Medical Quality of Service for Optimized Ultrasound Streaming in Wireless Robotic Tele-ultrasonography System

Nada Y. Philip

A THESIS SUBMITTED IN PARTIAL FULFILLMENT OF
THE REQUIREMENTS OF KINGSTON UNIVERSITY
FOR THE DEGREE OF DOCTOR OF PHILOSOPHY

Faculty of Computing, Information Systems and Mathematics
Kingston University, London

At the request of the university the following figures have not been digitised:

Acknowledgement

First I would like to express my sincere appreciation and gratitude to my supervisor - Professor Robert S. H. Istepanian, he is patiently guided me and helped me throughout the entire time of this research.

I would also like to thank Faculty of Computing, Information Systems and Mathematics, Kingston University for providing me with this opportunity to fulfil this research.

I have had the pleasure of being a member of the MINT research centre and MOMED group. My thanks go to all the members of this group. Especial thanks goes for the support of Dr. Maria Martini, Dr. David Wertheim and Dr. Henry Wang. And also special thanks for the help and friendship of Mr. Ala Sungoor, Dr. Salim Garawi, Dr. Ying. Zou and Mr. Nilesh Prag.

I am very grateful to Mr. Tom Geake for his support and advice on thesis writing. My appreciation and gratitude goes to Ms. Bee Tang who has provided invaluable administration guidance and support throughout this research.

My appreciation also goes to Dr. Nazar Amso from Cardiff University and Dr. Phil Shorvon from Central Middlesex Hospital / London for their kind medical suggestions and help.

I would like also to acknowledge the support of Vodafone/ UK, especially Dr. Nigel Jefferies for the help in the provision of mobile network facilities for this study.

My thanks also go to Prof. Aura Ganz and Ms. Y. Chu from University of Massachusetts/ Amherst.

This thesis could not have been accomplished without the love, support and patient of my family, my parents, my husband, my lovely daughter Sarah, my aunt and my brothers. Thanks for their support.

Finally, I would like to thank all of those who have helped me and showed their support. They are always in my mind and with my best wishes.

Abstract

Mobile healthcare (m- health) is a new paradigm that brings together the evolution of emerging wireless communications and network technologies with the concept of 'connected healthcare' anytime and anywhere. There are two critical issues facing the successful deployment of m-health applications from the wireless communications perspectives. First, wireless connectivity issues and mobility requirements of real-time bandwidth demanding m-health applications. Second, the Quality of Service (QoS) issues from the healthcare perspective and their required levels to guarantee robust and clinically acceptable healthcare services.

This thesis consider the concept of medical QoS (m-QoS) issues for typical bandwidth demanding m-health application (tele-ultrasound streaming) in 3G and 3.5G wireless environments. Specifically this thesis introduces a new concept of m-QoS that provide a sub-category of quality of services from the m-health perspective. A wireless robotic tele-ultrasonography system is adopted in this research as the m-health application. Accordingly the m-QoS metrics and its functional bounds for this m-health application are defined. To validate this concept a new optimal video streaming rate control policy is proposed based on the Q-learning approach to deliver the ultrasound images over 3G and 3.5G environments.

To achieve these objectives an end-to-end architecture for streaming M-JPEG compressed ultrasound video over 3G and 3.5G communication network is developed. Through this a client-server test bed is developed to capture the ultrasound images and adaptively varying its frame rate and the quality and send to the other end. The new rate control algorithm was implemented via this test bed.

This thesis shows the performance analysis of the proposed rate control algorithm in terms of achieving the defined m-QoS over 3G and 3.5G wireless connections.

In collaboration with medical expert in ultrasonography field, subjective image analysis are also carried out to validate the quality of the processed images.

Contents

Glossary

16QAM: 16-Quadrature Amplitude Modulation (16QAM)
3G: Third Generation
3.5G: 3.5 Generation
4G: Fourth Generation
3(GPP)2: Third Generation Partnership Project 2
ACK: Acknowledgments
AMC: Adaptive Modulation and Coding
AIMD: Additive Increase and Multiplicative Decrease
ADC: Analogue-to-Digital Converter
AFR: Arrival Frame Rate
ARQ: Automatic Repeat reQuest
ATM: Asynchronous Transfer Mode
AB: Available Bandwidth
BO: Buffer Occupancy
CABAC: Context Based Adaptive Binary Arithmetic Coding
CQI: Channel Quality information
CR: Channel Rate
CS: Circuit Switched
CIF: Common Intermediate Format
CN: Core Network
CRC: Cyclic Redundancy Check
DCH: Dedicated Channel
DPCCH: Dedicated Physical Control Channel
DOF: Degree-Of-Freedom
DAM: Diagnostic Acceptability Measure
DL: DownLink
DLL: Dynamic Link Library
DSCQS: Double Stimulus Continuous Quality Scale
DSIS: Double Stimulus Impairment Scale
EDR: Echographic Diagnosis Robot
EV-DO: EVolution-Data Optimized
FTP: File Transfer Protocol
FIFO: First In First Out
FACH: Forward Access Channel
FEC: Forward Error Correction
GGSN: Gateway GPRS Service Node
GPRS: General Packet Radio Service
GOP: Group Of Picture
GMSC: Gateway Mobile Switching Centre
GSM: Global System for Mobile communications
H.264/AVC:H.264/Advanced Video Coding
HARQ: Hybrid Automatic Repeat reQuest
HS-DSCH: High-Speed Downlink Shared CHannel
HS-DPCCH:High-Speed Dedicated Physical Control CHannel
HSPA: High Speed Packet Access

HS-SCCH: High-Speed Shared Control CHannel
HSDPA: High Speed Data Packet Access
HSUPA: High Speed Uplink Packet Access
HVS: Human Visual System
ICMP: Internet Control Message Protocol
IETF: Internet Engineering Task Force
IP: Internet Protocol
ISDN: Integrated Services Digital Network
ITU-R: International Telecommunications Union - Radiocommunication
ITU-T: International Telecommunications Union – Telecommunications standards
JBIT: Java Based Interface for Telerobotics
JPEG2000: Joint Photographic Experts Group 2000
LabVIEW: **Lab**oratory **V**irtual **I**nstrumentation **E**ngineering **W**orkbench
LAN: Local Area Network
LPC: Linear Prediction Coding
MB: Macroblock
MC-DCT: Motion-Compensated Discrete Cosine Transforms
MAC: Medium Access Control
MDP: Markov Decision Process
ME: Mobile Equipment
M-Health: Mobile- Healthcare
MIDSTEP: Multimedia Interactive DemonStrator Tele-Presence
MIMD: Multiplicative Increase and Multiplicative Decrease
M-JPEG: Motion-JPEG
MOS: Mean Opinion Score
MAC: Medium Access Control
MPEG4: Moving Picture Experts Group 4
M-QoS: Medical-Quality of Service
MSC/VLR: Mobile services Switching Centre / Visitor location register
MSE: Mean Squared Error
MTU: Maximum Transit Unit
MVS: Medical Video Streaming
NACK: Negative Acknowledgment
NI-IMAQ: National Instrument – IMage AcQuisition
NMSE: Normalized Mean Square Error
OTELO: mObile Tele-Echography using an ultra-Light rObot)
PSNR: Peak Signal to Noise Ratio
QCIF: Quarter Common Intermediate Format
QI: Quality Index
QoS: Quality of Service
QPSK: Quadrature Phase Shift Keying
QS: Quantization Step
Q-USR: Q-learning-based Ultrasound Streaming Rate control
PS: Packet Switched
RACH: Random Access CHannel
RAN: Radio Access Network
R-D: Rate-Distortion
RL: Reinforcement Learning
RLC: Radio Link Control
RNC: Radio Network Control
ROC: Receiver Operating Characteristic

ROI: Region Of Interest
RSVP: ReSerVation Protocol
RTP: Real-time Transport Protocol
RTT: Round Trip Time
SA: Streaming Agents
SGSN: Serving GPRS Service Node
SSCQE: Single Stimulus Continuous Quality Evaluation
SSIM: Structural SIMilarity
TCP: Transmission Control Protocol
TFRC: TCP friendly Rate Control
TTI: Transmission Time Interval
UDP: User Datagram Protocol
UE: User Equipment
UIQ: Universal Image Quality
UL: UpLink
UMTS: Universal Mobile Telecommunications System
US: Ultrasound Streaming
USB: Universal Serial Bus
UTRAN: UMTS- Terrestrial Radio Access Network
VI: Virtual Instrument
VQEG: Video Quality Experts Group
VOIP: Voice Over IP
W-CDMA: Wideband - Code Division Multiple Access
XTP: Xpress Transport Protocol

List of Tables

List of Figures

Introduction

1.1 Evolution of Telemedicine and e-health

In recent years telemedicine and e-health systems have become increasingly important areas of healthcare delivery in several countries world wide. In general telemedicine has been defined as the use of telecommunication to provide diagnostic and therapeutic medical information between patient and doctor without either of them having to travel [1, 2, 3].

More recently the definitions involved in the identification of "e-health" as an umbrella term, with definitions such as "a new term needed to describe the combined use of electronic communication and information technology in the health sector, the use in the health sector of digital data, transmitted, stored and retrieved electronically for clinical, educational and administrative purposes, both at the local and at distance" [4].

Revised definition advocate that telemedicine remains linked to medical professionals, while e-health is derived by non-professionals, namely patients that with their interests drive new services even in the healthcare field mostly for their empowerment through access to information and knowledge [5].

However, the recent advances in Mobile, Multimedia and Network technologies presents a paradigm shift in future health care delivery systems. The synthesis of the two terms 'mobility' and 'healthcare' is currently introducing new areas of research and development that will bring new medical applications and services closer to large scale realization that were not possible in 20th century telemedical services.

The recent advances in wireless communication and network technologies with increased bandwidth and data rate capability has resulted in further evolution of e-health systems. M-Health is a new and emerging concept that was first introduced in 2000 as 'unwired e-med' in [6]. Mobile healthcare (M-Health) can be defined as 'mobile computing, medical sensor, and communications technologies for healthcare'. This emerging concept represents the evolution of e-health systems from traditional desktop "telemedicine" platforms to wireless and mobile configurations [7].

The increased availability, miniaturization, performance, enhanced data rates, and the expected convergence of future wireless communication and network technologies around mobile health systems will accelerate the deployment of M-health systems and services within the next decade.

It is evident that organizations and the delivery of health care are being underpinned by the advances in M-health technologies. These advances are giving rise to a range of reforms in the way in which some healthcare services are currently delivered. In the near future, the increasing medical data traffic and demand from different clinical applications and mobile medical scenarios will be compatible with the increased data rates of the current third generation (3G) and beyond 3G systems. Specially, in a society penetrated by 3G systems, home medical care and remote diagnosis will become common. Check-up by specialists and prescription of drugs will be enabled at home and in under-populated areas based on high resolution image transmission technologies and remote surgery, and virtual hospitals with no resident doctors will be realized. Preventive medical care will also be emphasized: for individual health management, data will constantly be transmitted to the hospital through built-in sensor and monitoring systems, e.g. in the patient's watch, accessories, or other items worn daily, and results will be fed back to the patient [7].

1.2 M-health

As described in the earlier section, the evolution of current 3G and beyond wireless communication and mobile technologies will be the major driving force for future development in m-health systems [7].

With current wireless technologies, patient records can be accessed by healthcare professionals from any given location by connection to the medical institution's information system. Physicians' access to patient history, laboratory results, pharmaceutical data, insurance information, and medical resources can be enhanced by mobile technology, thereby improving the quality of patient care. For example handheld devices are used in home health care. In recent years there has been increased research on M-health technologies using current 3G-wireless communication systems [10-17].

There are some limitations to the existing 3G wireless technologies on their deployment strategies in health care. Some of these issues can be summarized as follows [7]:

1) The lack of an existing flexible and integrated "m-Health-on-demand" linkage of the different mobile telecommunication options and standards for healthcare services. This lack of linkage and compatibility with integrated services exists due to the difficulty of achieving operational compatibility between the different mobile technologies, terminals and devices standards, and "M-health protocols."

2) The high cost of current wireless links, such as between satellites and global mobile devices and the limitation of existing practical wireless data rates. This is also combined with the availability of secure mobile Internet connectivity and information access.

3) Health-care is a very complex industry that is difficult to change. Organizational changes are very often required for health-care institutions to benefit from e-Health and m-Health services.

4) The short-term and long-term economic consequences and working conditions for physicians and health-care experts using these technologies are not yet fully understood or properly investigated.

5) The methods of payment and reimbursement issues for e-Health and m-Health services are not yet fully developed and standardized.

6) There is a lack of integration between existing e-Health services and other information systems, e.g., referral and ordering systems, medical records, etc.

The above are some of the factors that have hindered the wider applications of mobile telemedicine technologies thus far across healthcare systems and on critical medical applications. A comprehensive review in m-health system and recent developments in this area are cited in [20].

In addition, there are two important critical issues from the technical perspective that are the focus of this thesis and these are summarised as:

1. The communication medium required to provide effective and accurate diagnosis and treatment, especially with bandwidth demanding services such as real-time tele-ultrasonography. It is well known that the evolution of mobile telecommunication systems from 3G to 4G will facilitate the provision of faster

data-transfer rates, thus enabling the development of telemedicine systems that require high-data rates and hence better diagnostic quality.

2. The Quality of Service (QoS) issue and their guarantee to provide robust m-health services and diagnostically acceptable quality. For m-health systems to be accepted clinically especially by healthcare services. Their services require to provide the users (patients, healthcare provider) with an acceptable QoS from the clinical perspective.

The research focus of this thesis will aim to address the above two research challenges.

1.3 Robotic Tele-ultrasonography systems

It is well known that demand is increasing for ultrasonography services that require expert opinion, since specialist experts are not available in remote areas, hence medical doctors in these cases have a limited amount of data (echography and radiography) to evaluate the level of the clinical symptoms and to make the decision to whether to send the patient, by ambulance, helicopter or to the closest hospital or to keep them at home. In approximately 50% of the diagnostic cases, patients are transferred to the hospital centre at night, to receive an ultrasound examination, and are sent back home a few hours later. Medical scenarios requested an echography examination as a first evaluation arise a several times a day in main hospital centres [21]. A study in Finland investigated whether teleradiology consultation would reduce unnecessary patient transportation and thereby save on opportunity and treatment costs, 81% of the patients examined via teleradiology, avoided unnecessary transportation, and 75% of those transported to a central hospital were operated on, immediately on arrival without further radiological study [22].

One of the first ultrasound telemedical studies on remote examinations were reported in the mid 1990s. Where the ultrasound video images acquired by the technician at the patient's side, transmitted to a medical expert via a communication link of 1.5 Mbps T-1 leased line [23]. In this system, the expert could communicate in real time with the technician so as to supervise the image acquisition. However, these earlier telemedical

systems were not efficient enough for proper medical validation because of their ad-hoc 'expert-dependency' of the relevant ultrasound examination.

To overcome the disadvantages of the above-mentioned simple remote echography, it would be necessary to enable the distant expert to take control of the displacement of the echographic probe, for example, by controlling a probe hold by a remote-controlled robot. Such systems using robotics are used in medicine and especially in surgery [24 - 26].

In particular robotized telemedecine offers great medical advantages for medical experts who want to perform skilled actions, from an expert centre for the benefit of a remotely located patient [32-34].

During the last decade, research centres have been involved with the development of robotic tele-ultrasonography applications. For most of these, the challenge has been the combination of the robotic performances or the quality of the transmitted image. Most of these projects introduced parallel robots to fit the medical requirements of a tele-ultrasonography examination over the abdominal area of the remote patient [29-31].

A different approach is proposed with the *OTELO* system (mObile Tele-Echography using an ultra-Light rObot) (that was a European funded project IST-2001-2004, 32516). The main objectives of the OTELO system were to perform, in real-time, a robotized ultrasonography examination on a remotely located patient, using several communication links from wired to wireless (3G and satellite) links options. The objective was to combine the development of a light weight robot with appropriate image compression techniques to offer the medical specialist a high performance tool for an efficient hand-to-eye coordination during the robotized tele-ultrasonography examination.

This thesis uses the OTELO system as the advanced mobile telemedical system platform.

1.3.1 The OTELO System: An overview

In this section an overview of the used robotic tele-ultrasonography platform is given. Further details on the system are presented in [58]. Ultrasound images and the probe-holder robot are two important elements of the overall tele-echography chain. They are dependant on each other and they contribute to make the system transparent for the expert who is the major actor of the tele-operated control loop.

The expert controls the remote probe holder robot by combining one degree-of-freedom (DOF) hand-free input device orientation and the received information as shown in figure 1.1. This information includes the ultrasound images and the position of the robot on the patient's body. When considering an ideal communication link there is no time delay between the emission of the real probe position data and the reception of the received image. Therefore the real ultrasound plane position corresponds, at any time, to the desired one given by the input device held by the expert. In a real tele-operated scenario, one should expect time delay in the communication link combined with a significant response time for the robotics and electronics system. The received ultrasound images do not correspond any longer to the desired ultrasound plane position given by the input device. The quality of the ultrasound image can also be altered by the chosen compression technique required by the communication link bandwidth. The resulting hand-to-eye coordination is then hindered.

Therefore the development of the robotics system is strongly linked with ultrasound image study when considering the performances of the tele-operated global chain.

The OTELO system consists of three parts as shown in figure 1.1:

- **The expert station:** where the medical expert remotely controls the positions and orientations of the distant ultrasound probe located on the patient's skin, with a dedicated one DOF hand free input device (also called fictive probe) fitted with a 6D localization sensor, the positions and orientations of the distant ultrasound probe located on the patient's skin. The specialist receives, in almost real-time depending on the available bandwidth, the patient ultrasound images. The information received at the expert station is integrated in an ergonomic graphic user interface. Furthermore a videoconferencing system between the two stations, enables the expert, the paramedic and the patient to communicate with each others during the robotized tele-echography examination.
- **The patient station:** which consists of a light weight 6DOF serial robot that holds the ultrasound probe available at the patient site, a compact ultrasound device, a control and communication portable unit and a videoconferencing system. A paramedic assists the patient. He positions the light weight robot on an anatomic reference point on the patient's skin according to the medical expert instructions and maintains it during the examination. A strain gauge force sensor, embedded in the probe holder, measures the contact force between the real probe and the patient's skin. The robot controller restricts this force for the patient's comfort and safety. Medical images from the ultrasound device are compressed before being sent to the expert. The patient station is mobile, is easily transportable and can be quickly set up on the place of use and connected to any available communication infrastructure using TCP/IP and UDP modes.
- **The communication link:** where the robotic and the medical data exchanged between the two stations, expert and patient, that includes ultrasound images, robot controls, haptic information, ambient images and audio instructions. Most of the bandwidth is used for ultrasound or ambient images transfer. Terrestrial links includes (e.g. ISDN), fixed and mobile satellite solutions or 3G technologies (e.g. UMTS). Further details of the performance analysis of OTELO system is presented in details in [58].

1.4 Wireless Medical Streaming for the Teleultrasonography System

This section introduces the concept of wireless medical streaming with focus on teleultrasonography. A brief introduction on streaming in robotic teleultrasonography is presented. There follows an introduction to wireless streaming issues and their effect on wireless (QoS) from medical prospective.

1.4.1 Ultrasound Streaming in Robotic teleultrasonography

In generally video streaming consists of the following stages [18]:

1- Partition the compressed video into packets

2- Start delivery of these packets

3- Decode and playback at the receiver while the video is still being delivered.

Figure 1.3 shows a typical video streaming scenario. It comprises a sending server that transmits data units of video over a packet network to a receiving client application. Video data are packetsized into data unites, and put in a sending buffer, ready to be transmitted by the server to the client. The purpose of the encoding buffer is to manage the generated bit rate by the encoder in order to match it with the channel bit rate. At the appropriate time the client sends data units to the decoder, for decoding and presentation. The purpose of the decoder buffer is to delay the decoding of the video streams for certain time called the play-back delay. The purpose of this delay is two-fold: to remove network delay jitter and to allow for recovery of lost packets using positive acknowledgments (ACKs) [19].

Figure 1.3. Block diagram of a typical video streaming system [19].

Streaming video can be in real time or pre-encoded (stored video). Real time video streaming may be interactive as in videoconferencing or not interactive e.g. broadcast of a sport event. In the real time case the time constraints are an important factor. In particular for m-health applications most medical video application require specific time delay bounds and other specific QoS constraints that are discussed in details in the subsequent chapters.

For a typical robotic tele-ultrasonography session the common scenario for the expert in ultrasonography field is communicating, controlling the robotic arm and acquiring ultrasound images or stream of images via the wireless link from the patient been scanned by ultrasound probe held by the robotic arm. The streaming of these medical images can be classified as real time interaction as explained above. The OTELO system is an advanced example of such m-health scenario.

In general videoconferencing is used increasingly in many telemedicine applications, including medical personnel education, peer consultation, patient education, and patient care [50]. In the recent years, the methods used to stream the ultrasound images is general video conferencing systems that are based on standard video codecs e.g. H263, MPEG4, M_JPEG etc...[27]. These video streaming codec systems have been carefully designed and developed over the years towards achieving good communication QoS for the general video conference users [28]. However in m-health applications, there are additional critical requirements of a medically approved service, especially in limited and variable wireless conditions. This thesis uses the term Medical Video streaming (MVS). The (MVS) such as in robotic tele-ultrasonography application, is the stream of ultrasound images that the patient (robotic) side transmits back to the medical expert side. In this work the term Medical Video Stream is used, when appropriate, to refer to the ultrasound image stream.

1.4.2 Challenges in Wireless Video Streaming

The rapid advances in both mobile communication and multimedia technologies, is making wireless video streaming a popular and demanding application. Current mobile terminals and PDA can send and receive videos anywhere and at anytime. However, there are a number of basic problems that affect wireless video streaming processes. In

general wireless video streaming suffers from the same problems that affect best effort IP services. These can be summarized as follows [18]:

- Bandwidth: The bandwidth available between two points in the Internet is generally unknown, limited and time-varying. If the sender transmits faster than the available bandwidth then congestion occurs, packets are lost, and there is a severe drop in video quality. If the sender transmits slower than the available bandwidth then the receiver produces sub-optimal video quality. The goal to overcome the bandwidth problem is to estimate the available bandwidth and then match the transmitted video bit rate to the available bandwidth.
- Delay jitter: The end-to-end delay that a packet experiences may fluctuate from packet to packet. This variation in end-to-end delay is referred to as the delay jitter. Delay jitter is a problem because the receiver must receive/decode/display frames at a constant rate, and any late frames resulting from the delay jitter can produce problems in the reconstructed video, e.g. jerks in the received video.
- Loss rate: Wired packet networks such as the Internet are affected by packet loss. Losses can have a very destructive effect on the reconstructed video quality. To solve this problem there is a need for streaming media systems to adaptively control its transmission rate according to the instantaneous network conditions

Specifically, these characteristics are unknown and dynamic. Therefore, a key goal of video streaming is to design a reliable system to deliver high-quality video over the network.

In addition to the above challenges wireless video streaming introduces specific additional constraints due to the following:

- Limited bandwidth availability
- Mobility and radio condition, handover that causes a period of no throughput at all as the radio is torn down and re-established. Fading effect due to path loss. These effects cause packet loss in terms of bit error.

The available bandwidth between two points in the wireless communication due to these constraints is stochastic, limited and time-varying [37]. Losses can have a very destructive effect on the reconstructed video quality. To combat these losses, usually a robust video streaming system is designed with error control to trade off the throughput

and the delay for reliability. Approaches for error control can be roughly grouped into four classes: (1) forward error correction (FEC), (2) ARQ (Automatic Repeat reQuest), (3) error concealment, and (4) error-resilient video coding [18, 37].

1.5 Medical Quality of Service (m-QoS)

This section introduces the concept of Medical Quality of Service (m-QoS) in medical video streaming (MVS) environment, with further details to follow in chapter 2. It is well known that traditional Quality of Service can be defined as a set of specific requirements for a particular service provided by a network to its users . In general, QoS can be divided into two levels [37]:

1- Network QoS: the QoS that the network and technology can offer to the user, e.g. bandwidth, time delay and reliability.

2- User QoS: the quality of the received services is it approved by the user, different users have different translation for QoS.

In M-health environments providing guaranteed QoS is a challenge and needing further research. In the selected ultrasound medical streaming environment of this work, three user QoS requirements are important in deciding the resulting throughput. These are summarized as:

1. Image quality,
2. Frame rate of the received images,
3. End-to-end delay.

In order to match the resulting bandwidth with the available network bandwidth, there must be a trade off between these QoS requirements in order to satisfy the medical (clinical) requirements and bounds with relevant metrics. This is the concept of m-QoS which can be defined as a sub category of QoS from the m-health perspective that represents:' *An augmented requirements of critical mobile health care applications and the traditional wireless Quality of Service requirements'*.

Several research attempts has been reported in the literature to study QoS in telemedicine applications. These are reviewed in chapter 2.

In this thesis the focus is on two main issues that are described briefly next and

detailed in the following chapters.

1.5.1 Optimisation issues of m-QoS

It is well known that the majority of engineering design problems can be represented as multiobjective in that there are several conflicting design aims, which need to be simultaneously achieved [42]. In our case the above defined m-QoS trade-off problem can be solved using multiobjective optimisation methods in order to find the optimal medical rate allocation that can satisfy the necessary m-QoS requirements. The details of these issues will be presented in chapter 4.

1.5.2 Rate Adaptation issues

As discussed earlier, the communication of compressed video requires a guaranteed QoS for efficient wireless transmission and reception. It is well known that due to the lack of QoS guarantees for IP multimedia applications and the variable error prone environment of wireless communication, the compressed video streaming applications should be reactive to the variation of network resources by detecting and adapting to network congestion optimally [43]. This is achieved by the detection of the available bandwidth during the video streaming process, and adapting video rate/quality accurately [44]. This will ensure the transmission of high quality pre-encoded video and at the same time ensure good network condition, with higher utilization.

For the bandwidth demanding m-health application addressed here, a concept derived from "Adaptive Control Theory" for the rate adaptation problem of the ultrasound streaming is adopted. This concept is summarised in figure 1.4 below. The "controller" in this case is the encoder that is needed to set its control parameters, which are the quality and frame rate of the transmitted images. The "process" represents the wireless environment that has to be measured its state and fed it to the adaptive control to predict the optimal frame rate and quality.

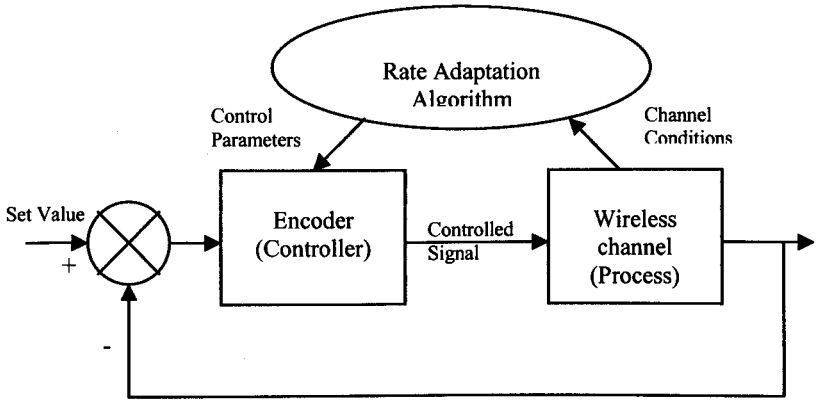

Figure 1.4. Block diagram of the m-health rate adaptation mechanism.

In real-time adaptive control theory; there are two adaptive control approaches: **Indirect** and **direct** [48]. In the **indirect** structure the process parameters needs to be estimated explicitly and accordingly the control parameters get estimated. On the other hand in **direct** structure the process parameters do not need to be estimated explicitly. Clearly the **direct** structure is better suited for real time wireless environment, since it is difficult to estimate the wireless channel model. Hence the concept of the optimal rate control is based on this approach.

In this research work the rate control problem is formulated as a Markov Decision Process (MDP). Moreover, a new scheme is proposed based on real time reinforcement learning method known as "Q-Learning" which is based on the direct adaptive control theory [36]. This scheme is named in this work as the Q-learning-based Ultrasound Streaming Rate control (Q-USR) algorithm. The block diagram Figure 1.5 below shows the basic idea of Q-learning approach. The adaptive controller is the decision maker known as the agent that monitors the environment state and assign actions accordingly. When the agent realizes this action, the environment's state changes, the agent receives the new environment's state and a signal of immediate reword from the environment, as a consequence of the previous action. Based on this information the agent updates its knowledge base. The process will get repeated until the agent reaches an optimal policy that assigns optimal actions that leads the environment to a better state that satisfies the control constrains. The main advantage of this method is that it does not require a prior knowledge of the state transition probabilities (explicit state transition model) in mobile communication networks, which are very difficult to estimate due to the large fluctuations in the link bandwidth of mobile networks.

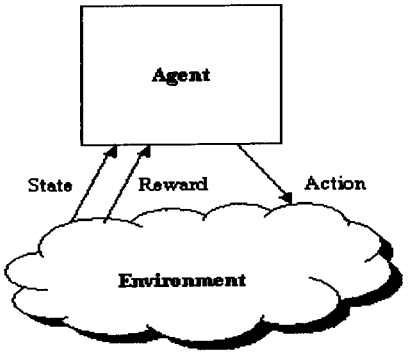

Figure 1.5. Q-learning functional strategy.

1.6 Research Contribution

The major contributions of this thesis can be summarized in the following challenges and objectives:

1. A new concept of **medical QoS (m-QoS)** that define a sub-category of the traditional Quality of Services from the m-health perspective is introduced.
2. A new optimal rate control policy is introduced based on Q-learning approach (Q-USR) to deliver optimal ultrasound streams over 3G and 3.5G networks to validate this m-QoS concept.
3. The development of a client-server test bed to test and validate the optimized ultrasound streams in 3G and 3.5G wireless networks.
4. Performance analysis of the system in 3G and 3.5G real-time operating network conditions and using different video codec to validate the algorithmic concepts defined above.

1.7 Structure of the Thesis

This thesis is structured as follows:

Chapter 2 : This chapter gives the background and a literature review with justifications for the main aspects of this multi-disciplinary research. It starts with a

background and brief review on QoS issues in wireless video streaming. Some previous work on medical video streaming is also presented. It presents some related work on the requirements of medical Quality of Service m-QoS defined earlier in implementation process of m-health applications. In addition it gives some examples of m-health applications and defines its important m-QoS requirements when implemented in integrated environments. One of the m-QoS metrics considered here is the medical image quality. This chapter introduces the quality measurements issues and techniques of medical images.

Chapter 3 : This chapter introduces and justifies the m-QoS metrics for the Ultrasound streaming in the robotic tele-ultrasonography system "OTELO" in wireless 3G environments. These are namely image quality index in terms of PSNR and SSIM, arriving frame rate and end-to-end delay. These metrics have been selected based on the medical requirements of tele-ultrasonography and the limitations of the 3G and 3.5G uplink data rate conditions.

Chapter 4 : The overall system block diagram of the medical video streaming system developed is introduced in this chapter. Specifically the Q-USR control algorithm is explained in details. In addition the performance of this algorithm will be given to show its optimization achievements. Further more a comparison in the performance of this system with and without the Q-USR control algorithm is given over 3G network and using H.263 video codec.

Chapter 5 : The implementation and experimental setup of the developed medical video streaming system is introduced in this chapter. The implementation issues are explained in terms of the techniques and software used.

Chapter 6 : This chapter shows the performance of the Q-USR control algorithm over 3.5G wireless communication link (HSDPA). A theoretical overview on HSDPA wireless communication system is provided. Some of the result is compared with the performance of this algorithm over 3G wireless communication link.

Chapter 7 : This chapter summarises the contributions of this thesis. In addition, directions for future research taking in to consideration the achievements of this study are discussed.

Chapter 2

Background and Related work

2.1 Introduction

This chapter presents the background of all the multidisciplinary issues of the thesis. These are summarised as follows:

1. An introduction to QoS control issues in the wireless video streaming environment is given first followed by related work on existing rate control techniques is presented.
2. A review of medical video streaming and some of the existing work and research in this area.
3. A summary of related work on the requirement of medical Quality of Service (m-QoS) defined earlier. In addition some examples of m-health applications are given along with a definition of the important (m-QoS) requirements when implemented in integrated environments.
4. One of the m-QoS metrics that considered here is the medical image quality. An introduction is given to image quality measurement techniques. Objective medical image quality measures and related work are discussed.

2.2 QoS Control in Wireless Video Streaming

This section presents some of the previous work on QoS control in wireless video streaming applications. First, an introduction to general end-to-end QoS frameworks in wireless video streaming environment is described.

2.2.1 End-to-End QoS in wireless video streaming

End-to-end QoS support is a multidisciplinary topic involving several areas, ranging from applications, terminals, networking architectures to network management, business models, and finally the main target, the end users. Enabling video streaming QoS through the Internet is difficult, and becomes more challenging when introducing QoS in video streaming in an environment the involves mobile hosts under different wireless access technologies, because available resources (e.g., bandwidth, battery life, etc.) in wireless networks are limited and change dynamically over time [53]. For wireless networks, since the capacity of a wireless channel varies randomly with time, providing deterministic QoS (i.e., zero QoS violation probability) is not practical. Hence the focus of this review will be on statistical (trade-off) QoS issues.

There are two main approaches for end-to-end QoS support in wireless video streaming: Network Centric QoS and End-system Centric QoS [53]. These are summarizes as follows:

1- **Network Centric QoS:** In this type of QoS the underlying network provides prioritized QoS support to satisfy data rate, delay bound, and packet loss requirements of different applications. In the prioritized transmission, QoS is expressed in terms of the probability of buffer overflow and/or the probability of delay violation at the link layer. However, at the video application layer, QoS is measured by the mean squared error (MSE) and/or peak-signal-to-noise ratio (PSNR). Thus, one of the key issues for end-to-end QoS provisioning using a network centric solution is the effective QoS mapping across different layers. More specifically, one needs to consider how to model the varying network and coordinate effective adaptation of QoS parameters at the video application layer and prioritized transmission system at the link layer. The best-effort nature of Internet has promoted the Internet Engineering Task Force (IETF) community to seek for QoS support through network layer mechanisms. Two different approaches have been introduced by the IETF community, which are IntServ and DiffServ [54, 55], respectively. IntServ was introduced in IP networks in order to provide guaranteed and controlled services in addition to the existing best-effort service. IntServ and reservation protocols, such as ReSerVation Protocol (RSVP), have failed to become a practical end-to-end QoS solution for lack of scalability and difficulty in that all elements in the network have to be RSVP enabled.

DiffServ was proposed to provide a scalable and manageable network with service differentiation capability. In contrast to the per-flow-based QoS guarantee in the IntServ, DiffServ networks provide QoS assurance on a per-aggregate basis.

The approaches to providing QoS in wireless networks are quite different from their Internet counterparts. The General Packet Radio Service (GPRS)/Universal Mobile Telecommunications System (UMTS) and IEEE 802.11 have total different mechanisms for QoS support. The Third Generation Partnership Project (3GPP)2 is the main standard body that defines and standardizes a common QoS framework for data services, particularly IP-based services. 3GPP has defined a comprehensive framework for end-to-end QoS covering all subsystems, from Radio Access Network (RAN) through core network to gateway node (to the external packet data network) within a UMTS network [56]. 3GPP has also defined four different UMTS QoS classes according to delay sensitivity: conversational, streaming, interactive, and background classes.

2- **End-System Centric QoS.** In particular, the end system employ various control techniques, which include congestion control, error control, and power control, to maximize the application-layer video quality without any QoS support from the underlying network. The advantage of end system control is that there are minimum changes required in the core network. However, the main challenge is how to design efficient and effective power/congestion/error control mechanisms.

This research focuses on the latter i.e. (*end-system centric based)* QoS since this type does not impose any requirements on the network conditions. In particular, the end systems employ control techniques that aim to maximize the video quality with minimum support from the transport layers.

As mentioned before the end-system QoS is applied at the application layer. The objective of application layer QoS control in a video streaming environment is to avoid congestion and maximize video quality in the presence of packet loss and bit errors. The application-layer QoS control techniques include congestion control, power control and error control. The focus of this thesis is on the medical video adaptation from the viewpoint of congestion control, i.e. how the rate of the compressed video should be manipulated so that the end-quality is optimized and satisfy the clinical and diagnostic

requirement. As a result, the issue of error control and power control is out of its scope. In addition to that, the techniques developed herein do not disallow or impede the use of error and power control techniques.

(i) Rate Control Mechanisms

It is well known that packet loss has a major effect on video presentation quality caused by network congestion. Thus, end-to-end congestion control mechanisms are necessary to help reducing packet loss and delay. Congestion control in video streaming applications takes the form of rate control. Rate control attempts to minimize the possibility of network congestion by matching the rate of the video stream to the available network bandwidth.

Rate control mechanisms can be located at the source end (source-based) or the receiver end (receiver-based) or at both ends (hybrid rate control). This work considers the use of source-based rate control mechanism as the other rate control mechanisms are preferably suitable for multicast streaming and our application is considered as a unicast streaming application [57].

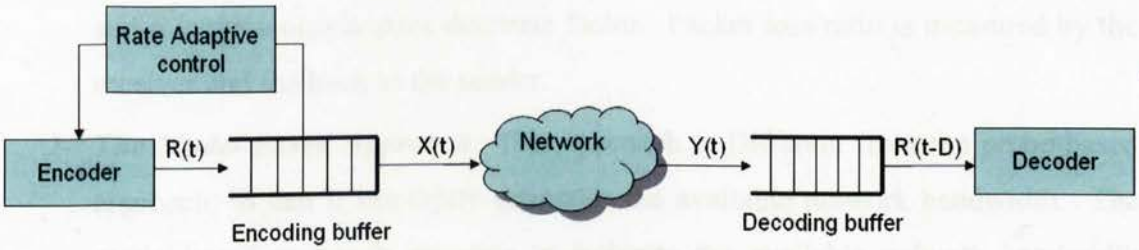

Figure 2.1 Adaptive rate control.

Figure 2.1 is a block diagram of a general source-based real-time video streaming system showing the rate control mechanism at the sender that adapts the video rate R(t) to the channel rate Y(t) to achieve the best quality at the receiver.

For source-based video streaming rate-control, two mechanisms are usually applied: **Probe-based** and **model-based** approach [57].

1- ***The probe-based approach*** is based on probing experiments. Specifically, the source probes for the available network bandwidth by adjusting the transmitting rate so that some QoS requirements are met, e.g., packet loss ratio is below a certain threshold the value of which is determined according to the minimum video perceptual quality required by the receiver. There are two ways to adjust

the sending rate: Additive Increase and Multiplicative Decrease (AIMD), and Multiplicative Increase and Multiplicative Decrease (MIMD). The probe-based rate control could avoid congestion since it always tries to adapt to the congestion status and keep the packet loss at an acceptable level.

For the purpose of illustration, the source-based rate control mechanism based on AIMD is described. The basic AIMD rate control algorithm can be represented in the following algorithm [57]:

$$
\begin{array}{l}
\textit{if } (P \leq P_{th}) \\
\quad r = \min((\ r + AIR\ );\ Max\ \ R) \\
\textit{else} \\
\quad r = \max((\ \alpha * r);\ Min\ \ R)
\end{array}
$$

Where P is the packet loss ratio; P_{th} is the threshold for the packet loss ratio; is the sending rate at the source; AIR is the additive increase rate; $MaxR$ and $MinR$ are the maximum rate and the minimum rate of the sender, respectively; and α is the multiplicative decrease factor. Packet loss ratio is measured by the receiver and fed back to the sender.

2- ***The Model-Based Approach:*** This approach is Different from the probe-based approach, in that it implicitly estimates the available network bandwidth. The model-based approach attempts to estimate the available network bandwidth explicitly. This can be achieved by using a throughput model of a TCP connection, which is characterized by the following formula [57]:

$$\lambda = \frac{1.22\,MTU}{RTT\sqrt{\rho}} \tag{2.1}$$

Where λ is the throughput of a TCP connection; MTU (Maximum Transit Unit) is the maximum packet size used by the connection; RTT is the Round Trip Time for the connection; and ρ is the packet loss ratio experienced by the connection. Under the model-based rate control, (2.1) can be used to determine the sending rate of the video stream. That is, the rate-controlled video flow gets its bandwidth share like a TCP connection. As a result, the rate-controlled video flow could avoid congestion in a way similar to that of TCP, and can coexist

with TCP flows in a "friendly" manner. Hence, the model-based rate control is also called "TCP friendly" Rate Control (TFRC) [56]. In contrast to this TCP friendliness, a flow without rate control can get much more bandwidth than a TCP flow when the network is congested. This may lead to possible starvation of competing TCP flows due to the rapid reduction of the TCP window size in response to congestion.

To compute the sending rate in (2.1), it is necessary for the source to obtain the MTU, RTT, and packet loss ratio. The MTU can be found through the mechanism proposed in [70]. In the case when the MTU information is not available, the default MTU, i.e., 576 bytes, will be used. The parameter RTT can be obtained through feedback of timing information. In addition, the receiver can periodically send the parameter to the source in the time scale of the round trip time. Upon the receipt of the parameter, the source estimates the sending rate λ and then a rate control action may be taken.

This work uses the probe-based approach instead of the model based approach because in addition to estimating the packet loss for the model based approach, it also has the disadvantage of additional requirements to estimate other factors such as the RTT. In general there is a large variation in end-to-end delay in wireless Internet [51]. Sending only a single acknowledgment to measure the RTT during a predefined period of time may be inaccurate and variable.

Further more in wireless networks, the end-to-end packet loss can be caused by either congestion loss due to buffer overflow or the erroneous loss occurred in the wireless link. Rate control mechanisms are interested in packet loss caused by congestion loss. Therefore there is a need for some sort of end-to-end packet loss differentiation and estimation [71]. Which requires some sort of monitoring agents at the edge of wired and wireless network to measure the conditions of the two types of networks separately [72, 73]. Some other methods adopt some heuristic method such as interarrival time or packet pair [74, 75]. In both approaches (probe and model based rate control) measuring the packet loss require this extra stage of packet loss differentiation.

This work uses the probe-based approach based on probing the wireless network to measure the available bandwidth instead of measuring the packet loss. There has been

a large amount of research in this area over the last two decades. Many techniques have been proposed, and some performance and comparative studies have been done [101]. For mobile networks estimating the Available Bandwidth (AB) is a very challenging task due to the heterogeneity of the current systems and the different traffic characteristics of different data flow. One possible way of AB estimation is the deployment of some software on every router to report the router's load continuously. Since the exact route between two nodes in an ad-hoc network usually is unknown and may change without notification to the application layer the end-to-end measurement of the AB should not require any infrastructure or pre-installed components at each node. To achieve that, common End-to-End bandwidth measurement methods can be applied [102]. In this research end-to-end bandwidth measurement approaches is used here to estimate the available bandwidth. Many state of the art AB measurements methods are proposed for example Pathchirp, Pathload, Spruce and Topp [101, 103]. However the best performed method over mobile networks is the PathChirp [101, 103]. PathCirp is based on sending streams of exponentially spaced packets called chirps, so the instantaneous input rate changes. Only one iteration is needed to get an AB estimation, since it probes the network with different input rates in each stream. However according to [102] available bandwidth estimation in wireless networks is associated with difficulties that can result in misleading bandwidth estimations. Some of these difficulties are the probing packet size and the cross traffic intensity. Above all, these techniques add extra traffic to the wireless communications because the basic principle of these techniques is to inject a set of measurement packets, the probe packets, into the network. The probe packets traverse the network path to a receiver node, which time stamps each incoming probe packets. By analyzing these time stamps estimates of the link capacity and/or the available bandwidth can be made.

This thesis proposes a novel technique based on Linear Prediction approach (LPC) [123]. Linear Prediction is a mathematical operation in which future values of a discrete-time signal are estimated as linear functions of previous samples. The current available bandwidth is estimated from previous bandwidth readings. More details are available in chapter 4.

2.2.2 Wireless Video Streaming Rate Control – Related Work

As mentioned earlier rate control is an important issue in both wired and wireless streaming applications. In recent years, there have been a number of efforts to design rate control schemes in the wireless environment, some of which are probe-based and others are model-based approaches. Examples of probe-based work are in [82, 83]. [82] describes an adaptive video streaming method which adjusts the video output rate according to the wireless network. It uses the RTP/RTCP protocol for transmitting the video packets and controlling the video rate. It uses the RTCP reports to measure the available bandwidth (AB) and packet loss. Then it uses this information to decide either to increase the rate or decrease or hold in the same style as in [81]. However because it is a wireless environment it performs a test when a loss is detected to check if this loss is due to burst error or congestion. The work proposed in [83] is a feedback rate control scheme for video streaming in wireless environment. This work uses UDP in the transport layer and proposes a control algorithm on the top of that layer to control the network congestion. This places the congestion notification tool at the base station by monitoring the buffer occupancy at the base station and feedback this information to the transcoder at the server side to control the streaming rate accordingly. The base station router buffer has two limits, a lower and an upper one to prevent underflow and overflow respectively, these two limits triggering the rate controller at the server.

As mentioned earlier, a widely popular rate control scheme for streaming in networks is the model-based TCP-friendly rate control (TFRC) scheme. There have been a number of efforts to improve the performance of TFRC in wireless environments [84 – 88]. Since the TCP-friendly rate calculation depends on the value of packet loss reported by the receiver. These approaches either hide end hosts from packet loss caused by wireless channel error, or provide end hosts with the ability to distinguish between packet loss caused by congestion and that caused by wireless channel error. An example of the former can be found in [84], where a TCP-aware local retransmission link layer approach was adopted. The proposed module here resides in a router or base station on the last hop and record every packet forwarded. It looks into the ACK packets and carries out local retransmissions when a packet is corrupted by wireless channel errors. While doing the local retransmission, the ACK packets are suppressed and not forwarded to the sender. An example of the second approach can be found in [85, 86], where explicit loss notification was applied to notify a TCP/TFRC sender when packet

loss was caused by wireless channel errors rather than congestion. End-to-end statistics were used in [87] to detect congestion when a packet was lost. In this work the interarrival times and relative one-way delay to differentiate between packet loss caused by congestion and that due to wireless channel errors. The relative one-way delay increases if there is congestion, while the interarrival time increases if there is a packet loss caused by wireless channel errors. The work in [88] proposed an optimal end-to-end rate control scheme that suggests using multiple TFRC connections for a given wireless streaming application.

The focus in this thesis is on media optimization rate control so the concentration is on the research work of optimized media transmission schemes. In the literature review it was noticed that media optimization rate control algorithms are mainly based on either Lagrangian optimization or dynamic programming [89, 90]. In [89] the rate control algorithm was proposed for robust video transmission over wireless channel with bursty channel errors. The rate control was integrated with ARQ error control. The encoder in this work uses the channel feedback and channel model to adjust the encoding rate. The rate control algorithm used here is based on Rate-Distortion (R-D) approach, in that the source rate can be reduced at the cost of reduced quality distortion at the destination. The optimization methods used to solve the R-D problem here are based on dynamic programming and Lagrangian multiplier methods. This work assumes an accurate channel model and the result shows any mismatch between the underlying channel behaviour and the assumed two-state channel model at the encoder causes degradation of the proposed rate control. The work in [90] covers two issues. The first proposes the use of streaming agents (SA) strategy to feedback information about the network status to the server. The second uses streaming optimization scheme called complexity-scalable ARQ. It is derived from a rate-distortion optimized application-level retransmission scheme [91, 92], that adapts to SA and possibly client feedbacks to optimize video quality. In the optimization part it uses dynamic programming method to solve the optimization equation. The wireless scenario assumed here is that the server is the wired side and the client is the wireless part. This means that they adopt a downlink scenario where the available bandwidth is not a problem as compared to the uplink bandwidth scenario that this PhD work is adopting. The work in [98] is based on a network-aware joint source channel coding and decoding (JSCC/D) approach, based on two controller units at the physical and the application

layers. The two controllers work together to provide control for both the source encoder and the channel coding to satisfy user requirements. A cross-layer rate control strategy is adopted.

2.3 Medical Video Streaming

This section reviews some of the earlier work on medical video streaming in the Tele-Ultrasonography medical field.

One of the earliest Tele-Ultrasound systems used for real time remote diagnosis was reported in 1995 [23]. This used a digital image capture and distribution system that supporting remote ultrasound examinations and real-time diagnosis. For transmission the image was digitized and encoded at a resolution of 640X480 pixels with colour plan 8 bits per pixel and then sent over the dedicated communication link of 1.5 Mbit/s T-1 leased line. At the receiver end the arrived frame was decompressed and displayed. For reliable transmission of each frame Xpress Transport Protocol (XTP) was used. XTP is a transport protocol that provides flexibility in adapting the transmitting rate to the available bandwidth of the underlying network. This system was based on wired communication link that differs from our mobile research work that has limited bandwidth.

In 1998, the Multimedia Interactive DemonStrator Tele-Presence (MIDSTEP), a tele-presence system was developed [35]. The project had the principle objective of realizing two telesurgery demonstration systems; one for 'local' telemanipulation over LAN and one for remote telemanipulation over WAN. Both utilized remote robotic manipulation of an ultrasound probe, controlled by an expert Ultrasonographer, to guide a surgeon at the patient site in performing simple invasive surgical tasks. The ultrasound images were acquired at a 384x288 resolution and compressed using 10:1 M-JPEG video coder and then transmitted to the expert side via Asynchronous Transfer Mode (ATM) communication technology. In this system a User Datagram Protocol (UDP) was used to transmit video packets with a rate control system to maintain a frame rate of better than 15 fps. This application required 10 fixed lines with total of 100Mbps data rates and fixed location for both Expert and Remote stations.

In 2000, a European project 'TeleInVivo' was developed with a similar approach: the echography was performed by a clinical expert standing next to the patient, ultrasound data being sent via satellite to a data base station and processed to reconstruct a 3D representation of anatomical region of interest [69]. A wavelet-based images compression algorithm was implemented for the size reduction of the image data sets to be transferred. The compression was lossy but very efficient in cases where bandwidth is the crucial issue. However this system still lacks the ability of two way interaction during the consultation process, and did not solve the problem of the presence of the specialist in the remote area.

A telerobotic system was introduced in [45]. In this system, the internet user could access and command a 2 DoF robot in a real time closed loop over the Internet, receiving both visual and force feedback. A Java Based Interface for Telerobotics (JBIT) system was developed to demonstrate the feasibility of the Internet based telerobotics equipment. The real video was realized using the H.263 compression technique with a rate of 4 frame/s performance over 28.8 Kbps modem connection, and the obtained results confirmed that real time closed loop operation over the Internet is possible. The system provided poor image quality with the 4 frame/sec transmitted over a 28.8 Kbps channel.

Another example of using video conferencing systems in telemedicine was reported in [31]. A group of researchers in the Department of Medical Informatics at Ehime University in Japan experimented with a tele-diagnosis system to control a Echographic Diagnosis Robot (EDR). Two wireless Local Area Network (LAN) bridges SB-1100 (ICOM Co. Ltd) connected Ehime University to a temporal examination room 1.4Km from the hospital at 10Mbps. This line speed was sufficient to communicate at 6Mbps bandwidth. In this experiment PCS-1600, Sony videoconference systems were used in streaming ultrasound images captured by the ultrasound probe. This videoconference system uses H.263 video coding technologies. The time delay was less than 1sec when the image size was Common Intermediate Format (CIF) (352x288 pixels). This work was based on a wireless LAN, a short distance field and not over a wireless telecommunication channel (e.g. UMTS); where the limited bandwidth and the added noise in terms of interference and mobility could significantly affect the performance. This work failed to satisfy the user requirements (expert) in terms of the received frame rate and quality. As that it uses a general videoconference system that it is not designed

for medical applications.

2.4 QoS in m-Health Application

Following the introduction in chapter one, this section reviews the latest research work specifically related to the general QoS in telemedicine applications and the mobile environment. In addition gives some examples of m-health applications and define its important m-QoS requirements when implemented in integrated tele-medical wireless environments.

QoS studies in telemedicine applications generally are not a mature subject yet. Several research works have been reported in the literature to evaluate the current technologies' capabilities to provide the required medical QoS by the telemedicine applications and point out the importance of QoS managements in telemedicine application [76-80]. In all these studies the argument was around three important QoS factors, which are the time, the bandwidth, and quality. As that it is well known in telemedicine application, medical data (especially real time data and emergency data) needs to be delivered to the remote end in a timely manner within the available network bandwidth and within the end user required quality (e.g. image quality in video streaming applications).

Recently developed mobile healthcare (M-Health) services allow healthcare professionals to monitor a mobile patient's vital signals and provide feedback to the patient anywhere and at any time. Due to the nature of current supporting mobile services platforms, m-health services are implemented with best-effort QoS. An example of a m-health system built with best effort QoS is the European project system MobiHealth [78].

All of the studies mentioned in this section considered the network centric based QoS study, where they tried to build isolated networks for medical applications only.

However the present view of medical environments is changing towards an integrated heterogeneous network scenario that can support a wide range of applications medical and non-medical applications [59]. Key factors to achieve this in a

heterogeneous environment are the ability to define the perceived QoS at the user interface level; how to relate this to underlying QoS supported within the underlying system, and how QoS-aware applications can adapt. Rather than isolating mobile systems as a special case, infrastructure and applications should be able to adapt to their environment, whatever that might be [60].

In conclusion, this work aims to introduce and study the medical QoS from the application user level prospective. In other words this work does not require users to have detailed knowledge of the resources needed and resource scheduling and allocation techniques in use. These underlying details are effectively hidden from the user. So far there is no such detailed study in the m-health environment.

In the medical video streaming in the robotic environment section above, the work in [23, 31, 35, 45] considered the issue of QoS management implicitly by adding some kind of rate controller that adapts to the environment. However none was done on mobile 3G/3.5G wireless communication environments and there was no evidence that the algorithm used provided an optimal solution that satisfies both the network conditions and the medical requirements.

Different m-health scenarios require different sets and levels of m-QoS requirements. Table 2.1 below gives some example of m-health applications and defines its important m-QoS requirements when implemented in an integrated environments [59].

The m-health applications in table 2.1 are the common applications in most m-health scenarios. The QoS metrics discussed in the table are generally ***Bandwidth, Timeliness and reliability.*** Specifically for bandwidth metrics the generated data rate of the application is considered. For timeliness metrics, the delay element is considered. And finally for reliability the packet loss element is chosen as that is the most common measurable element for reliability [60].

Remote control applications – This category includes the remote control of medical equipment, such as robotic control signals in the OTELO system. These applications require a continuous but very low bandwidth and can not tolerate delay and data loss.

Real-time critical applications – These include remote monitoring of patients physiological functions (e.g. monitoring cardiac signals). These applications require continuous small bandwidth and cannot tolerate any delay and packet loss.

Real-time noncritical applications – this category include real-time ultrasound image streaming, video conference for remote consultations, and Voice over Internet Protocol

(VOIP). These applications are delay sensitive. In terms of data loss, these applications can tolerate some data loss. However, this is a relative problem. In real-time ultrasound image streaming the tolerable data loss is less than that for ambient video conference applications. Apart from the VOIP, this type of application requires a wide bandwidth.

TABLE 2.1 – MEDICAL QOS (M-QOS) REQUIREMENTS IN M-HEALTH APPLICATIONS [59]

m-health application	Example	Medical QoS requirements		
		Data rate /Bandwidth	Delay /Timelines	Packet loss /Reliability
Real-time critical applications	-Real-time physiological monitoring	10-100 kb/s	Require low delays, < 300 msec	Cannot tolerate packet loss, ~ 10^{-6}
Real –time non-critical applications	-Medical Videoconference system (video and audio)	10 kb/s – 1 Mb/s	Require low delays, 10 msec-250 msec	Can tolerate low packet loss, < 10^{-4}
Mobile web-based medical consultation	- Patient's record access and sharing and download of medical data and files	1-10 Mb/s	Can tolerate delay, < 1sec	Cannot tolerate packet loss.
Remote control applications	- Robotic control signal (OTELO system)	<< 1 kb/s	Require low delay < 200 msec	Cannot tolerate packet loss.

Mobile web-based medical consultation – These are typically used in medical and consultation scenario and GP offices, such as web browsing, interactive access to patients' records, file sharing and download of medical images and videos. These applications require high bandwidth. Although, this type of applications can tolerate some delay, but no data loss.

Some other user QoS requirements exist in m-health applications like security and ubiquity issues, but these are out of the scope of this PhD work and further details can be found in [59].

As mentioned before, the m-health platform used in this thesis is the OTELO system. The detailed issues of m-QoS of this system are explained further in chapter 3.

2.5 Quality issues in Medical Video streaming

2.5.1 Artifacts in video streaming process

In general end-to-end transmission of video material is subject to two sources of artifacts; encoding artifacts and transmission artifacts. Encoding artifacts are mainly due to the fact that the vast majority of video compression, are based on motion-compensated discrete cosine transforms (MC-DCT) and quantisation of the resulting transform coefficients [28]. This type of artifact can be seen as blocking effects, blurring, temporal edge noise and jerky jagged motion. However, transmission artifacts are a common source of impairment of the compressed video bitstream when transmitted over a packet network. Two different types of network transmission characteristics cause transmission artifacts: packet loss and end-to-end delay. As that in video encoding technologies, such as MPEG2 and H.263, they use inter coding techniques that lead to the dependencies of the video frames. Where a loss of a macroblock may corrupt subsequent macroblocks, until the decoder can re-synchronise. Another problem arises when blocks in subsequent frames are predicted from a corrupted macroblock which will cause a temporal propagation of errors until the next intra-coded macroblock is available.

2.5.2 Medical Video Quality Measurements

Chapter 1 stated that one of the m-QoS metrics is the quality of the medical images. In general the quality of an image is an attribute with many possible definitions and interpretations. One can define the quality of an image based on the question [38]: How well does an image communicate the information required by an observer? This is called the intelligibility of the image. For example, an image used in diagnostic imaging is good if it enables an observer to make the right diagnosis (diagnostic image quality). A more technical definition of image quality relates to the question: How much does an image deviate from an ideal image of the scene? This is called the fidelity of the image (technical image quality). There are three approaches used to measure the medical image quality, that are presented briefly here [94]:

1- Simulation and statistical analysis of a specific application of the images, e.g., diagnostic accuracy in medical images measured by clinical simulation and statistical analysis. In this evaluation approach, the methodology of the Receiver Operating Characteristic (ROC) curves has dominated historically, but a variety of other approaches have been used in which radiologists may be called upon to perform various interpretive tasks. Radiologists detect and localize the disease, make measurements of various structures, and make recommendations for patient management. But the ROC method is very weak in practical applications because it is inconvenient, costly and not real time [95].

2- Subjective Measures: this measures the clarity of the image and how well it offers diagnostic information to the medical expert. This usually done by psychophysical tests or questionnaires with numerical ratings. Subjective quality of a reconstructed image can be judged in many ways. A suitably randomized set of images can be presented to experts or typical users who rate them, often on a scale of 1 to 5, where 1 is Bad and 5 is Excellent. Subsequent statistical analysis can then highlight averages, variability, and other trends in the data. Such subjective testing is also known as Mean Opinion Score (MOS) and the descriptive rating called the Diagnostic Acceptability Measure (DAM) [94]. The subjective method for image evaluation is standardized in the International Telecommunication Union - Radiocommunication (ITU-R) BT.500-11 [96]. Depending on what contextual factors influencing user perception need to be derived, three testing procedures are most commonly used. Double Stimulus Continuous Quality Scale (DSCQS) is one of these methods where the viewers are shown several pairs of video sequences, which consist of the reference and test sequences. The reference and test sequence are shown to the user twice in a random alternating fashion. Double Stimulus Impairment Scale (DSIS) is another type of subjective assessments that is similar to DSCQS but the reference sequence is always presented before the test sequence and there is no need for the pair to be shown twice. The viewers rate the second clip with reference to the first on an overall impression scale. The third way is Single Stimulus Continuous Quality Evaluation (SSCQE). This method allows the viewers to assess dynamically the quality in a continuous manner. The viewers are shown the sequence to be evaluated and they rate the instantaneous perceived quality by continuously adjusting a side slider on the DSCQS scale (from bad to excellent).

Continuous quality sores are obtained by periodically sampling the slider value. Subjective measures in general are complicated, not in real time and expensive. They require the physical availability of the medical expert and accordingly different medical experts give variable opinions on the same image. This known as inter- and intra-observer variability.

3- Objective measures measure the fidelity of an image or technical image quality. They are based on computable objective distortion measures such as Peak-Signal-to-Noise-Ratio (PSNR).

$$PSNR = 10.\log\left[\frac{255^2}{\frac{1}{NM}\sum_{i=0}^{N-1}\sum_{j=0}^{M-1}\left(x(i,j)-y(i,j)\right)^2}\right] \qquad 2.2$$

where $x(i,j)$ refers to the pixel (i,j) in the original image and $y(i,j)$ to the pixel (i,j) in the test image; both images are of size N x M.

This is well known to be an indicator of quality but is recognized to be uncorrelated with the Human perception, two images with the same PSNR may have very different appearance and errors [39, 40]. In recent years, researchers have made much progress in developing objective perceptual image quality algorithms that predict image quality closely mirroring human judgments [41]. It is generally easy for Human Visual Systems (HVS) to assess the quality of two similar images and decide on which one looks better. This issue has encouraged a group of researchers in [97, 40] to develop an objective-based quality measurement method known as Universal Image Quality (UIQ) index and its late version Structural SIMilarity (SSIM) index that proposed an alternative way to think about image quality assessment based on a new philosophy that based its assessment decision between the original and the distorted image on structural distortion difference. All these research efforts to design objective video quality measurements models have generated recent standardisation activities. Video Quality Experts Group (VQEG) and the ITU-study Group 9 (SG9) are the main bodies that work together to deal with the video quality measurements models standardisation issues [99, 100].

In conclusion video quality methods based on objective measurement approach are less complicated and less expensive and are suited to real time applications, especially if that

method considers the HVS characteristics as in the case of the SSIM index. The SSIM index implements a new philosophy in image quality measurement that is based on the concept that the main function of the human eyes is to extract structural information from the viewing field, and the human visual system is highly adapted for this purpose. Therefore, a measurement of structural distortion should be a good approximation of perceived image distortion. In this method, the quality index (Q) models any distortion as a combination of three factors:

1- Loss of correlation,
2- Mean distortion,
3- Contrast distortion.

This is defined as [97]:

$$Q = \frac{\sigma_{xy}}{\sigma_x \sigma_y} \cdot \frac{2\overline{x}\overline{y}}{(\overline{x})^2 + (\overline{y})^2} \cdot \frac{2\sigma_x \sigma_y}{\sigma_x^2 + \sigma_y^2}, \quad -1 < Q < 1 \tag{2.3}$$

Where

$$\overline{x} = \frac{1}{L}\sum_{i=1}^{L} x_i, \qquad \overline{y} = \frac{1}{L}\sum_{i=1}^{L} y_i,$$

$$\sigma_x^2 = \frac{1}{L-1}\sum_{i=1}^{L}(x_i - \overline{x})^2, \qquad \sigma_y^2 = \frac{1}{L-1}\sum_{i=1}^{L}(y_i - \overline{y})^2,$$

$$\sigma_{xy} = \frac{1}{L-1}\sum_{i=1}^{L}(x_i - \overline{x})(y_i - \overline{y}),$$

x, y and L are the original image, the test image and the number of pixels in the portion of the image under processing respectively.

This is a special case and an earlier version of SSIM called UQI. SSIM can be defined as in the following equation [40]:

$$SSIM = \frac{(2\overline{y}\overline{x} + c_{ssim\_1})(2\sigma_{xy} + c_{ssim\_2})}{(\overline{y}^2 + \overline{x}^2 + c_{ssim\_1})(\sigma_y^2 + \sigma_x^2 + c_{ssim\_2})}, \quad -1 < SSIM < 1 \tag{2.4}$$

Where c_{ssim_1} and c_{ssim_2} are constants used to calculate SSIM. The universal Quality Index (UQI) correspond to the special case of (2.4) $c_{ssim\_1} = 0$ and $c_{ssim\_2} = 0$, which produces unstable results when either $(\overline{y}^2 + \overline{x}^2)$ or $(\sigma_y^2 + \sigma_x^2)$ is very close to zero.

The dynamic range of SSIM is [-1,1]. The best value 1 is achieved if and only if y=x.

This method was used in measuring the quality of medical images in [95] in addition to other objective and subjective methods to train a neural network to develop a system to mimic radiologists' perception. However, there is not yet enough evidence about the suitability of using this model in real time applications. The work in [52] has used the SSIM quality index in addition to the PSNR quality index to test the quality

An earlier work [28] has suggested the use of objective quality measurements in determining the physical degradation of transmitted ultrasound images via an ISDN communication link. This work was inspired by the fact that there were no standards for teleultrasound image quality. The DICOM radiology image standard does not extend to video [28]. It suggested the use of Normalized Mean Square Error (NMSE), Pixel Density Histogram, Contrast Wedge Intensity plots and Fourier Spectra Analysis methods separately to measure the difference between the original and the distorted image. The result was not consistent as it depended on the image content and degree of degradation.

The work in [52] has used the SSIM quality index in addition to the PSNR quality index to check the quality of transmitting medical images in real time wireless video environment.

Chapter 3

m-QoS Issues for 3G Ultrasound Streaming

3.1 Introduction

This chapter presents the conformance of the m-QoS defined earlier with the relevant functionality and requirements of the ultrasound medical imaging acquired by the OTELO robotic system over 3G networks. An overview of a 3G communication network is described in the first section. This is followed by details of the m-QoS metrics and their functional modalities.

3.2 An Overview on (3G) Communication Network

In this section an overview on the 3G network communication will be given. Universal Mobile communication services UMTS (3G) are designed for multimedia communication that enhance the normal person-to-person communication with high quality images and video, and access to information and services on the Internet. This is due to the higher data rates and new flexible communication capabilities of third generation systems [104].

The supported downlink bit rates by UMTS are [105]:

- 144 kbits/s satellite and rural outdoor
- 384 kbits/s urban outdoor
- 2048 kbits/s indoor and low range outdoor

However for the uplink the practical bit rate achieved is in the rage of 64 kbits/s.

The overall architecture of the UMTS system is shown in figure (3.1) [37]. Functionally the UMTS network elements can be divided into three parts:

- UMTS- Terrestrial Radio Access Network UTRAN, that handles all radio-related functionality. The Access network domain or UTRAN manages specifications of the access technology of the UMTS, that is the wideband Code Division Multiple Access (W-CDMA). It controls and manages the radio

resources. The Radio Network Control (RNC) provides data link layer services and the Node B supplies the physical (radio) channel access.

- Core Network (CN), which is responsible for switching and routing calls and data connections to external networks. At the core network, UMTS reuses the (Global System for Mobile communications) / (General Packet Radio Service) GSM/GPRS network elements. The (Mobile services Switching Centre) / (Visitor location register) MSC/VLR and Gateway Mobile Switching Centre (GMSC) performs transcoding (e.g. voice coding) and bridges the cellular network to the public-switched telephone network. Serving GPRS Service Node (SGSN) and the Gateway GPRS Service Node (GGSN) functionality is similar to those of MSC/VLR and GMSC respectively. However they are typically used for Packet Switched (PS) services (e.g. Internet) services.

- User Equipment (UE), that provides the interfacing issues with the user and radio interface. The UE consists of two parts, the mobile equipment (ME) and the UMTS subscriber identity module (USIM) which holds the subscription information.

Figure 3.1 shows the relationship between the core network and the radio access networks. The UMTS standards are structured so that the internal functionality of the network elements is not specified in detail. Instead, the interfaces between the logical network elements have been defined. In the UTRAN part each Node B is responsible for connecting many end user terminals, UEs, to the UTRAN through the Uu interfaces. The lub interface connects a Node B and an RNC. The UMTS core network consists of two domains: the Circuit Switched (CS) service domain and the packet-switched service domain. These two domains are responsible for providing appropriate services to the circuit-switched traffic such as voice and the packet-switched traffic such as web and other Internet Protocol (IP)-related applications, respectively. Therefore two types of interfaces are used to connect the UTRAN and the Core Network, lu-CS and lu-PS, connect the circuit-switched service domain and the packet-switched service domain to the UTRAN, respectively.

Figure 3.1. The UMTS network architecture [37].

3.2.1 UMTS Quality of Service Support

In general, applications and services can be divided into different groups, depending on how they are considered. Like new packet-switched protocols, UMTS attempts to fulfill QoS requests from the application or the user. In UMTS four traffic classes have been identified [104]:

- Conversational
- Streaming
- Interactive, and
- Background classes.

The main distinguishing factor between these classes is how delay-sensitive the traffic is: the conversational class is meant for very delay-sensitive traffic, while the background class is the most delay-insensitive. The UMTS QoS classes are summarised in table 3.1 [104].

TABLE 3.1. UMTS QOS CLASSES [104]

Traffic class	Conversational class Real Time	Streaming class Real Time	Interactive class Best Effort	Background class Best Effort
Fundamental characteristics	- Preserve time relation (variation) between information entities of the stream - Conversational Pattern (stringent and Low delay)	- Preserve time Relation (variation) between information entities of the stream	- Request response pattern - Preserve payload content	- Destination is not expecting the data within a certain time - Preserve payload content
Example of the application	Voice	streaming video	web browsing	telemetry, emails

3.2.2 End-to-End QoS issues in the OTELO system over 3G network

The adopted communication scenario between the Expert (hospital) side and the Patient side in the OTELO system is shown in figure 3.2. The patient side is the wireless side and the Expert station is the wired side. The access technology here is thus composed of several systems: the local bearer service providing the service cellular phone user, the UMTS bearer service, and the external bearer service providing service to the wired hospital side computer user. This is lustrated in figure 3.2 as well. Without the support of the required QoS indicators by all segments of the network from end to end, one cannot claim that one has a QoS support. UMTS has its own share in providing the QoS but the end-point bearer services also need to support similar QoS indicators in order to complete the end-to-end process.

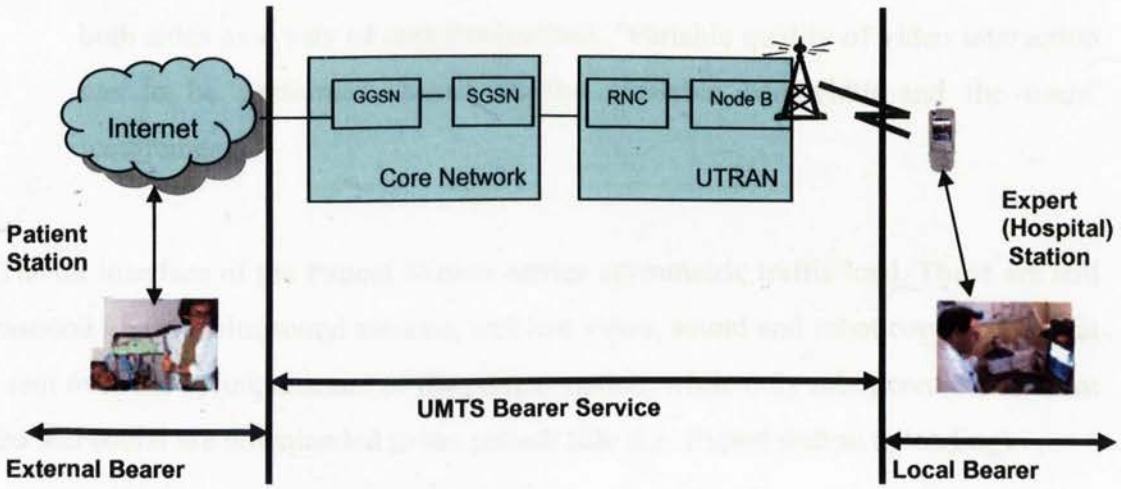

Figure 3.2. End-to-End QoS realization in the OTELO system over 3G network

3.3 3G Functional Modalities of the OTELO System

OTELO can be considered as a bandwidth-demanding data traffic advanced m-health system, with challenging classes of QoS requirements, as medical ultrasound images, robotic and other data have to be transmitted simultaneously. Such QoS requirements are summarized in Table 3.2, which is partly based on [108].

Figure 3.2 shows the general 3G connectivity of the OTELO system and the interface requirements. In this scenario, it is assumed that the OTELO Patient Station is connected to the OTELO system via the 3G network and the OTELO Expert station is connected to the OTELO system via specialist hospital LAN network.

The OTELO functional modalities require four types of medical and robotic data to be transmitted synchronously or simultaneously between the expert station and the patient station:

- Robotic real time control data associated with fictive feedback sensors data with an average data rate of 5-6 kbps in both directions (Patient-to-Expert and Expert-to-Patient).
- Ultrasound still images: this needs no real-time transmission, and is transmitted in only one direction (Patient-to-Expert station).
- Stream of ultrasound images: During the tele-ultrasonography examination, a stream of Ultrasound images must be transmitted from the patient site to the expert site. This has to be synchronized with the movement of the robot control data.
- Videoconference: Ambient video and sound have to be interacted between both sides as a way of communications. Variable quality of video interaction has to be performed, based on the available bandwidth and the users' requirements.

The air interface of the Patient Station carries asymmetric traffic load. These are still ultrasound images, ultrasound streams, ambient video, sound and robot control data that are sent over the uplink channel of the patient station, while only robot control, ambient video and sound are downloaded to the patient side (i.e. Expert station uploading).

From Table 3.2, it can be seen that for the OTELO system the most bandwidth-demanding traffic is the medical Ultrasound Streaming (US) data. For this reason, the focus of this thesis is on the transmission of US data in wireless environments. According to the communication link limitations, various scenarios can be identified with respect to the data traffic that should be sent simultaneously so as to enable the performing of the medical examination, as explained briefly in the following medical diagnostic scenario of this medical robotic system [108]:

1. During the hardware and session preparation, only voice and text messages exchange are required between both ends.
2. The medical expert remotely controls the robot (which would already be properly oriented above the patient body), according to the received ultrasound images or ambient video information alternatively. Throughout the process, the expert will be adjusting the pressure on the patient's body.
3. Through the ultrasound scanning and organs location and diagnosis, a satisfactory Ultrasound image stream transfer on real-time is needed, no ambient video is necessary.
4. After locating the area of examination, high quality still Ultrasound images transfer need to be received. This is because the data rate used for the communication link makes a difference in conjunction with the compression standards used.
5. The expert will then analyse and validate the incoming images and information clinically, in co-operation with the patient side with the help of high quality videoconferencing. Then real-time continuous communication can still be available until one end terminates the connection (more likely the patient, as the customer who needs the service).

TABLE 3.2
OTELO MEDICAL DATA REQUIREMENTS

OTELO- Medical Data	Data Description	Relevant QoS requirements			Data Flow direction, Patient-to-Expert (P-to-E) Expert-to-Patient (E-to-P)
		Bandwidth - Data Rates (Kbps)	Timelines – Delay (msec)	Reliability – Packet loss	
Still US Images	Gray Scale, CIF 352x288 Pixel - with quality 37dB	23 kbps	Can tolerate delay	non	Up-link P-to-E
Still US Images	Gray Scale, QCIF 176x144 Pixel - with quality 37 dB	7 kbps	Can tolerate delay	non	Up-link P-to-E
Stream US Images	Gray Scale, CIF 352x288 Pixel – with 7 fps and quality 35 db	86 kbps -not possible on 3G limited uplink bandwidth	----------	$\sim 1*10^{-4}$	Up-link P-to-E
Robotic Arm Data Control	100-200 Hz	5-6 kbps	100 msec	non	UP or Down Link E-to-P and P-to-E
Stream US Images	Gray Scale, QCIF 176x144 Pixel – with 5 fps and quality 36 dB	23 kbps	148 msec	$\sim 1*10^{-4}$	Up & Down P-to-E and E-to-P
Videoconference (Ambient video)	QCIF 176x144 Pixel - with 7 fps and quality 33 dB	20 kbps	250 msec	Can tolerate loss	Up & Down P-to-E and E-to-P
	CIF 352x288 Pixel – with 5 fps and quality 33 dB	35 kbps	250 msec	Can tolerate loss	

As mentioned above voice and ambient video (videoconference) is used in the OTELO system as a tool of communication between the Expert and the patient in the process of the tele-ultrasound scanning. However, due to the limited bandwidth this type of data can be transmitted before or after the transmitting of the ultrasound data.

The classification of the OTELO traffic may be mapped to the three major traffic classes presented earlier. The best-suited UMTS QoS class for video streaming is service class 'Streaming RT' which preserves the time relation (variation) between information entities of the stream. However, for medical image sequences with real-time (RT) requirements, the 'Conversational RT' class would be necessary. The OTELO system is considered for conversational pattern (stringent and low delay) and for the real-time interactions.

In this study the 3G communication link is tested using the 3G-UMTS Vodafone data service. The selected US streams were transmitted over the available 3G network data rates. The currently supported 3G-uplink bandwidth was measured as shown in figure 3.3 which shows a sample measured 3G uplink bandwidth that averages around 56 kbps for the Vodafone 3G network. This rate is specifically related to the Patient station

uplink that represents the specific communication bottleneck of this 3G wireless telemedical connectivity channel. The method used to measure the real time currently supported 3G-uplink bandwidth is by uploading a large amount of data via large files transfer using File Transfer Protocol (FTP). The Vodafone mobile connect 3G data card **(Appendix C)** was used in this experiment. The received data was monitored and analysed via Ethereal - network protocol analyzer software [112]. Then using this data the 3G-uplink bandwidth capability (B_l) was measured using the following formula [58]:

$$B_l = \frac{S_1 + S_2 + ... + S_n}{T_n} \tag{3.1}$$

Where $S_1, S_2, \ldots, S_n$ are the arrived packet size since time 1 to the current time T_n.

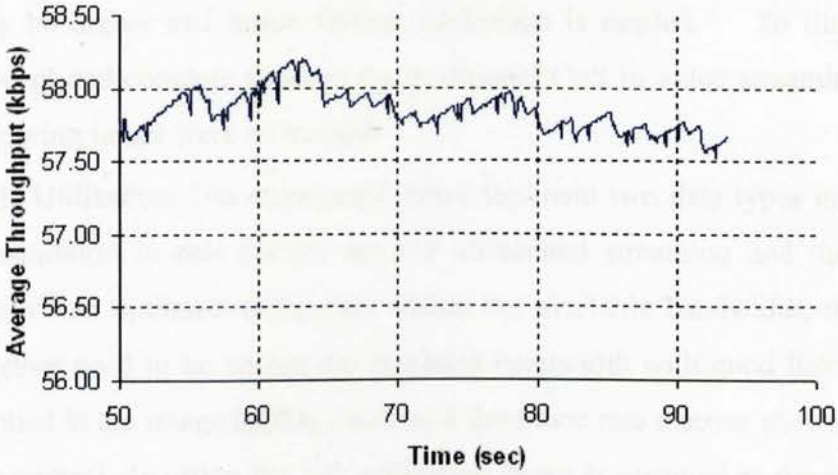

Figure 3.3. The measured 3G-uplink available bandwidth.

3.4 m-QoS for the Ultrasound Streaming

It is well known that the main quality of service metrics in video streaming environments is summarized in the Utilization, Packet Loss, End-to-End delay and Delay jitter that needs to be guaranteed by the delivering network in order to provide a satisfactory video streaming services [37]. For the concept of m-QoS introduced earlier, additional metrics and functional bounds related to the OTELO medical platform are added as explained earlier. These are summarized in table 3.3.

TABLE 3.3
MEDICAL QOS (M-QOS) FOR MOBILE ROBOTIC TELE-ULTRASONOGRAPHY

m-QoS metrics	Functional Bounds
Image quality (PSNR) – QCIF 176X144 CIF 352X288	> 36 dB > 35 dB
Structural SIMilarity (SSIM) Quality Index	> 0. 9
Frame Rate – QCIF 176X144 CIF 352X288	> 5 fps > 7 fps
End-to-End Delay	< 350 ms

The m-QoS metrics and functional bounds shown above are specified by the earlier clinical evaluation during the extensive real time implementation of the OTELO system [106-108]. However, lower frame rates are acceptable only when the probe movement is slow. On the other hand, in the case of cardiac echography, the minimum frame rate may be higher and hence further evaluation is needed. To illustrate the (m-QoS) concept and compare them to the traditional QoS in video streaming environment, the following issues were addressed:

1- Utilization: As mentioned above the main two data types needing simultaneous transmission in this system are the ultrasound streaming and the robotic data. To achieve an optimum utilization within the available bandwidth, these data combined together need to be within the available bandwidth with good link utilization. This is implied in the image quality index and the frame rate metrics shown in table 3.2. In the rate control algorithm the link utilization factor is assumed as the constraint of how far the image quality can be reduced or increased. So two image size formats are considered and the relevant frame rate to occupy the available bandwidth optimally.

2- Packet loss: Transmission impairments, such as packet loss, will impact differently on the medical experts' perception depending where the loss occurs within the video clip. Measuring the average packet loss cannot predict the impact on an expert viewer's perception since packet loss can produce a wide range of different qualities [39]. Therefore packet loss effect is implied in the image quality index metrics shown in table (3.2).

3- End-to-End delay: this is an important issue that is explicitly identified in table (3.2). Streaming video requires bounded end-to-end delay so that packets arrive at the receiver in a timely fashion to be decoded and displayed. If a video packet does not arrive on time, the play out process will pause, which is annoying to human eyes. For this robotic m-health application the end-to-end delay is the round trip response to the

Expert hand movement that controls the robotic head, in the mean time, is receiving continuous ultrasound streams in real time. Figure 3.4 shows the complete round trip path delay over Expert-Patient-Expert links.

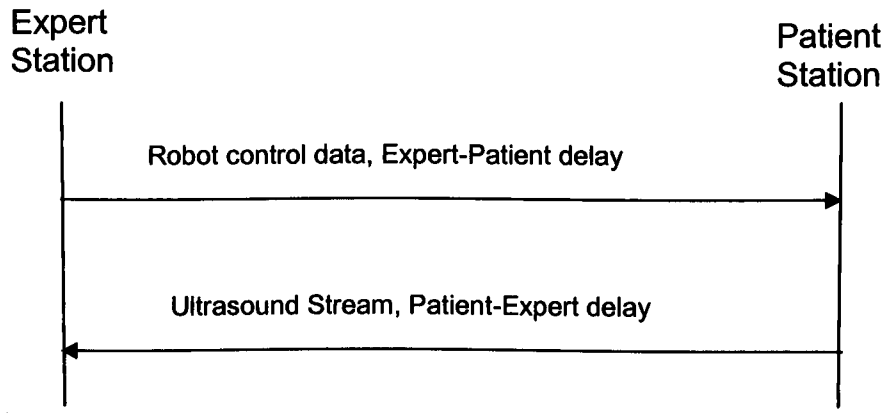

Figure 3.4 End-to-End delay measurements for OTELO system.

According to previous work on OTELO 3G performance analyses [108], the robot control data (robot payload packet size = 16 Bytes) delay from the Expert to the Patient station was shown to be in average of 100 msec and with very low standard deviation, which can be neglected. According to previous technical experiments and real medical trails of the OTELO system the recommended End-to-End delay was < 350 msec [21, 106, 107]. This means that the Ultrasound streaming delay (from the Patient station to Expert) should be < (250) msec.

3- Delay jitter: This is implicitly implied in the arriving frame rate metrics above in table 3.2. The recommended delay jitter for normal video streaming applications is within 2 sec. This is also acceptable for the current medical platform. The delay jitter effect has been taken care of by the decoder buffer as we will see in the next chapter.

Hence, we can conclude that for a typical bandwidth demanding applications a new sub-category is required in addition to the traditional wireless QoS issues to validate clinically the acceptable quality of the medical data and images received. These are summarized in table 3.4.

The QoS metrics discussed in table 3.4 are generally Bandwidth, Timeliness and reliability [60]. Table 3.4 shows the relationship between these three QoS metrics and both the m-QoS and the general wireless video streaming QoS.

TABLE 3.4 – QOS, M-QOS AND WIRELESS QOS COMPARISON

QoS	m-QoS	Wireless QoS
Reliability	Medical image quality index - QI	Packet loss
Bandwidth		Utilization
	Frame rate	
Timeliness		Delay & Delay jitter
	End-to-End delay	

3.4.1 Objective Quality Index

In order to achieve high compression for the transmission over mobile radio channels with low bit rates, it is important that both the spatial resolution and the format rate (temporal resolution) to be reduced compared to standard television pictures [112]. Therefore the image formats used were as follows:

1. Gray scale Common Intermediate Format (CIF) (352x288), which is the most common input format over the range of bit rates considered in this mobile application (which is 64 kbps for 3G and 350 kbps for High Speed Data Packet Access (HSDPA) 3.5G links).
2. Gray scale Quarter Common Intermediate Format (QCIF) (176x144), which is used as another option under the criteria of the Region of Interest (ROI). This is when the Physician at the expert side decided to select a ROI in the Ultrasound scanning and study more the case.

As mentioned in table 3.1 Quality evaluation of the ultrasound images transmitted by OTELO system, suggested that the minimum threshold for accepted medical US image quality is PSNR > 35 dB for CIF image size and >36dB for QCIF respectively.

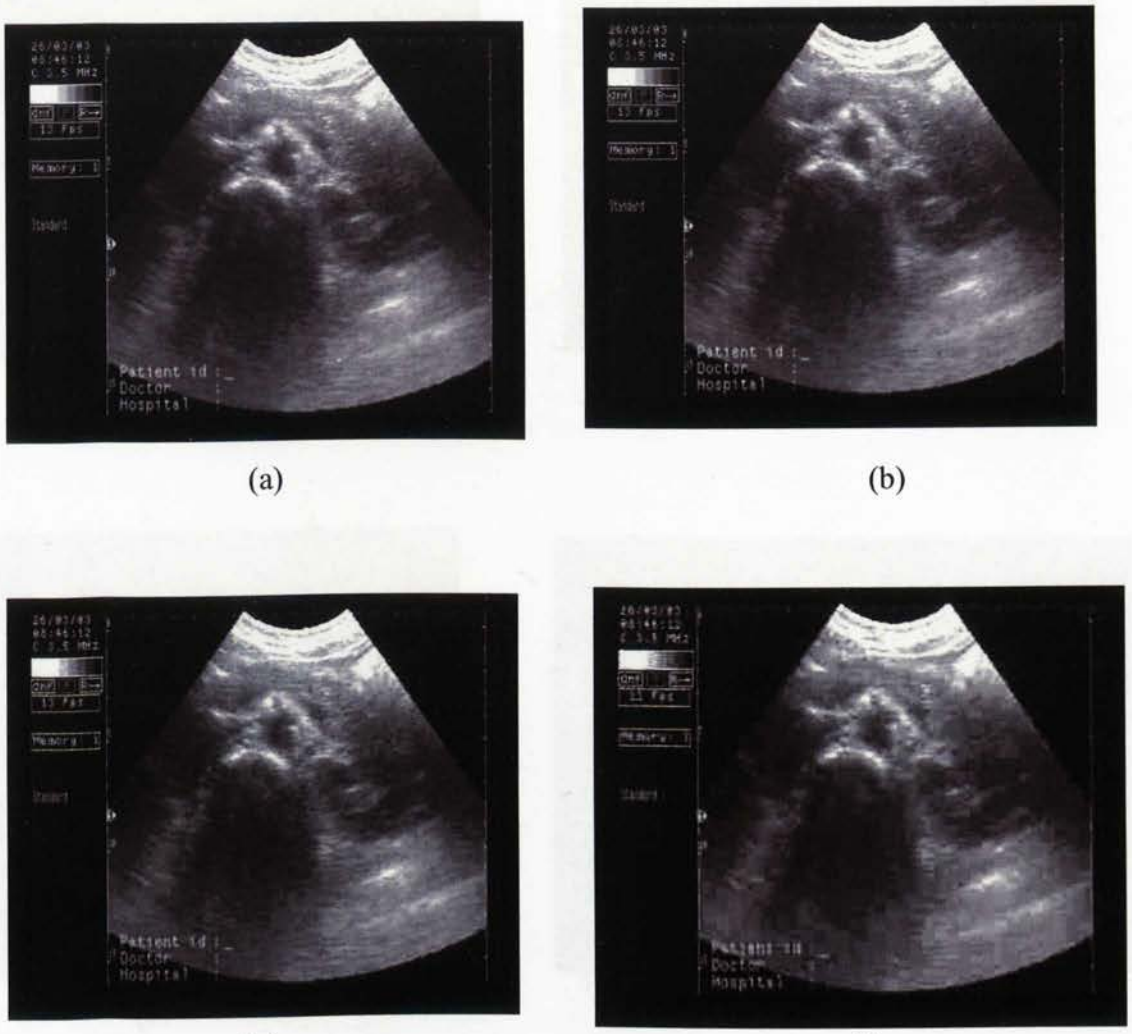

Figure 3.5. Frame 20 of ultrasound Images for abdomen, acquired by OTELO system. (a) Original , uncompressed, (b) compressed with PSNR = 38 dB, (c) compressed with PSNR = 35.1 dB and (d) compressed with PSNR = 33.6 dB.

Figure 3.5 illustrate the effect of the selected PSNR bound of 35dB on the image quality. The compression technique used was Joint Photographic Experts Group 2000 (JPEG2000), since JPEG2000 provides better compression efficiency than other well known compression techniques e.g. JPEG. Figure 3.5(c) shows a reasonable image quality with PSNR value of 35.1 dB.

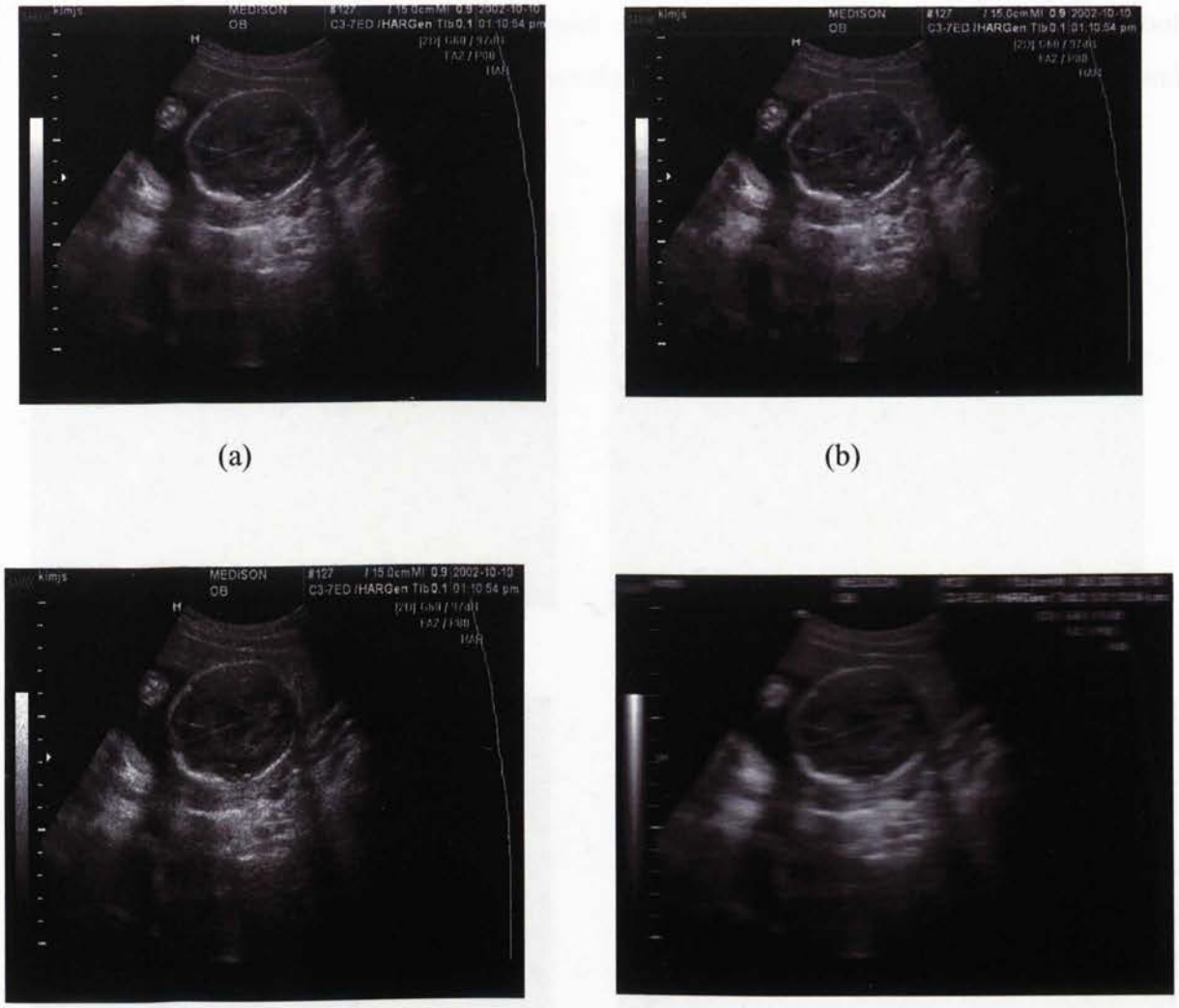

Figure 3.6. comparision of an ultrasound image with different types of distortions, all with PSNR value of 35 dB. (a) Original image (b) JPEG compressed image, SSIM = 0.75 (c) With speckle noise, SSIM = 0.85 (d) Blurred Ultrasound image, SSIM = 0.7.

However, the subjective evaluation of the compressed image is not necessarily proportional to the objective evaluation measures. Images with nearly identical PSNR value have drastically different perceptual quality. The (SSIM) quality index measurement technique had proven to be well matched to perceived visual quality [40]. Therefore the SSIM image quality index is considered in this work. Figure 3.6 shows an ultrasound image with different distortion, each adjusted to give PSNR of 35dB. The distortion factors considered here are compression, blurring effects and speckles noise effect. The (SSIM) quality index is also measured. The results show an average SSIM index for these distorted images with values less than 0.9.

However, figure 3.7 shows ultrasound images under the same type of distortion but with different values. The result shows that the value of 0.9 gives good perceptual and diagnostic image quality.

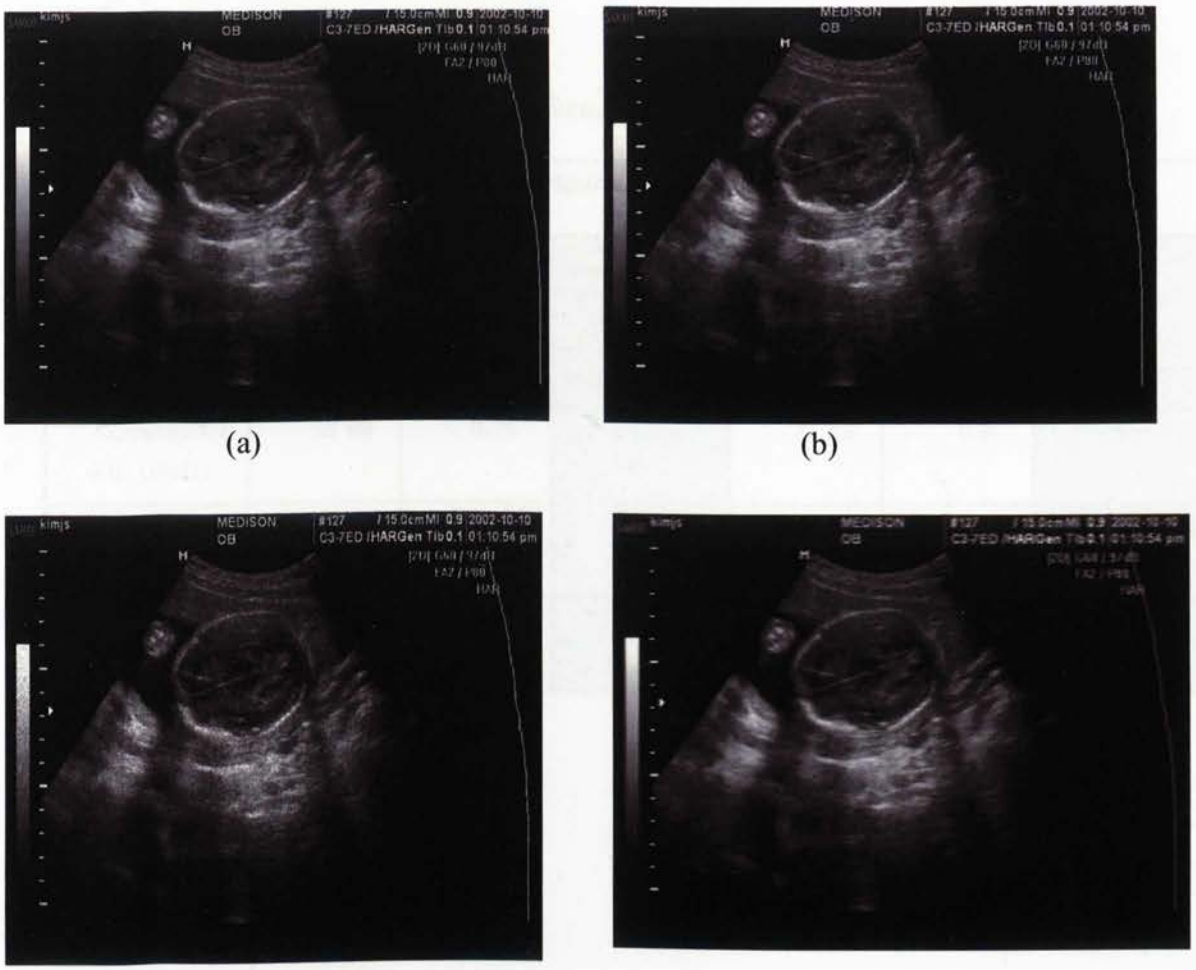

Figure 3.7. Ultrasound images with different types of distortion, all with SSIM = 0.9. (a) original, (b) Compressed with JPEG, (c) with speckle noise effect and (d) Blurred ultrasound image.

In order to validate these results of SSIM index of ~ 0.9 is an indication of a good quality medical image, subjective quality measures Mean Opinion Score (MOS) [94, 138] were used to assess the visual quality of the processed images in figures 3.6 and 3.7, in which four observers (two expert and two non-expert) were asked to evaluate the quality of the processed test.

$$MOS(k) = \frac{1}{M}\sum_{i=1}^{M} S(i,k) \tag{3.2}$$

Where S(i,k), is evaluation score of image k by viewer i,

M, number of observers

Table (3.5) summarises the comparative percentage average MOS achieved by these experiments. It is clear from this table that SSIM 0.9 attains a subjective gain in the range of 80%.

TABLE 3.5 – PERCENTAGE AVERAGE MOS FOR THE TESTED US IMAGES

	Experiment 1 – Figure 3.6			Experiment 2 – Figure 3.7		
Image Artifact	PSNR	SSIM	Subjective measures – percentage average MOS	PSNR	SSIM	Subjective measures- percentage average MOS
Compression with (JPEG)	35 dB	0.75	52%	37 dB	0.9	85%
with Speckle Noise	35 dB	0.85	80%	35.5 dB	0.9	75%
Blurred image	35 dB	0.7	45%	38 dB	0.9	80%

3.5 Summary

In this chapter m-QOS metrics in 3G ultrasound streaming environment was defined and investigated. First an overview on 3G communication network was introduced in terms of its main system blocks data rate capabilities and QoS issues. The OTELO system functional modalities and the adopted ultrasound scan scenario was demonstrated.

The m-QoS metrics for 3G ultrasound streaming in OTELO system was defined and justified. The m-QoS metrics identified in this system was ultrasound image quality in terms of PSNR and SSIM indices, the ultrasound stream frame arriving rate and the system end-to-end time delay. These metrics was defined and justified by the medical expert in addition to the theoretical and experimental approaches.

Chapter 4

Q-Learning based Ultrasound Streaming Rate Control Algorithm

4.1 Introduction

This chapter presents the proposed Q-learning ultrasound streaming rate algorithm (Q-USR) designed specifically for the robotic ultrasound streaming application previously described. In addition the performance of this algorithm will be given to show its optimization achievements. Furthermore a comparison of the performance of this system with and without the Q-USR control algorithm is given over 3G network and using H.263 video codec is given.

4.2 The Q-USR Controller structure

This section describes the Q-USR algorithm designed specifically for the current wireless ultrasound streaming application. Figure 4.1 illustrates the structure for the proposed adaptive rate control architecture. The sender is represented here as the patient (robotic) station where patient body is scanned by the OTELO system and the generated images are streamed in real time to the expert station on the other side over 3G/3.5G wireless networks.

In the OTELO environment and for 3G network connectivity, the optimal frame rate and image quality issue defined in chapter 3 cannot be attained for the following reasons:

1. Over a relatively variable and low-data rate wireless channel, the variable network conditions are not predictable from the expert station end. For example rates below 64 Kbps may lead to clinically unacceptable image artifact or require operation at low frame rates, resulting in low temporal resolution and long end-to-end delay.

2. Channel data rate availability and the congestion variation may lead to a fluctuating quality of performance above and below the required quality setting of the medical expert.

As shown in figure 4.1, the adaptation algorithm is located at the patient station, where the encoding process is performed by the video encoder and controlled by feedback information acquired from different location within the network.

The feedback information that the Q-USR controller requires are the Channel Rate (CR), the Arrival Frame Rate (AFR) and the image Quality Index (QI).

This feedback information is fed to the wireless network feedback analysis block that feeds the CR to the encoder buffer management in order to calculate the Buffer occupancy (Bo) which will be used as the state of the environment in the Q-USR controller. The AFR and the QI variables are used by the Q-USR controller block as to parameters in the cost function c(x,a) to obtain the optimal actions that will be used by the encoder to adapt the rate accordingly. The encoded image streams will pass through the encoder buffer and then be packetized and transported via the UDP transport protocol to the lower layers. This process is illustrated in figure 4.1.

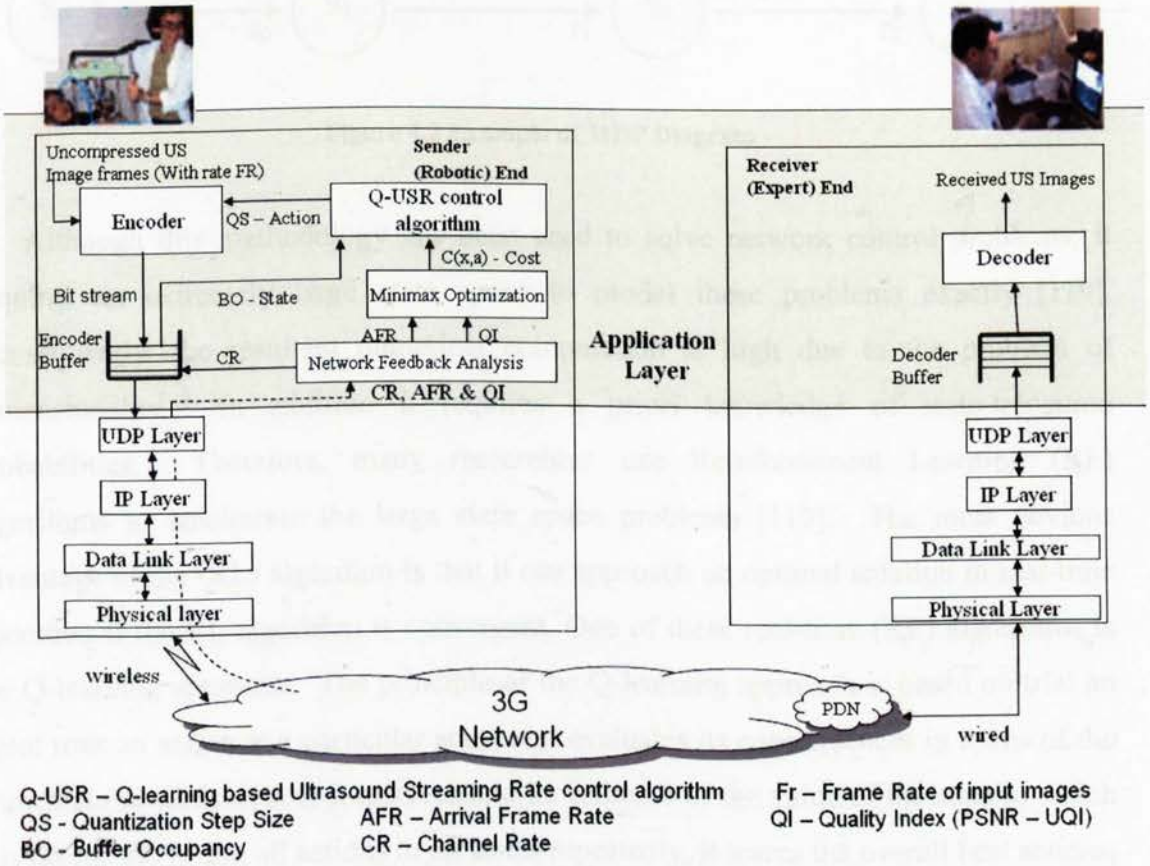

Q-USR – Q-learning based Ultrasound Streaming Rate control algorithm
QS - Quantization Step Size
BO - Buffer Occupancy
AFR – Arrival Frame Rate
CR – Channel Rate
Fr – Frame Rate of input images
QI – Quality Index (PSNR – UQI)

Figure 4.1 Q-USR control structure for ultrasound streaming.

4.3 Design of Q-USR controller

In the Q-USR algorithm, the rate controller policy is modelled as a discrete-time Markov Decision Process (MDP) problem. MDP provide a mathematical framework for modeling the decision-making process in situations where outcomes are partly random and partly under the control of the decision maker. More precisely a Markov Decision Process is a discrete time stochastic control process characterized by a set of states; in each state there are several actions from which the decision maker must choose. For example for a state (s) and an action (a), the relevant state transition function P determines the transition probabilities to the next state. The decision maker earns a reward (r) (or a penalty) for each state visited. The states of the MDP possess the Markov property. This means that if the current state of the MDP at time step k is known, transitions to a new state at time step $k + 1$ are independent of all previous states. This is illustrated in figure 4.2

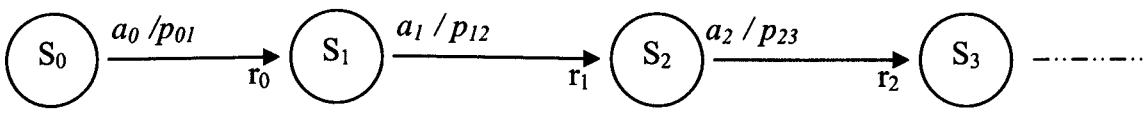

Figure 4.2 Example of MDP Diagram

Although this methodology has been used to solve network control problems; it requires an extremely large state space to model these problems exactly [119]. Consequently, the resultant numerical computation is high due to the problem of dimensionality. In addition it requires a priori knowledge of state-transition probabilities. Therefore, many researchers use Reinforcement Learning (RL) algorithms to ameliorate the large state space problems [119]. The most obvious advantage of the (RL) algorithm is that it can approach an optimal solution in real-time operation if the RL algorithm is convergent. One of these real-time (RL) algorithms is the Q-learning approach. The principle of the Q-learning approach is based on trial an agent tries an action at a particular state, and evaluates its consequences in terms of the immediate rewards or cost it receives and its estimate of the value of the state to which it is taken. By trying all actions in all states repeatedly, it learns the overall best actions, judged by long term discounted return and without knowing the state-transition behavior.

Figure 4.3 illustrate the Q-USR controller concept and specifically the interaction between the Q-learning controller and the wireless medical video streaming environment in terms of the states, the actions and relevant costs.

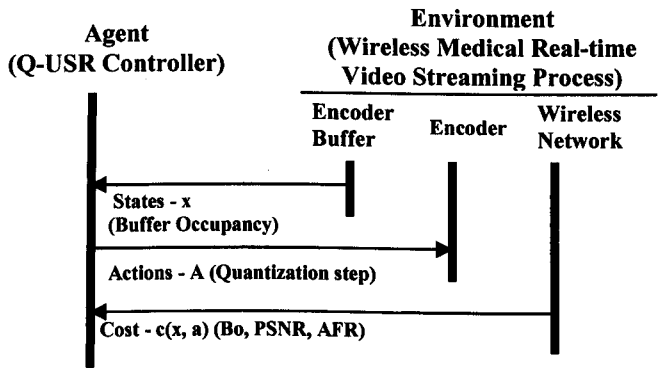

Figure 4.3 Q-USR concept model and functionality.

The Q-USR algorithm can be summarised in the following steps:

Step 1: Let us define the system state at time step k as:

$$x_k = Bo_k \tag{4.1}$$

Where Bo_k is the Buffer occupancy state at time step k.

In this particular application, (10) buffer occupancy percentage states is defined in the range of 10% to 100%. The reason for this selection is to have a small state space and consequently reduce the time for the Q-learning algorithm to converge.

Step 2: Based on the system state x_k, the video streaming rate controller will determine an *action* (A_k). The action A_k is defined as the scaling factor that affect the quantization metrics and eventually affect the quality of the compressed image. The range of values used for the scaling actor (actions A_k) is taken to be in the range of 1 to 100, where values towards 1 give high compression and hence low quality images, but values towards 100 gives low compression and high quality images. In this work (10) values of actions in the range of (10 – 100) have been chosen.

Step 3: Once the state-action pair (x, A) has been determined, an immediate cost $c(x,A)$ is defined as shown in Eq. (4.2) [42]:

$$c(x,A) = \max\left\{\begin{array}{l} \max\left\{\dfrac{\varepsilon_1 - Bo}{\omega_1},0\right\}, \\ \max\left\{\dfrac{QI - \varepsilon_2}{\omega_2},0\right\}, \\ \max\left\{\dfrac{AFR - \varepsilon_3}{\omega_3},0\right\} \end{array}\right\} \tag{4.2}$$

Where ε_1=50%, ε_2=36dB (if PSNR is used as a quality index as described in chapter 3) and ε_3=5 fps are the bounds (these values are chosen experimentally) for the buffer occupancy (Bo), the Quality index (QI) and the arrival frame rate (AFR) respectively. The ε_2 and ε_3 values were chosen to reflect the m-QoS bounds shown in Table 3.3. In this application the variables ω_1, ω_2 and ω_3 are positive weighting chosen experimentally with values 0.1, 0.5 and 10 respectively. Such values have been selected with the goal to give more weight to Bo and less weight to AFR.

The value of $c(x,A)$ assesses the immediate cost obtained by the assignment of action (A) at state x. The basic idea is to enforce an assignment of lower cost to the actions that provide less buffer occupancy, higher quality (QI) and higher arrival frame rate (AFR). Equation (4.2) represent a multiobjective optimization design problem with three objective functions that need to be satisfied. One approach to solve multiobjective design problems is to formulate the problem as a set of algebraic inequalities that must be satisfied for a successful design [42]. The design problem is expressed as

$$\phi_i(p) \le \varepsilon_i \qquad for \quad i = 1,....,n \tag{4.3}$$

Where $\phi_i(p)$: $i = 1,....,n$, are the design objective functions, where (p) denotes the design parameters. (ε_i) are real numbers representing the tolerable values of the objective functions (ϕ_i). The aim is to find the value of (p) that simultaneously satisfies the set of inequalities.

In this work the minimax method has been used in order to combine the three objective functions together as shown in Eq. 4.2 above [42]. The objective of this method is to find the best value of the controller parameters (quantization step size) that minimizes the maximum value of the cost function $c(x,A)$ as shown in Eq. 4.2.

Step 4: The objective of the learner is then to find an optimal policy *(A)* for each *(x)*, which satisfies some cumulative measure of the cost $c_k = c(x_k, A_k)$ defined in Eq. (4.2) received over time. An evaluation function, denoted by *Q(x,A)*, which is referred as the total expected discounted return (or cost) from the initial sate-action pair (*x, A*) over an infinite time horizon, is given by

$$Q(x,A) = E\left\{\sum_{k=0}^{\infty} \gamma^k c(x_k, A_k) | x_0 = x, A_0 = A)\right\} \tag{4.4}$$

Where E is the expectation operator and $0 \le \gamma < 1$ is a discount factor that is experimentally selected as $\gamma = 0.8$.

The (Q-USR) rate control algorithm is designed to determine an optimal action, denoted by A^*, which minimizes the Q-function represented in Eq. (4.4) above. The minimization of the Q-function represents the fulfillment of the m-QoS requirements defined earlier. Based on the Bellman's theory in Dynamic Programming (Bellman & Dreyfus, 1962) cited in [36], there is at least one optimal policy that satisfies the minimization of the Q-function represented in (4.4), which is $Q^*(x,A)$.

Hence, Eq. (4.4) can be re-written as:

$$Q^*(x,A) = C(x,A) + \gamma \sum_y P_{xy}(A) \min_B (Q^*(y,B)) \tag{4.5}$$

Where $C(x,A) = E\{c(x,A)\}$.

Eq. (4.5) indicates that the Q function of the current state-action pair can be represented in terms of the expected immediate cost of the current state-action pair (C(*x,A*)) and the minimum Q-function of the next state y and action B. $P_{xy}(A)$ is the state transition probability from state x with action A to the next state y.

Since it is difficult to find the immediate cost C(x,A) and the state transition probability $P_{xy}(A)$ to solve equation (4.5). The Q-learning approach, allows the optimal rate control to be achieved without *a priori* knowledge of C(x,A) and $P_{xy}(A)$ [36]. To find the optimal $Q^*(x,A)$, the Q-USR algorithm computes the values of (Q) in a recursive method using available information (x, A, c(x,A)), where x is the current

states, and A and c(x,A) are the action for current state and its immediate cost of the state-action pair, respectively. The Q-learning process searches for $Q^*(x,A)$ in a recursive manner using available information. The Q-learning rule is defined as:

$$Q(x,A)=\begin{cases} Q(x,A)+\alpha\Delta Q(x,A) & if\ A=A^* \\ Q(x,A) & Otherwise \end{cases} \tag{4.6}$$

where α is the learning rate $0 \le \alpha \le 1$ (α in this work is chosen to be 0.5).

And

$$\Delta Q(x,A^*)=\{c(x,A^*)+\gamma \min_B Q((y,B)\}-Q(x,A^*) \tag{4.7}$$

Since only one state-action pair is chosen for evaluation in each learning epoch, for the Q-learning rule, only the Q value of the chosen action pair is updated, while others are kept unchanged. In (4.7) the operation of $\min_B Q[(y,B)]$ is executed by comparing the Q values of all the possible action candidates for state (y) and then choosing the desired action (B) with minimal (Q) value.

4.4 Buffer occupancy measurement

As explained in section 4.3, the Q-USR controller represents the system states as the encoder Buffer Occupancy (Bo) state. The encoder buffer model used here to measure the Bo(t) at time t, is based on the following Equation, as given in [116]:

$$Bo=\frac{Fs-(Cr/Fr)}{Bs}+Bo \tag{4.8}$$

Where *Fs* and *Bo* are the frame size and the buffer occupancy respectively. *Cr* and *Fr* are the channel and the frame rates respectively. The buffer size (Bs) is assumed here to be 2 frame sizes. That is for example, if the channel rate is Cr = 128kbits/s and frame rate of 15f/s, the mean number of bits allocated per frame are 8,533.33 bits then the selected buffer size will be 17,066.66 bits. Figure 4.4 shows the results of the arrived frame delay achieved in streaming Motion-JPEG (M-JPEG) ultrasound images via system structure scenario shown in figure 4.1. The image selected was QCIF

(176x144). From the experimental results one may conclude that the maximum delay is less than 1 sec. Therefore the selected 2 frame size buffer size is adequate for this situation.

In this work the frames are displayed as they arrive according to the channel rate condition. This means that the decoding buffer is implemented in such a way that it waits for all bits corresponding to a given frame to arrive and be present in time for decoding.

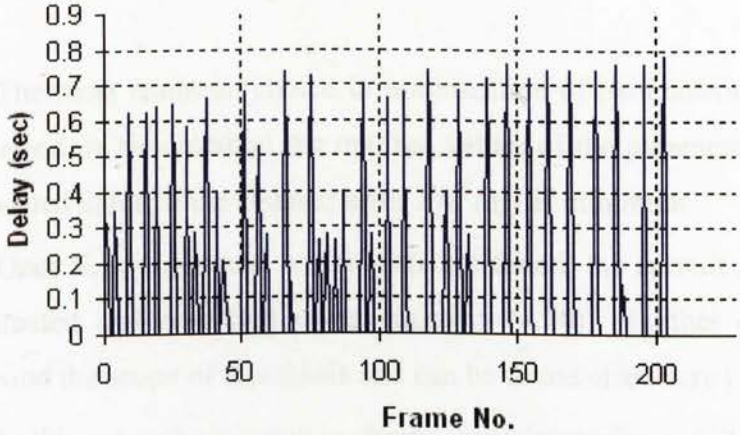

Figure 4.4 Arrived Frame delay of M-JPEG streaming of QCIF Ultrasound images over real time 3G uplink bandwidth.

4.4.1 Available Bandwidth Estimation

It is well known that monitoring the available bandwidth in a wireless application is important especially in the current application. As that monitoring the loss rate is not sufficient due to the heterogeneity of the network links. For example, if the loss is due to congestion, video quality can then be decreased whereas if the loss is due to link error, no such action is necessary. Moreover, in video streaming applications, such estimates can be used to determine the new video rate if the quality is to be increased.

As mentioned in chapter 2 the method used here to measure the available bandwidth is based on the Linear Predictive coding approach (LPC) [123]. LPC is mostly used in audio signal processing and speech processing for representing the spectral envelope of a digital signal of speech in compressed form, using the information of a linear predictive model.

The basic concept is to model the available bandwidth as follows:

$$\bar{x}(n) = -\sum_{i-1}^{p} a_i x(n-i) \tag{4.9}$$

where $\bar{x}(n)$ is the predicted available bandwidth value, $x(n - i)$ is the previous observed available bandwidth values, p is the order of the prediction polynomial, and a_i the predictor coefficient. The error generated by this estimate is given as:

$$e(n) = x(n) - \bar{x}(n) \tag{4.10}$$

Where $x(n)$ is the true signal value.

The most common choice in optimization of parameters a_i is the root mean square criterion. In this method the optimal values of the parameters a_i is found such that the expected value of the squared error $E[e^2(n)]$ is minimum.

Once the polynomial coefficients are found, the current available bandwidth can be estimated and predicted using equation (4.10). Further details of this method are beyond the scope of this thesis and can be found elsewhere [123].

In this work the p value is chosen experimentally as (12), since this represented the best result, in terms of minimum error $E[e^2(n)]$. Figure 4.5 shows the comparative performance of the estimated available bandwidth.

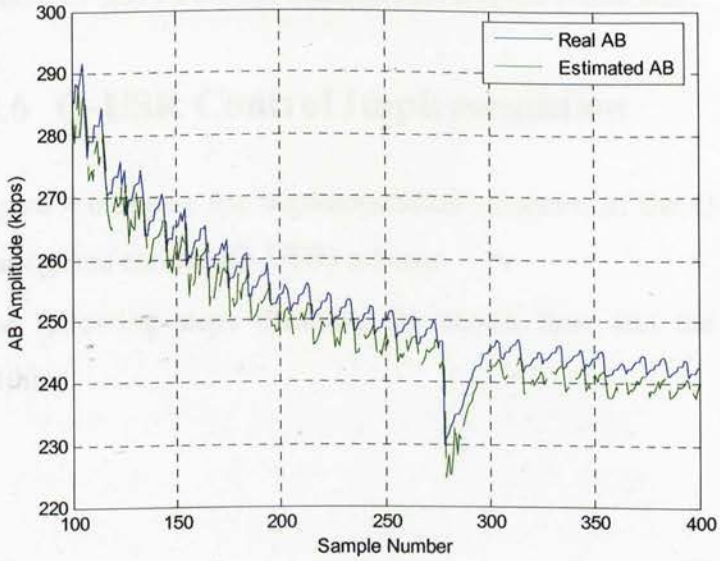

Figure 4.5. Comparative performance of the estimated Available Bandwidth (AB) using LPC and the real Available bandwidth.

4.5 Quality Index Estimation and Arrival Frame Rate Estimation

The quality index is estimated at the sender by comparing the processed image frame (decompress the image at the sender) with the image frame before compression. The Quality index used here is PSNR indicator. If one assumes that there is some sort of error concealment technique applied at the receiver that can detect and fix the error caused by wireless transmission on the damaged received images. However SSIM index can be used as well, the technique and software used to calculate the SSIM is as in [40].

A similar technique used by [114] is another option that can be used to measure the received image quality based on non-reference techniques where there is no need for the image before transmission to be available for quality measurement and comparison. This value of the received image quality can be fed back to the sender and by using some sort of modeling the current image quality can be predicted based on the quality measures of the previous images and hence the rate control algorithm can be modified accordingly. However, such option can be pursued in future work.

The arrival frame rate estimation is achieved using the following equation:

$$AFR = Cr / Fs \tag{4.11}$$

Where Cr and Fs are the channel rate and the frame size.

4.6 Q-USR Control Implementation

Figure 4.6 shows the implementation structure of the Q-learning-based Ultrasound streaming rate control (Q-USR) scheme.

The following steps illustrate the action flow and the sequences of the Q-USR algorithm.

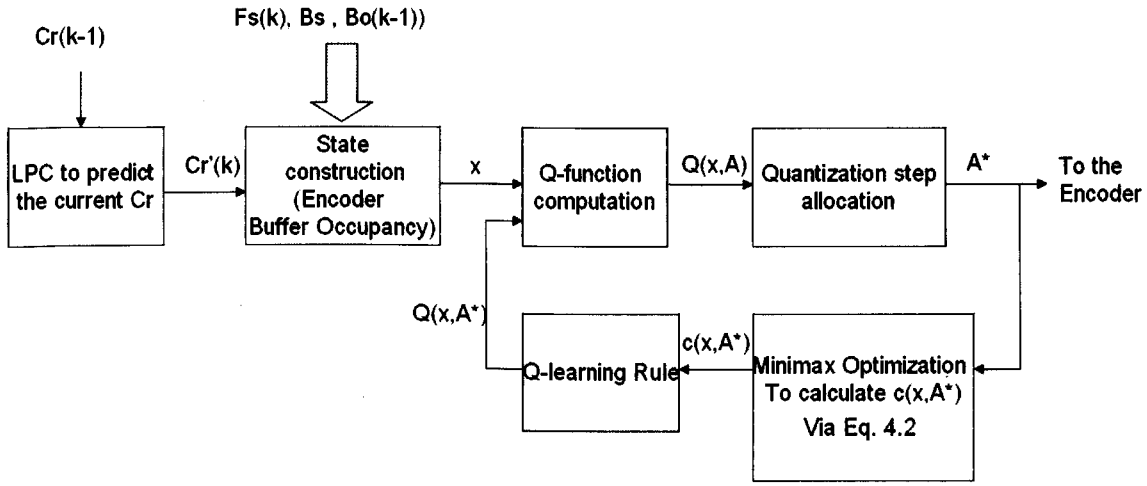

Figure 4.6 Implementation steps of the Q-USR algorithm.

1. **State-Action Construction**

   Construct the current state $x_k = Bo_k$ and find a set of all possible actions for state x, denoted by A(x).

2. **Q-Value Computation**

   For the set of state-action pairs {(x,A)| AЄA(x)}, compute the respective Q(x,A) values. This is a raw in the Q matrix, the raw for state x and a number of actions (columns).

3. **Quantization Step Allocation**

   Determine the optimal action A^* such that the value of $Q(x, A^*)$ is minimum, i.e., $Q(x, A^*) = \underset{A \in A(x)}{Min}[Q(x, A)]$.

4. **Q-Value Update**

   Observe the immediate cost $c(x,A^*)$ and use the Q-learning rule (4.6) to adjust the values of Q(x,A). Since only one action pair is chosen for evaluation in each learning iteration, for the Q-learning rule, only the (Q) value of the chosen action pair is updated, while others are kept unchanged. Also in 4.6, the operation of $\underset{B}{Min}[Q(x, B)]$ is executed by comparing the (Q) values of all the possible action candidates for state y and then choosing the desired action B with minimal Q value.

4.6.1 Parameter Initialisation

Before the Q-USR control is performed for the online operation, it is necessary to assign a proper set of initial values. An appropriate initialization can provide a good relationship between the input parameters and the decision output for an event at the beginning of system operation such that the transient period of the Q-learning procedure would be short. In this work the initial values for the Q matrix depends on the channel bit rate (3G/3.5G) and the encoder type (M-JPEG or H.263, H264 codec) used. For worst case scenario the Q-matrix is initialized offline by assuming the channel rate to be less than 50 kbps (< 3G uplink channel rate) and the encoder type to be M-JPEG (only intra-frames (I)). For the states-action values and as mentioned in section 4.2 there are 10 buffer occupancy states ranging from 1 to 10 in equal steps of 1 and 10 quantization steps in the range of 10 to 100 in steps of 10. The image size is QCIF (176x144) and the buffer size is 2 frame size. For this offline setting the initial Q-matrix was set to zero value before running the Q-USR control algorithm.

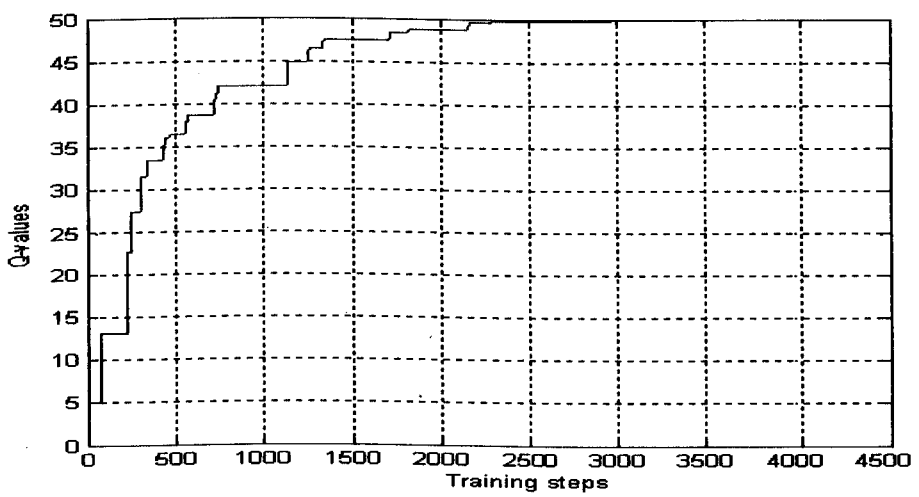

Figure 4.7 The learning curve

Figure 4.7 shows the performance improvement during the training phase, the final control policy is obtained after 2300 learning steps.

The achieved Q-matrix for this offline setting is shown in figure 4.8:

First minimum Q value at state 4

Actions [Quantization step {1(10) to 10(100)}]

First minimum Q value at state 1

	1	2	3	4	5	6	7	8	9	10
1	134	80	50	50	50	50	50	50	50	50
2	116	70	50	50	50	50	50	50	50	50
3	98	60	50	50	50	50	50	50	50	50
4	80	50	50	50	50	50	50	50	50	50
5	70	50	50	50	50	50	50	50	50	50
6	60	50	50	50	50	50	50	50	50	50
7	50	50	50	50	50	50	50	50	50	50
8	50	50	50	50	50	50	50	50	50	50
9	50	50	50	50	50	50	50	50	50	50
10	50	50	50	50	50	50	50	50	50	50

States [Buffer Occupancy {1(10%) to 10(100%)}]

Figure 4.8 Sample of Q-matrix after convergence

4.6.2 Initial Performance Evaluation

In order to illustrate the optimization issue of the Q-USR algorithm in selecting the optimum quantization step that satisfies the required QoS metrics described in (Eq. 4.2). Figure 4.9(a) shows that at minimum cost we have a quantization step size of value 30 and by applying this value to the M-JPEG encoder it achieves an arrival frame rate of 3.75 fps figure 4.9(d), quality of 32.5 dB of PSNR figure 4.9(c) and still within the chosen buffer Occupancy of 50% figure 4.9(b). However, the achieved PSNR is not ~ 35dB. This can be fixed by modifying the weighting values in equation 4.2 to trade some of the arrival frame rate achieved (3.75 fps) to get better PSNR (~35dB).

The achieved PSNR (32 dB) and frame rate (3.75 f/s) are lower than the m-QoS required for a medically approved tele-ultrasonography, as shown before in table (3.3). This due to the limitation in M-JPEG optimization performance. The M-JPEG encodes video frame by frame (intra compression I-frames only) and has no motion compensation (inter-frames (P & B) and hence gives larger frame sizes after compression and accordingly the generated data rate is high. For example for this case with a PSNR of 32.5dB and AFR of 3.75 f/s the generated data rate is 63.75 kbps.

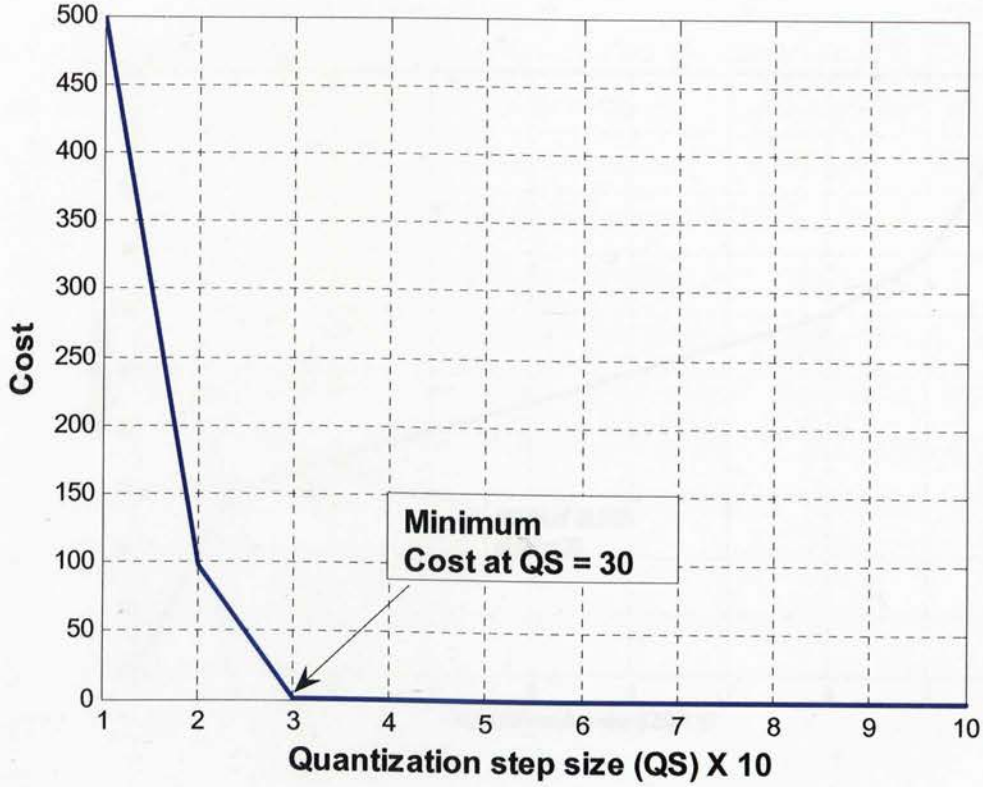
Cost
500
450
400
350
300
250
200
150
100
50
0
1
2
3
4
5
6
7
8
9
10
Minimum
Cost at QS = 30
Quantization step size (QS) X 10

-a-

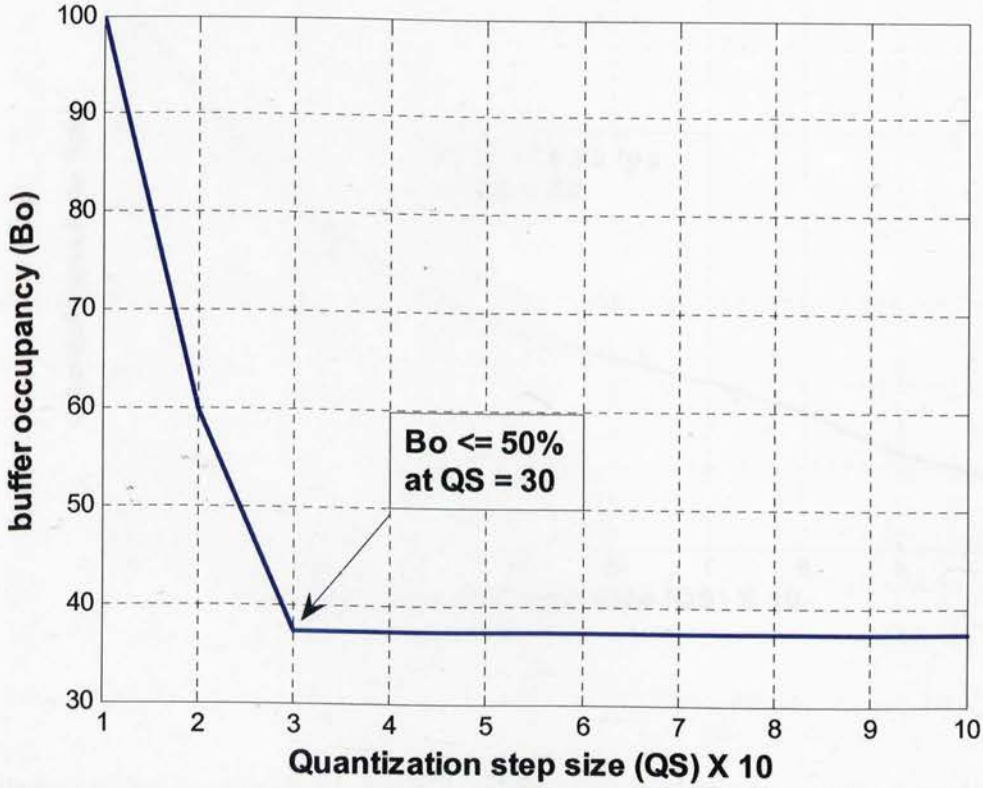
buffer occupancy (Bo)
100
90
80
70
60
50
40
30
1
2
3
4
5
6
7
8
9
10
Bo <= 50%
at QS = 30
Quantization step size (QS) X 10

-b-

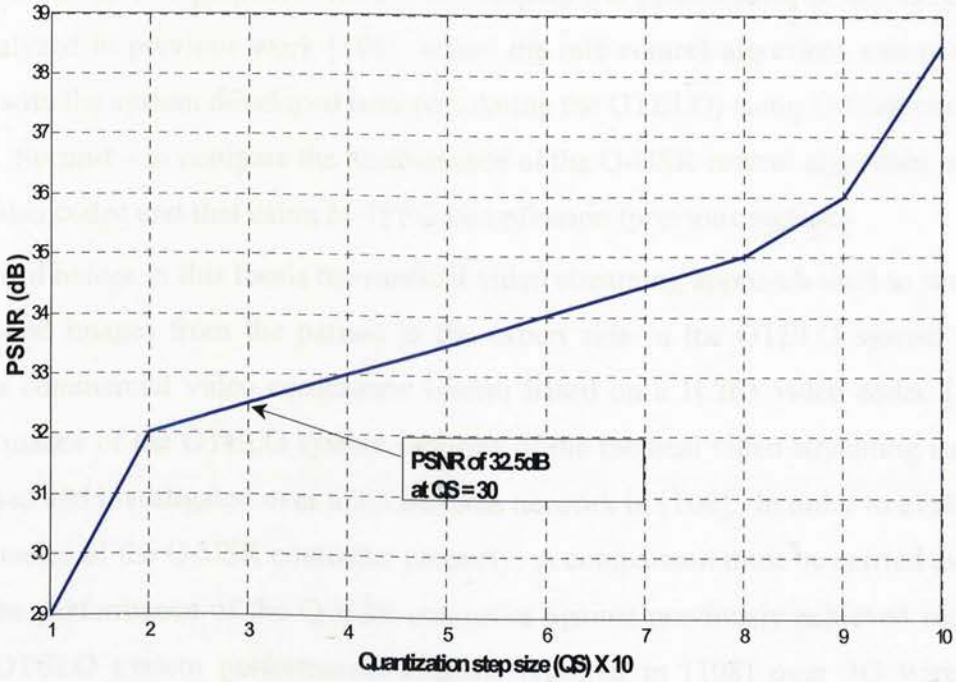

-c-

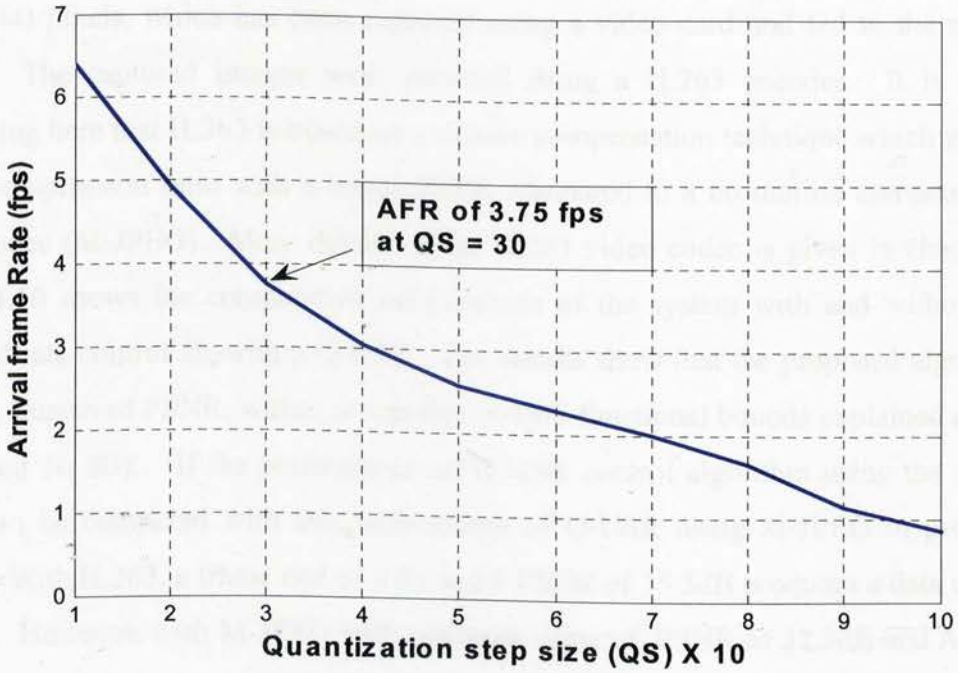

-d-

Figure 4.9 Cost –a-, Buffer Occupancy –b-, PSNR –c- and Arrival frame rate –d- against the Quantization step size (QS) for M-JPEG video streaming over simulated 3G communication link of 64 kbps data rate.

4.6.3 Performance analysis of Q-USR controller over 3G connectivity

This section serves two purposes: **first** – to compare the performance of the OTELO system analyzed in previous work [108], where the rate control algorithm was not Q-USR, and with the system developed here (emulating the OTELO) using Q-USR control algorithm. **Second** – to compare the performance of the Q-USR control algorithm using a H.263 video codec and that using M-JPEG compression (previous section).

As mentioned before in this thesis the medical video streaming approach used to stream the ultrasound images from the patient to the expert side in the OTELO system was based on a commercial video conference system based on a H.263 video codec [46]. The performance of the OTELO system in terms of the medical video streaming issues was analysed and investigated over a 3G wireless network in [108]. In order to evaluate the performance of the Q-USR controller properly. A comparison must be carried out to compare the performance of the Q-USR controller against previously achieved results with the OTELO system performance analysis reported in [108] over 3G wireless network.

The ultrasound scanner data stream used is at a rate of 13 fps and resolutions of QCIF (176X144) pixels, which has been captured using a video card and fed to the patient station. The captured images were encoded using a H.263 encoder. It is worth mentioning here that H.263 is based on a motion compensation technique which gives a higher compression ratio with a better PSNR compared to a no motion compensation based codec (M-JPEG). More details of the H.263 video codec is given in chapter 5. Figure 4.10 shows the comparative performance of the system with and without the proposed rate control algorithm Q-USR. The results show that the proposed algorithm achieves improved PSNR, within acceptable m-QoS functional bounds explained earlier (5 fps and 36 dB). If the performance of Q-USR control algorithm using the H.263 codec can be compared with the performance of Q-USR using M-JPEG in previous section. With H.263, a frame rate of 5 f/s and a PSNR of 35.5dB produces a data rate of 37 kbps. However, with M-JPEG with optimum value of PSNR of 32.5dB and AFR of 3.75 the generated data rate is 63.75 kbp. This due to the fact that the H.263 compression is based on motion compensation which produces in average smaller compressed frame sizes.

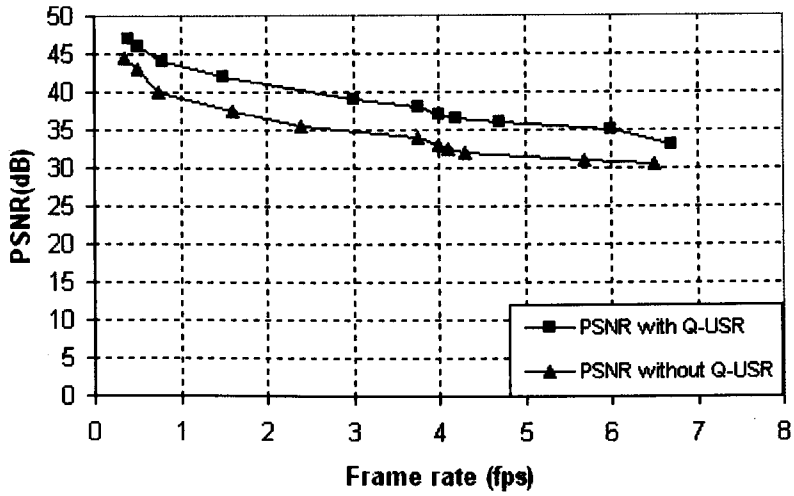

Figure 4.10 Comparative performance of the received ultrasound images PSNR as a function of the arrival frame rate with and without the Q-USR control algorithm.

The implementation and experimental set up issues of the overall Q-USR system is explained in chapter 5.

4.7 Summary

This chapter presented the proposed Q-learning ultrasound streaming rate algorithm (Q-USR). First an overview of the end-to-end wireless ultrasound streaming system building block was given. Then an initial performance of this algorithm was given to show its optimization achievements. Further more a comparison in the performance of this system with and without the Q-USR control algorithm was given over 3G network and using H.263 video codec. The results show a noticeable gain in the PSNR value when the Q-USR control algorithm is used.

Chapter 5

Implementation and Experimental Issues

5.1 Introduction

This chapter describes the experimental setup and implementation issues of the Q-USR controller for medical video streaming in robotic tele-ultrasonography system. The chapter describes both simulation tools used and the emulation system representing the OTELO functionality.

5.2 Experimental Set-up.

Due to the non-availability of the real-robotic system during the period of the study experimental set-up is designed to emulate the performance of the robotic system and the ultrasound streaming functions. Figure 5.1 shows the experimental setup of the system and the emulation of the ultrasound streaming system. The system is implemented based on the client-server software design architecture. The server represents the patient side of the OTELO system and the client side represents the expert side of the OTELO system. The focus of this work is on the wireless video streaming of the ultrasound images, the client-server system represents the real time video streaming process of the ultrasound images. In order to reflect the OTELO scanning scenario mentioned in chapter 3, robotic control data needs to be simulated here and to be sent as extra traffic in both link directions. As shown in figure 5.1 the patient station is implemented on a laptop PC where the ultrasound scanner machine (**Appendix A**) is connected via an Analogue-to-Digital converter (ADC) (**Appendix B**). The patient station captures the ultrasound images via a USB connection, processes the data (compressing it) and transmits it over a 3G/3.5G wireless link (via Vodafone data card modem (**Appendices C&D**)). This information traverses the 3G/3.5G network and then via the Internet and wired network it is delivered to the hospital (expert) station. The hospital (expert) station is the client side where this medical information is delivered. At the patient station an artificial phantom was used to emulate the human

body. The experiments were done at the MINT Centre.

The software used for the client-Server system introduced above is designed and implemented based on previous work by [117]. The software has been modified in order to:

- Deal with the transmission of different data types (ultrasound streaming and robotic control) and controls (network condition monitoring).
- Implement the ultrasound image acquisition module
- Allow the system to deal with different video coding techniques
- Implement the rate control algorithm
- Implement the packetization technique for the UDP packets
- Implement the Network monitoring techniques in terms of bandwidth estimation.

The software language used in this work is based on a commercial development platform – LabVIEW® for Windows [115], that has easy and fast developments capabilities, C language and MATLAB® [120]. LabVIEW (**Lab**oratory **V**irtual **I**nstrumentation **E**ngineering **W**orkbench) is a platform and development environment for a visual programming language from National Instruments (**Appendix E**). In LabVIEW, a user interface can be built by using a set of tools and objects. The user interface is known as the front panel. The appropriate code using graphical representations of functions can be added to control the front panel objects. For the communication transport protocols TCP and UDP sockets have been used appropriately depending on the transferred media type.

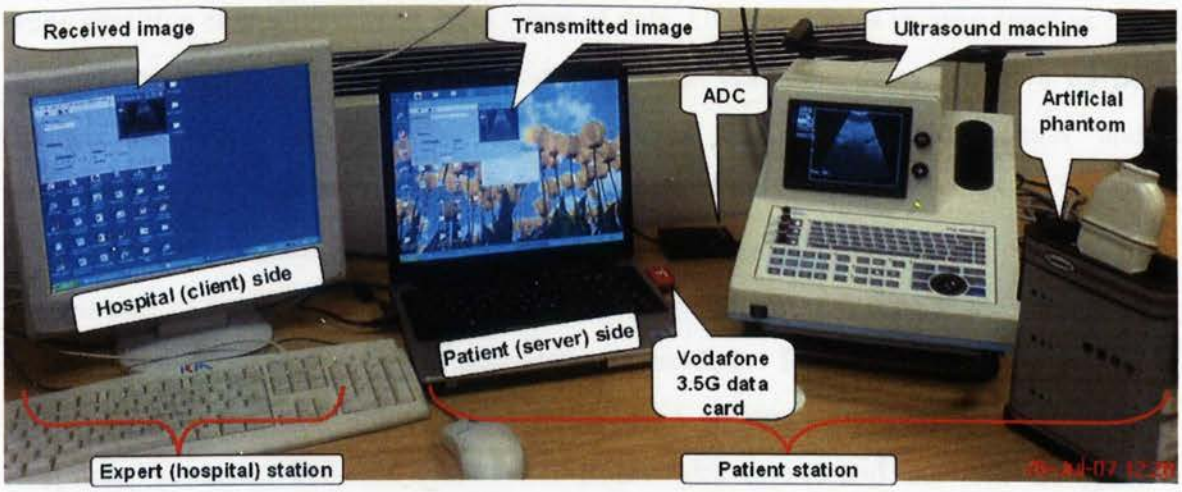

Figure 5.1 3G/3.5G Wireless experimental & Simulation Setup.

C Programming language was used to implement the Q-USR control algorithm. C language programs can easily be integrated with LabVEIW. At the early stages of this work MATLAB software was used to simulate the functionality of the Q-USR algorithm. MATLAB was also used to implement the estimation process of the available bandwidth that includes the implementation of the LPC method, as discussed in section 4.4.1.

5.2.1 Transmission Protocols and Packitization issues

Table 5.1 shows the medical data and the control flow transmitted and received in this system. These are: the ultrasound streams, the robotic control data and the network monitoring control.

TABLE 5.1 MEDICAL/ROBOTIC DATA AND THEIR CORRESPONDING PROTOCOLS

Data Type	Transmission protocol	Flow
Robotic control data	UDP/IP	Patient to expert station
Ultrasound streaming	UDP/IP + Congestion control arrangement (Q-USR)	Patient to expert station
Network monitoring control data	TCP/IP	Expert to patient station

For the patient to expert direction, which is the uplink side of the mobile communication, there are two types of data, the ultrasound streaming and the robotic control data. These two types of data need to be considered in parallel. Due to the delay sensitive characteristics of these types of data, UDP protocols is considered as the transport protocol. The TCP is unsuitable for such real time delay sensitive traffic because of the congestion control mechanisms that include slow starts and retransmissions, which bring extra delays to this type of data traffic.

At network level the IP protocol does not provide any guarantee for the delivery of packets due to the best-effort service of the IP protocol. In real time video streaming application some transport layer mechanism is needed. The most popular transport protocol-layer used for such purposes is the IETF (Internet Engineering Task force) Real-time Transport Protocol (RTP) RTP provides end-to-end network transport functions suitable for real-time data transmission. These functions include payload type

identification, sequence numbering, timestamping and delivery monitoring. Therefore, video frames are segmented and encapsulated into RTP packets, which are then embodied in the packet structure of the underlying protocols, namely UDP and IP.

However in this work and for the optimized ultrasound streaming packets the Q-USR control algorithm (as discussed in chapter 4) was used on top of the UDP/IP protocol as the congestion control layer. For the Robotic control data the UDP/IP protocol was chosen for its small generated traffic. Packet loss on the robotic control could effect the mechanical functionality of the robotic control system, but previous work on the OTELO system with an uplink of (64Kbps, in case of 3G communication link) had shown the reliable functioning of the robotic system in the patient station with the minimal packet loss of (< 0.5%) [58]. Therefore no congestion control was used for transmitting of the robotic control data in this work.

For the network monitoring control data TCP/IP protocol was used in order to provide reliable delivery of the control information.

(i) TCP and UDP in LabVIEW Implementation

TCP is a connection-based protocol, which means that sites must establish a connection before transferring data. A connection is initiated by waiting for an incoming connection or by actively seeking a connection with a specified address. In establishing TCP connections, the following issues needed to be addressed [115].

- The TCP Open Connection function is used to establish a connection with a specific address and port. If the connection is successful, the function returns a network connection refnum that uniquely identifies that connection. This connection refnum is used to refer to the connection in subsequent Virtual Instrument (VI) calls. The TCP Listen VI is used to create a listener and wait for an accepted TCP connection at a specified port. If the connection is successful, the VI returns a connection refnum, the address, and the port of the remote TCP client.
- The TCP Read function and the TCP Write function are established.
- Use of the TCP Close connection function to close the connection to the remote application.

The following set-up functions were allocated for the UDP connectivity [115]:

- UDP open function - The UDP Open function was used to open a UDP socket on a port. The UDP Open function returns a network connection refnum that uniquely identifies the UDP socket. This connection refnum was used to refer to this socket in subsequent UDP functions (e.g. read, write and close UDP).
- UDP write/read function - The UDP Write function was used to send data to a destination, and the UDP Read function used to read that data. Each write operation requires a destination address and port. Each read operation contains the source address and port. UDP preserves the datagram bytes specified for each command sent.
- UDP close function.

(ii) UDP Packetization Issues

At the stage of UDP packetization each encoded ultrasound frame was divided into a number of UDP packets. Each UDP packet had a header size of 42 Bytes. Depending on the video codec used, the choice of the packet size in video streaming communication is a challenging issue [118]. Choosing a small UDP packet size means generating more packets per frame and hence larger frame size due to the added header of 42 Bytes and error control redundancy. On the other hand, choosing large packet size is not feasible in wireless communication, as those packets can be dropped if the wireless link suffers fading or mobility error. When the packet size is large, dropping a packet means losing frame information that will affect the decoding process.

In 3G wireless communication, one of the uplink physical channels used to transmit data is the Dedicated Channel (DCH). DCH is a bi-directional channel with both uplink and downlink connections. It can have bit rates from a few kbps to 384 kbps depending on the maximum link power and the cell capacity. However the setting up time to select a DCH channel for transmission can take a long setting up time. Therefore other transmission channels are used for example Forward Access Channel (FACH) and Random Access Channel (RACH) that require less set-up time but can carry lower bit rate. Choosing between theses channel (DCH, RACH/FACH) depends on the packet scheduler buffer threshold in the Medium Access Control (MAC) layer. If the packet size is low then RACH/FACH is used. Otherwise DCH is used. Figure 5.2 illustrates an algorithm for selecting the transport channel and its bit rate, details of this algorithm

can be found elsewhere [104]. According to [104] the recommended packet size to use in DCH is in the range of (128-512) Bytes.

Experimentally in this work, using the packet size range above, it was found that the best reliable connectivity in this application can be achieved by choosing a packet size of 300 Bytes.

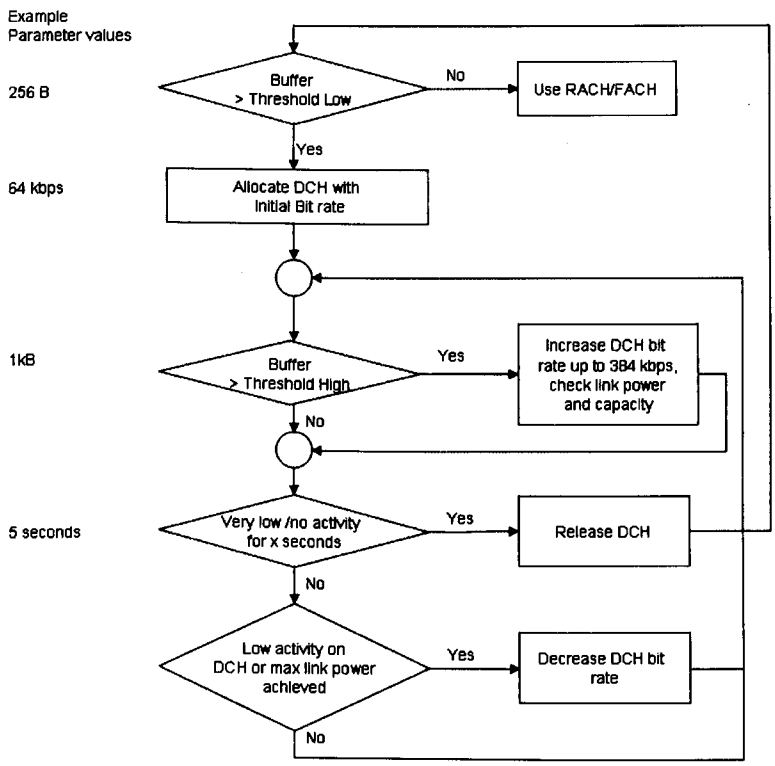

Figure 5.2 DCH-Data rate selection algorithm [104].

In this thesis a fixed UDP packet size was used. However, some research suggests using variable packet size [118]. In video codecs based on motion compensation (e.g. H.264 and Moving Picture Experts Group (MPEG4)), each packet will carry some motion compensation information (i.e. motion vector). For high amounts of motion in a video sequence, small packet sizes give better quality. However, for low amounts of motion, large packet sizes give better quality. Hence, it would be useful to have an optimization algorithm that determines the optimum packet size according to the motion amount in the video sequence [118]. This additional work is beyond the scope of this thesis and can be considered as future work to facilitate clinical applications requiring clear images of organs in rapid motion.

5.3 Patient End connectivity

The patient end software architecture and a snapshot of the patient user interface screen are shown in figure 5.3. This side transmits two types of data in parallel, the real time ultrasound streams and the emulated robotic control data. The emulated robotic data control is implemented via a signal generator that generates 16 Byte every 70 msec. That corresponds to the data of real robotic manipulator.

Due to the large amount of data generated by the real time ultrasound images and the limited wireless bandwidth, compression was needed for this type of data.

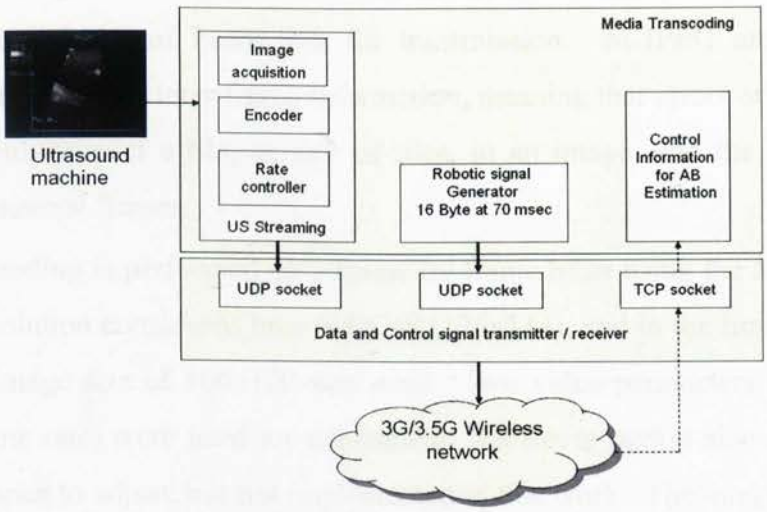

-a-

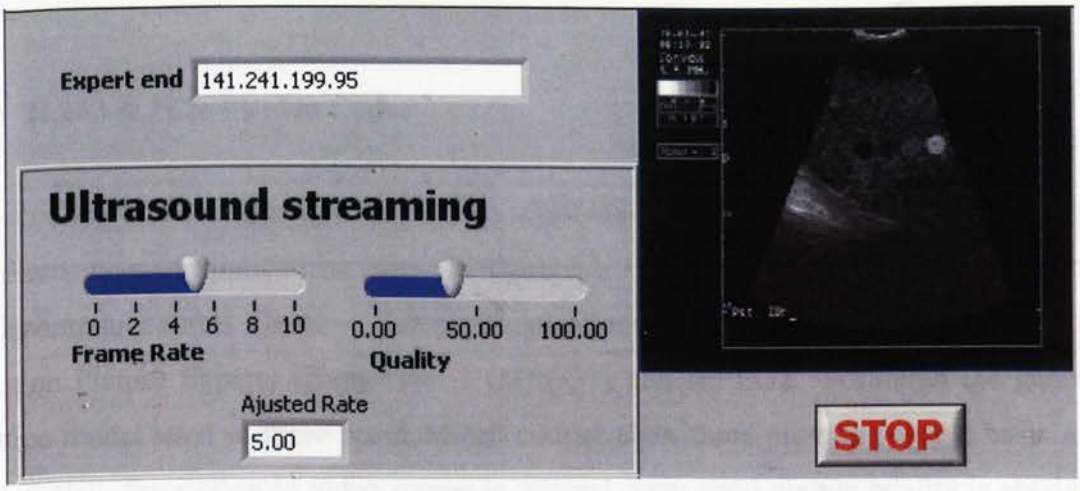

-b-

Figure 5.3 Patient station (server), a- software architecture, b- snapshot of the user interface screen.

5.3.1 Video codec used

In this work three types of video codecs have been used: Motion- joint picture expert group (M_JPEG), H.263 and H.264/Advanced Video Coding (H.264/AVC). Details of each codec is summarized below:

(i) Motion-JPEG

Motion-JPEG video transmission format has gained popularity due to several attractive features [27]. The main advantages that concern this thesis work is that M-JPEG uses no inter-frame compression, which results in low latency transmissions. The quality of the image will vary greatly based on the speed and quality of the codec as well as the availability of bandwidth for transmission. M-JPEG architecture uses normal JPEG tiles and no inter-frame information, meaning that errors or packet loss on the network only impact a tile, or row of tiles, in an image, and the error does not propagate for several frames.

The video coding is performed on a frame-by-frame basis using the M-JPEG codec. The image resolution considered here is QCIF (176x144), and in the limited bandwidth condition an image size of 100x100 was used. Two video parameters (image quality and video frame rate) were used for adjustment. However packet size can be used as another parameter to adjust, but not implemented in this work. The image quality index range used was 10 – 100 with frame rate range of 1-10 fps.

(ii) H.263 & H.264 Video Codec

Several international standards have been adopted for video compression, each serving a different type of application: Joint Photographic Experts Group (JPEG), International Telecommunications Union – Telecommunications Standards Sector (ITU-T) H.261, Motion Picture Experts Group type 1 (MPEG1) and MPEG2. Although the general source model used in these standardized coding algorithms provides only a basic and incomplete description of video scenes in general, very good picture quality is obtained at several megabits per second; picture quality is acceptable for some applications up to 64 kbps. However, below 64 kbps these algorithms lead to blocking artifacts or require operation at low frame rates, resulting in low temporal resolution and long end-to-end delay. Therefore, the H.263 codec was developed to work in low bit rates (as low as 28

kbps) and to improve the video quality considerably [121].

For the continuous fast demand of multimedia services in wireless networks and specifically in 3G wireless systems, the H.263 codec was adopted [122]. The choice was based on the manageable complexity of the encoding and decoding process, as well as on the maturity and simplicity of the design. The H.263 codec application used in this work was based on a H.263 codec based client/server application developed by the OTELO research group; screenshots of this application is shown in figure 5.4 [46]. At the server (patient) end application the compression parameters and the transmitted frame rate can be set.

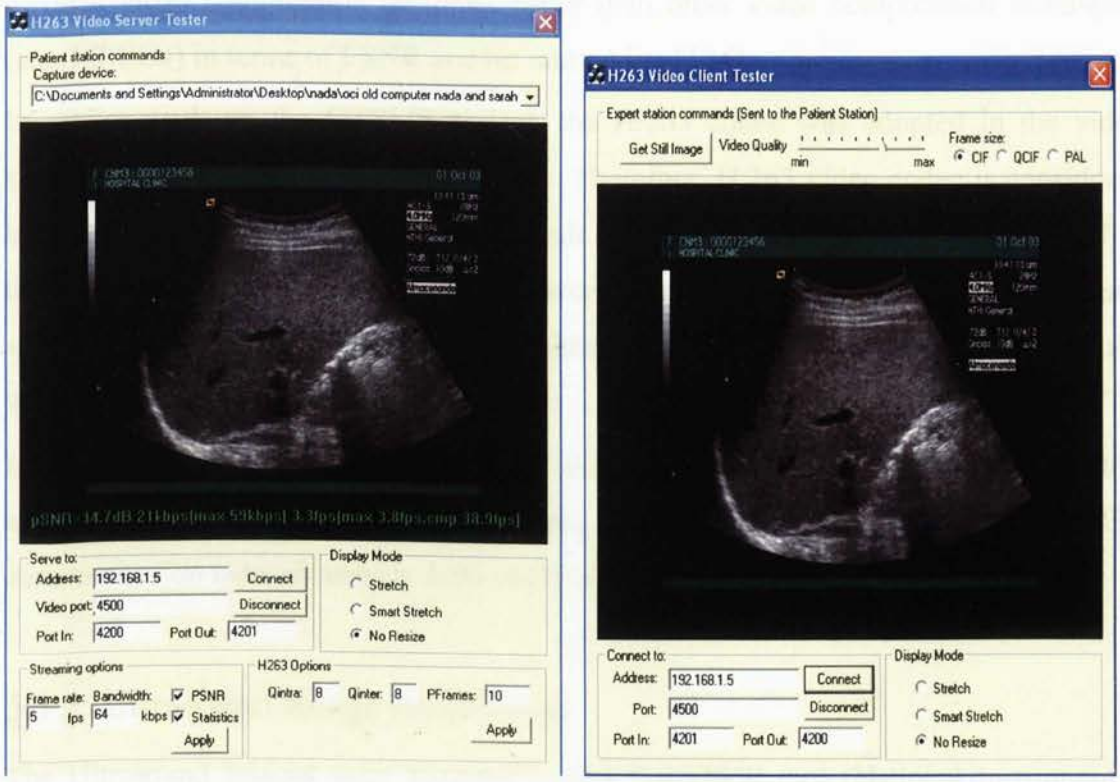

(a) **(b)**

Figure 5.4 Client/ Server application based on H.263 codec, (a) server (patient) end, (b) client (hospital) end [46].

The evolution of video coding for telecommunication applications continued. Throughout this evolution the effort was to maximize the coding efficiency while dealing with the diversity of network types and their characteristic formatting and loss/error robustness. A new video coding standard was finally approved in 2003 known as H.264/AVC. The main characteristic of this standard was to give double coding efficiency (halving the bit rate necessary for a given level of quality) in comparison to any existing video coding standards for a variety of applications.

In general, the available bandwidth and therefore the bit-rate over the radio link are limited and the costs for a user are expected to be proportional to the reserved bit rate or the number of transmitted bits over the radio link. Thus, low bit rates are likely to be typical, and compression efficiency is the main requirement for a video coding standard to be successful in a mobile environment [122]. However, due to the special mobile communication characteristics in terms of varying channel condition such as fading and shadowing, video coding to be applicable in wireless environment has to be error resilient. Hence, the H.264/AVC video codec is now considered the main codec in wireless multimedia applications [122]. In addition, H.264 video compression in medical video compression performs better than other video compression techniques (e.g. MPEG4) in terms of PSNR and bit rate saving [124].

In earlier work on the OTELO project, the H.263 codec was adopted in the video streaming services over 3G network [58]. Therefore, H.263 video codec is considered here in order to compare the achieved result of the Q-USR controller with that used in the OTELO project trials over a 3G network [108]. In these trials the H.263 based videoconference system was used in the ultrasound streaming. The comparative results were shown earlier in section 4.7.

In this work the H.264/AVC codec is also used to test the proposed rate control algorithm Q-USR and it's effectiveness in medical applications [124]. The communication network used is 3.5G wireless network.

5.3.2 Ultrasound Image Acquisition

The Ultrasound images were acquired by the LabVIEW tool (National Instrument – IMage AcQuisition (NI-IMAQ) for Universal Serial Bus (USB) Cameras connectivity) [115]. This embedded tool with LabVIEW allows the system to acquire the ultrasound images continuously from imaging devices connected to the computer via a USB connection. The rate of the acquisition is controlled by the designed system, this rate control is taking here as the frame rate control. Figure 5.5 shows the basic building blocks of this tool using the LabVIEW simulation tool.

Figure 5.5 LabVIEW model of the image acquisition using NI-IMAQ for USB interface connection [115].

5.3.3 Q-USR control algorithm implementation

The rate control algorithm Q-USR is written in MATLAB®. LabVIEW can execute external MATLAB® scripts. To make this work MATLAB must be installed on the computer to use MATLAB Script Nodes in LabVIEW.

5.3.4 Robotic Control Implementation

The Robotic control data implementation is as simple as generating 16 Byte string every 70 msec. This is shown in figure 5.6. This needs to be executed in parallel with the Ultrasound streaming process. As mentioned above the transport protocol used is UDP.

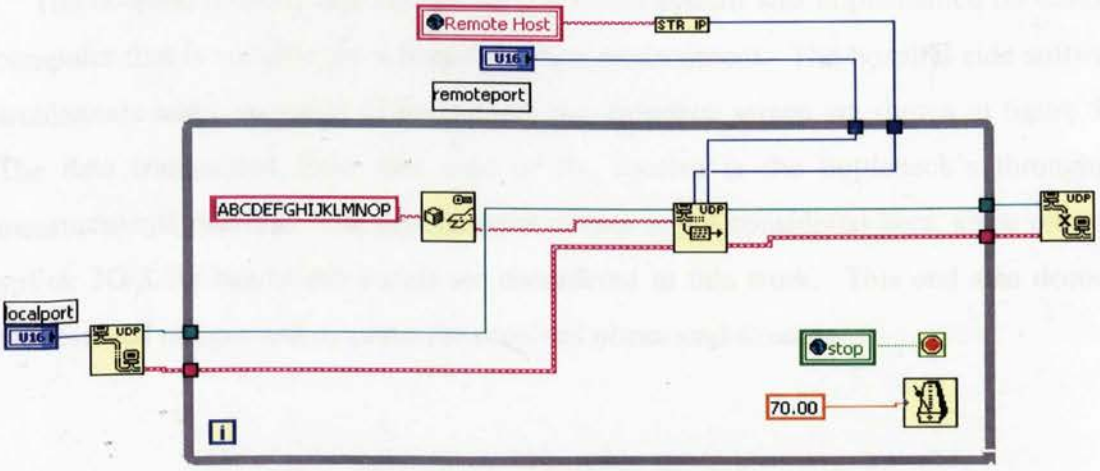

Figure 5.6 Robotic control data implementation

5.3.5 Control Information for bandwidth estimation

The patient side receives the control information for available bandwidth estimation via datasocket server which is based on the TCP protocol, as shown in figure 5.7. The patient station use this information to predict the next value of the available bandwidth by running the LPC program written in MATLAB via using a MATLAB script node in the LabVIEW platform.

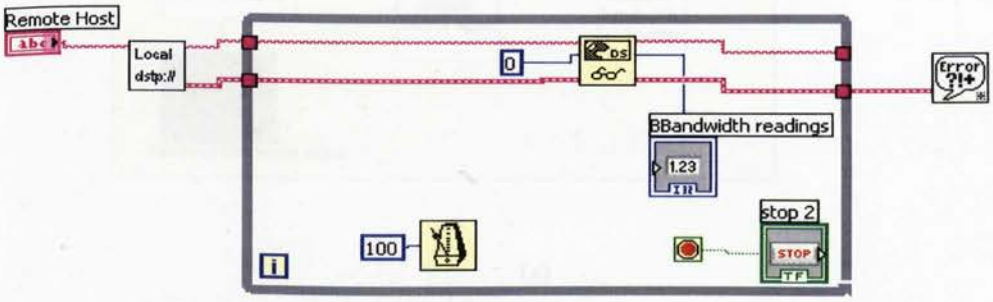

Figure 5.7 Control information for the Available bandwidth estimation model

5.4 Hospital (Expert) end

The hospital (expert) end unit in the emulation system was implemented on desktop computer that is suitable for a hospital office environment. The hospital side software architecture and a snapshot of the patient user interface screen are shown in figure 5.8. The data transmitted from this side of the system is the bottleneck's throughput measurements reading. The robotic control data is not considered here, since only the uplink 3G/3.5G bandwidth issues are considered in this work. This end also decodes the received images and displays the received ultrasound streams.

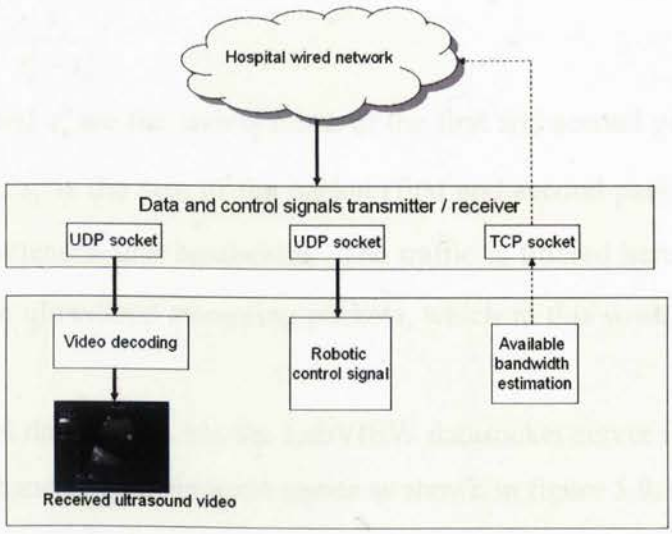

(a)

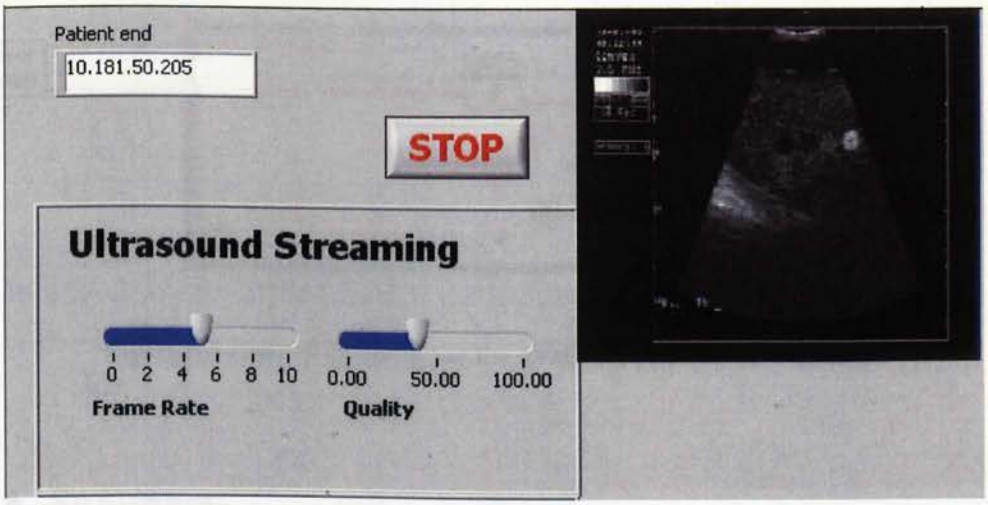

(b)

Figure 5.8 hospital end (client), (a) software architecture, (b) snapshot of the user interface screen.

5.4.1 Available Bandwidth estimation model in hospital end

The available bandwidth estimation block shown in figure 5.7 is used to monitor the incoming ultrasound stream packets in terms of packet size, delay and estimate average throughput (link bottleneck). The method used to measure the link bottleneck is based on "The packet pair property of First In First Out (FIFO)-queuing networks" approach

that predicts the difference in arrival times of two packets of the same size traveling from the same source to the same destination [129]:

$$b_1 = \frac{s_1}{t_n^1 - t_n^0} \tag{5.1}$$

Where t_n^1 and t_n^0 are the arrival times of the first and second packets respectively at the destination, s_1 is the size of the packet (first and second packet size are constant) and b_1 is the bottleneck link bandwidth. The traffic is filtered here only to pass the wanted packets (the ultrasound streaming packets, which in this work are kept constant to 300 Bytes).

This control data is sent via the LabVIEW datasocket server in real time to the patient station for bandwidth estimation issues as shown in figure 5.9.

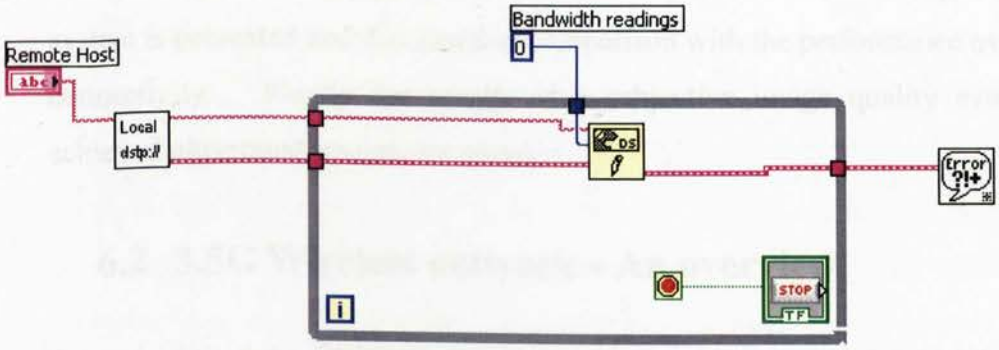

Figure 5.9 LabVIEW model for the Available bandwidth estimation

5.5 Summary

The work in this chapter presented the experimental setup and implementation issues of the Q-USR controller for medical video streaming in the robotic tele-ultrasonography system. The OTELO functional modalities were emulated in this work in terms of the robotic control data. The system was implemented based on the client-server approach. The programming language used was LabVIEW. The communication link used was real time 3G and 3.5G network. A real ultrasound scanning machine was used with an artificial phantom to represent the human body. Three types of video codec was considered M-JPEG, H.263 and H.264.

Chapter 6

Performance Analysis of Q-USR controller over 3.5G network connectivity

6.1 Introduction

In this chapter the performance of the proposed Q-USR control algorithm for robotic ultrasound streaming over 3.5G network connectivity is investigated. First an overview of the 3.5G network structure is presented. Then the experimental set-up of the Q-USR controller system over 3.5G network is illustrated. In addition the performance of the system is presented and discussed in comparison with the performance over 3G network connectivity. Finally the results of a subjective image quality evaluation of the achieved ultrasound images are given.

6.2 3.5G Wireless network – An overview

At present time, two 3.5G standards are deployed in commercial mobile networks that are capable of handling video streaming and video telephony services. One is the 3GPP [132] standard, HSDPA (High Speed Downlink Packet Access) and the other is the 3GPP2 [133] standard, EV-DO (Evolution-Data Optimized). HSDPA is based on the evolved Global System for Mobile Communications (GSM) specifications, EV-DO is based on evolved Code Division Multiple Access (CDMA) specifications. The focus of this thesis is on the HSDPA standard that is currently deployed in the UK.

6.2.1 High Speed Downlink Packet Access

Current 3G systems do not provide adequate throughput for high data rate applications. To enhance downlink performance, high speed downlink packet access (HSDPA) technology is introduced which is often referred to as 3.5G to differentiate the fundamental difference between 3G and 4G [134].

Since the early 1990's companies have been developing telecommunications technologies in order to provide higher bandwidths that would allow video

transmissions. The result of their efforts gave rise to UMTS, as defined by the ITU.

UMTS went through a series of releases from early 1999, Rel-99, Rel-4, Rel-5, Rel-6 and Rel-7 (Rel is abbreviation for Release). Rel-5 introduced some significant enhancements to UMTS including HSDPA architecture in 2002. Rel-6 was completed in March 2005 introducing further enhancements to UMTS including HSUPA (High Speed Uplink Packet Access). Rel-7 focuses on providing real-time interactive services such as push-to-talk over cellular, picture and video sharing and video over IP. UMTS adopted a generic term High Speed Packet Access (HSPA) to refer to both improvements, HSDPA and HSPUA, in the radio interface in the Rel-5 and 6 [134]. Brief details of these are explained here, for more completeness, further details on these issues can be found in [134].

The main enhancement and changes in HSDPA structure is in the physical layer. These are summarised as follows [135]:

Hybrid Automatic Repeat reQuest (HARQ): Error control in release 99 provides retransmission at the Radio Link Control (RLC) level. While in HSDPA the retransmission is done at the physical layer (using HARQ) under the control of the Node B, allowing many errors to be corrected quickly without the need for the RLC layer and the RNC to be involved. HARQ is different from the traditional ARQ. ARQ assumes that after a number of retransmission attempts, a correct message will eventually be received. HARQ, by contrast, makes use of all the received transmissions to recover the original message. Figure 6.1 shows an illustration of the process of HARQ in HSDPA. In Figure 6.1 the packet is first received in the buffer in the Node B. The Node B keeps the packet in the buffer even if it has sent it to the user. In the case of a packet decoding failure, retransmission automatically takes places from the Node B without RNC involvement. However, if this physical layer operation is failed due, for example, to a signaling error the RNC-based retransmission may still be applied on top using RLC acknowledge mode.

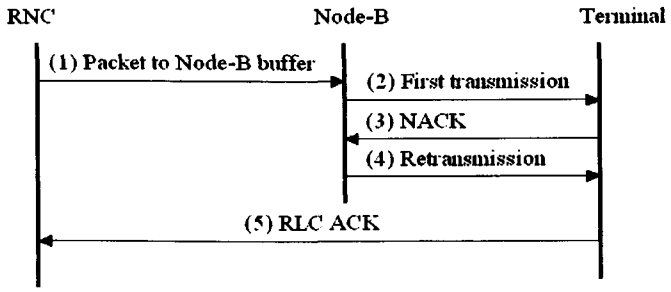

Figure 6.1 Node-B retransmission handling (HARQ)

New physical channels: HSDPA provides new physical layer channels for data transmission and signaling. Several new channels have been introduced for HSDPA operation for data transmission and signaling. Figure 6.2 shows the channels needed for the HSDPA operation. For user data transmission there is the high-speed downlink shared channel (HS-DSCH). For the associated signaling there are two channels: high-speed shared control channel (HS-SCCH) in the downlink and high-speed dedicated physical control channel (HS-DPCCH) in the uplink direction. The new uplink channel HS-DPCCH is used to send the acknowledgment (ACK/NACK) in case of the HARQ and to carry the Channel Quality information (CQI) to inform the Node B scheduler the data rate the terminal is capable of. The Release 99 based dedicated channel (DCH) is the key part of the HSDPA operation. HSDPA is always operated with the DCH running in parallel as shown in figure 6.2. In the downlink operation, the signaling for packet data service is carried on the DCH. In case of the circuit-switched data then the service always runs on the DCH. In the uplink direction the user data always go on the DCH (when HSDPA is active). The Dedicated physical data channel (DPDCH) carries user data while the dedicated physical control channel (DPCCH) carries the necessary physical layer control information.

Figure 6.2 Channels needed for HSDPA operation in Release 5 [134].

Frame length and scheduling: HSDPA reduces the radio frame length from 10ms in 3G to 2msec in 3.5G. This means a shorter Transmission Time Interval (TTI). In other words, the scheduling of the cell radio resources is re-evaluated every 2msec. This requires fast scheduling by moving the scheduling functions from the Radio Network Controller (RNC) to Node B allowing a faster response to user data on arrival and to changing network conditions.

Adaptive Modulation and Coding (AMC): HSDPA is capable of varying both the modulation and coding schemes on a frame by frame basis in order to make the best possible use of the current radio conditions. This AMC operation is based on the downlink channel quality. Mobile devices provide the channel quality feedback to the transmission station by a Channel Quality Indicator (CQI). The code rate can change between 1/4 and 3/4. If the code rate is k/n, for every k bits of useful information, the coder generates totally n bits of data, of which n-k are redundant for error control purposes. In addition to the Quadrature phase shift keying (QPSK) modulation, HSDPA can use the 16-Quadrature Amplitude Modulation (16QAM). Where in QPSK modulation the phase can vary between four possible states, allowing two bits to be transmitted at a time. 16QAM the amplitude is also varied in four steps, to give the 16 possible states; allowing four bits to be sent at once and hence doubling the data rate

[135]. However 16QAM is more sensitive to noise than QPSK, Therefore HSDPA has the ability to trade off between bandwidth and error rate by varying code rate. In a system with AMC, users close to the Node-B are typically assigned higher order modulation with higher code rates (e.g. 16 QAM with a 3/4 code rate), and the modulation-order and/or code rate generally decreases as the distance to the Node-B increases.

This collectively improved the data rate in HSDPA technology to peak rates (in the range of 1.8 Mbps to 14.4 Mbps in downlink). Currently available HSDPA deployment support only 1.8 Mbps in the downlink and 384 kbps peak data rate in the uplink.

6.2.2 HSDPA terminal capabilities

HSDPA specifies 12 categories for mobile devices. Categories 1 to 10 support QPSK and 16QAM modulations. Categories 11 and 12 include QPSK only support and have lower capacity than some of the lower categories. Depending on the category supported, the resulting maximum downlink data rates vary between 0.9 and 14.4 Mbps. A Category 12 device provides peak downlink data rate up to 1.8 Mbps and uplink speed up to 384 Kbps. A Category 10 device can provide a higher data rate. It can support downlink speed up to 14.4 Mbps (average at 1.5 Mbps) and uplink average up to 384 Kbps (average at 128 Kbps). The available mobile terminals are mostly Category 12 (peak rate up to 1.8 Mbps DL and 384 Kbps UL) devices and newer devices conform Category 5/6 (peak rate up to 3.6 Mbps DL and 384 Kbps UL). Category 12 type were used in this study.

6.2.3 Uplink connection in HSDPA

So far an overview of the HSDPA operation has been demonstrated. The main enhancement on HSDPA as compared to WCDMA was in the downlink communication (from the Node-B to the mobile terminal). The enhancement was mainly to increase the downlink data rate for users. However this benefited the uplink data slightly to reach 384 kbps peak data rate as compared to the Release 99 WCDMA uplink data rate of 64 kbps. According to [134] this is also due to the fact that currently WCDMA operators can offer laptop connectivity to the Internet and corporate Internet with the maximum bit rate of 384 kbps in the uplink

In the uplink direction the user data always go on the DCH (when HSDPA is active) [134]. The data transferred on DCH channel is protected by the channel coding scheme by applying the error detection and correction procedures to the data during the transport channel processing in DCH. Transport channel processing is the functionality that transforms the transport blocks delivered by the MAC layer to bits transmitted on physical channels [134]. In DCH channel the error detection is provided by cyclic redundancy check (CRC) coding and the error correction is by a combination of convolution code with turbo decoding. . Convolution coding and turbo coding are types of Forward Error Correction (FEC). For convolution coding, both rate 1/2 and 1/3 are considered and for turbo coding only 1/3 code rate is considered [136]. The code rate is controlled by the inner and outer loop power control mechanisms.

The use of the channel coding (convolution or turbo coding) aims to fix as many errors as possible in the UTRAN, and then the error-detection function (CRC) checks whether the result was correct. If not correct then retransmission is requested by applying the ARQ error control mechanism [130]. Figure 6.3 shows the ARQ operation. The user data is sent to the RNC, the RNC send ACK/NACK signal back to the mobile terminal and accordingly the retransmission happen [104].

Figure 6.3 Release '99 Uplink retransmission control [104].

6.3 Real Time 3.5G performance analysis

This section presents the experimental set up and results of the ultrasound streaming system controlled by the proposed Q-USR controller over a real time 3.5G network (as

provided by the current Vodafone operational networks in UK).

6.3.1 Experimental set-up

The experimental setup is shown in figure 6.4. As mentioned before in chapter 5, the ultrasound images are sent from the patient side via the Vodafone broadband data card (**Appendix D**), then via the IP network to the LAN network of the Expert side. The experiments were carried out at Kingston University, MINT laboratory, London.

It is worth mentioning here that the Vodafone data connectivity card used in this work is of category 12 with a data rate of 1.8 Mbps on the (downlink) and 384 kbps in the (uplink).

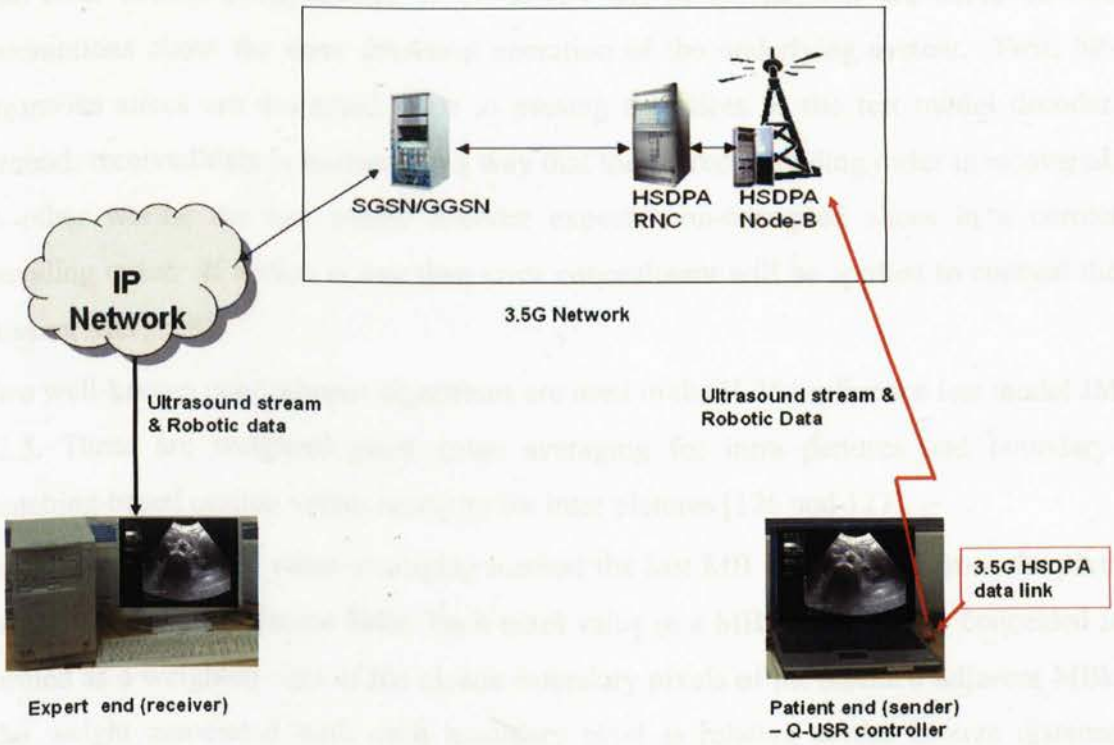

Figure 6.4 Real time 3.5G experimental set up.

The traffic analysis of the end-to-end wireless/wired link was then carried out with the desired packets separated from the background traffic generated by other applications using the link.

The experimental tests were carried out under different real 3.5G network loading conditions especially at peak working hours reflecting the different network conditions.

(i) Error control issues

As mentioned in section 6.2.3 above, the error control issues are taken care of by the lower layers of the mobile communications. It has been noticed that in bad network conditions, there will be more ARQ retransmissions, which add extra traffic on the link and hence affect the link throughput. Therefore in this work, the network conditions considered is the average throughput of the bottleneck link (3.5G uplink) only, and leaves the error control issues to the lower layers.

H.264/AVC video coding is based on a sequential encoding of frames [139]. Within each frame video encoding is typically based on sequential encoding of Macroblocks (MB)s (usually in the size of 8x8 pixels). In addition the H.264 encoding process groups certain numbers of MBs into slices.

The error detection capabilities of the H.264 test model decoder are based on two assumptions about the error detection operation of the underlying system. First, bit-erroneous slices are discarded prior to passing the slices to the test model decoder. Second, received data is buffered in a way that the correct decoding order is recovered. In other words, the test model decoder expects non-corrupted slices in a correct decoding order. If a slice is lost then error concealment will be applied to conceal the missing MB [128].

Two well-known concealment algorithms are used in the H.264 reference test model JM 12.3. These are weighted pixel value averaging for intra pictures and boundary-matching-based motion vector recovery for inter pictures [126 and 127].

In the weighted pixel value averaging method the lost MB is concealed from the pixel values of spatially adjacent MBs. Each pixel value in a MB needing to be concealed is formed as a weighted sum of the closest boundary pixels of the selected adjacent MBs. The weight associated with each boundary pixel is relative to the inverse distance between the pixel to be concealed and the boundary pixel [128].

In the motion vector recovery algorithm, the motion activity of the correctly received slices of the current picture is investigated first. If the average length of a motion vector component is smaller than a pre-defined threshold (currently 1/4 pixels), all the lost slices are copied from co-located positions in the reference frame. Otherwise, motion-compensated error concealment is used, and the motion vectors of the lost MBs are predicted from the neighboring concealed motion. The image is scanned MB-column-

wise from left and right edges to the center of the image. Consecutive lost MBs in a column are concealed starting from top and bottom of the lost area toward to center of the area. This processing order is used to ensure that lost MBs at the center of an image are concealed using as many neighboring concealed MBs as possible [128].

However, in this work the error concealment option in the decoder attributes is set to OFF in order to test the Q-USR performance that is based at the encoder and adapt to the network conditions in terms of throughput variations.

(ii) Ultrasound stream codec (H.264) issues

The ultrasound scanner is set to produce medical data streams at a rate of 13 fps and a resolution of (320X240) pixels. Then these images are acquired using a video card and fed to the laptop at the patient station. At the patient side the image size is reduced to QCIF (176X144) pixels to suit the wireless communication link limited bandwidth. H.264/AVC codec is used for the video encoding and is implemented with H.264 reference model version JM12.3 [125]. In this test model the image format used is YUV (color space model of one 1 (Y) luminance and two (U & V) chrominance), so the ultrasound image needs to be converted first to YUV format. The Group of Picture (GOP) selected here is of (IPPPP...) type with 10 frames per group. Table 6.1 shows the experiments setting for the H.264 codec used in this US streaming.

TABLE 6.1 H.264 CODEC SETTING FOR US STREAMING

Image size	QCIF (176X144)
Image format	YUV (4:2:0)
GOP size	10 frames
GOP type	IPPPPPP.....
Frame rate	Variable according to Q_USR
QP (for I and P)	Variable according to Q-USR
Slice mode	OFF
Symbol mode	CABAC (Context Based Adaptive Binary Arithmetic Coding)
Output file mode	Annex B (not for RTP)
Partition mode	No data partition (per slice)

The H.264 encoding process is very complex as compared to the decoding process so its software requires high PC resources in terms of temporary memory. As mentioned in chapter (5) of this thesis the software used to implement this system is LabVIEW that also requires significant computing resources. The ultrasound streams were then encoded offline under different quantization steps (QP) and different frame rates to avoid the problems of different software conversion format problems. These quantization steps and frame rates were the optimal value obtained by applying the Q-USR algorithm. Table 6.2 shows the details of the pre-encoded ultrasound streams in terms of the generated data rate, the Q-USR optimal control values (quantization step and Frame Rate) and the average PSNR of the ultrasound images. Experimentally it has been noticed that the data rate range used in table 6.2 can cover different 3.5G data rate variations. At the expert end, the decoding software was converted into a Dynamic-Link Library (DLL) file that can be run safely inside the LabVIEW platform system.

TABLE 6.2 H.264 PRE-ENCODED FILE DETAILS

Bit rate (kbps)	Q-USR optimal control values		PSNR (dB)
	Quantization step (QP)	Frame rate (fps)	
20	40	6.98	30.74
32	35	7.54	34.06
40	35	9.43	34.06
64	30	9.3	37.75
80	25	6.478	41.79
128	25	10.36	41.79
200	20	9.246	42.54
300	15	8.058	50.79

6.3.2 Performance Analysis

The 3.5G experimental setup is designed to measure the End-to-End m-QoS system performance when transmitting the ultrasound image streams under the proposed Q-USR controller functionality. In particular the following performance metrics are

discussed:

- Average throughput of the ultrasound image streams
- End-to-end transmission time, delta time and delay jitter of the received packets
- Medical image quality in terms of PSNR quality index
- Arrival frame rate AFR.
- Encoder buffer occupancy performance
- Image visual quality – objective and subjective measures

(i) Throughput

In a WCDMA system, the transmissions of users interfere with each other. Users can increase their data rates by increasing their transmission signal to noise ratio, but simultaneously this will increase the system noise level and then reduce the maximum data transmission capacity of other users [130]. This is based on Shannon's information theory that deals with the problem of maximizing the amount of transmitted information over noisy communications channel. According to this theory the maximum channel capacity in noisy communication environment can be determined from the following equation [130]:

$$C = W \log_2(1 + S/N) \tag{6.1}$$

Where W is the channel bandwidth, S is the power of the signal, and N is the power of the noise. Higher maximum channel capacity can be achieved by increasing the bandwidth or the signal power. The signal-to-noise ratio is usually given as the ratio of energy level per bit (E_b) to the energy level per Hertz (N_0) (i.e. E_b / N_0).

Since the channel capacity depends on the number of users, the experimental tests were carried out at different real 3.5G network loading conditions especially at peak working hours. Figure 6.6 shows the average throughput of the ultrasound stream (US) captured from the expert (robotic) end. This average throughput is achieved by transmitting ultrasound image streams with a PSNR of (37.75 dB) and an average frame rate (9.3 fps). Figure 6.6 shows that generally the average throughput was approximately 62 kbps. These results are within the minimum m-QoS requirement for the OTELO system given in chapter 3.

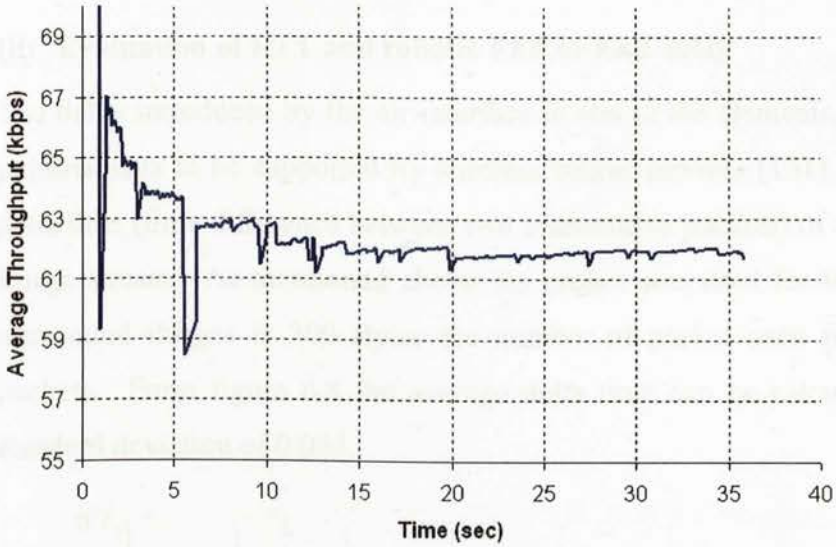

Figure 6.6 Average 3.5G throughput of the received ultrasound streams at PSNR (37.75dB) and Frame rate of (9.3 fps).

Figure 6.7 indicates that the achieved data rate (for PSNR of 37.75 dB and frame rate of 9.3 fps) is within the bandwidth capability of the uplink 3.5G link of approximately of 360 kbps. The experiments to test the 3.5G uplink bandwidth capability were done by continuous uploading of files with large sizes and measuring the average throughput achieved at the receiver.

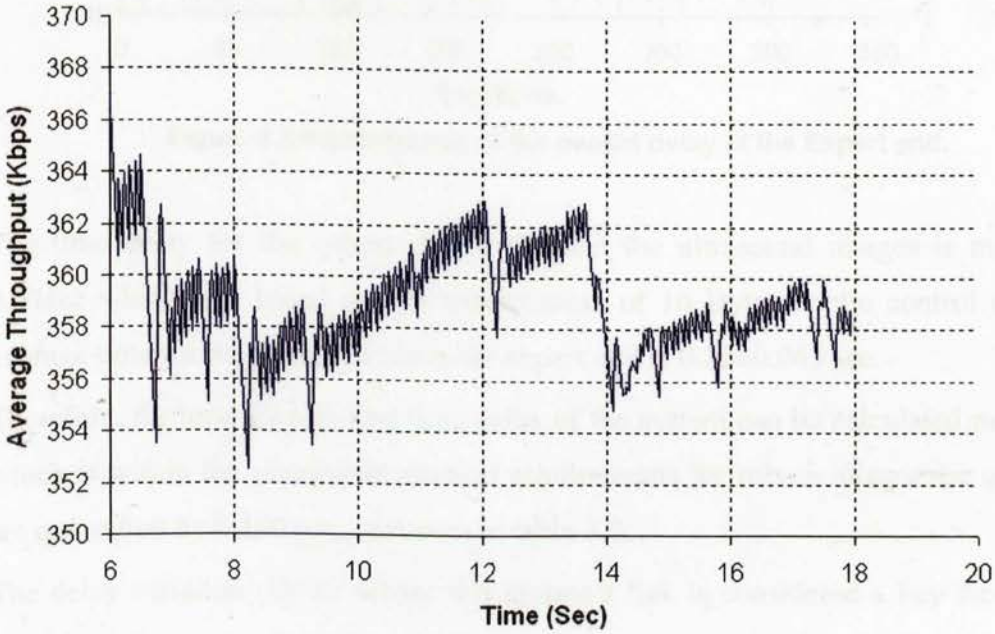

Figure 6.7 The 3.5G-uplink bandwidth capability.

(ii) Evaluation of RTT and robotic End-to-End delay

The delay introduced by the air interface is one of the elements, which define the QoS requirements to be supported by wireless bearer services [131]. Figure 6.8 shows the delta time (time difference between two consecutive packets) of the received ultrasound image stream. As mentioned above the packet size used for the packetization of the ultrasound images is 300 Bytes the number of packet used for this analysis is 300 packets. Form figure 6.8 the average delta time can be calculated as 0.12 sec with standard deviation of 0.063.

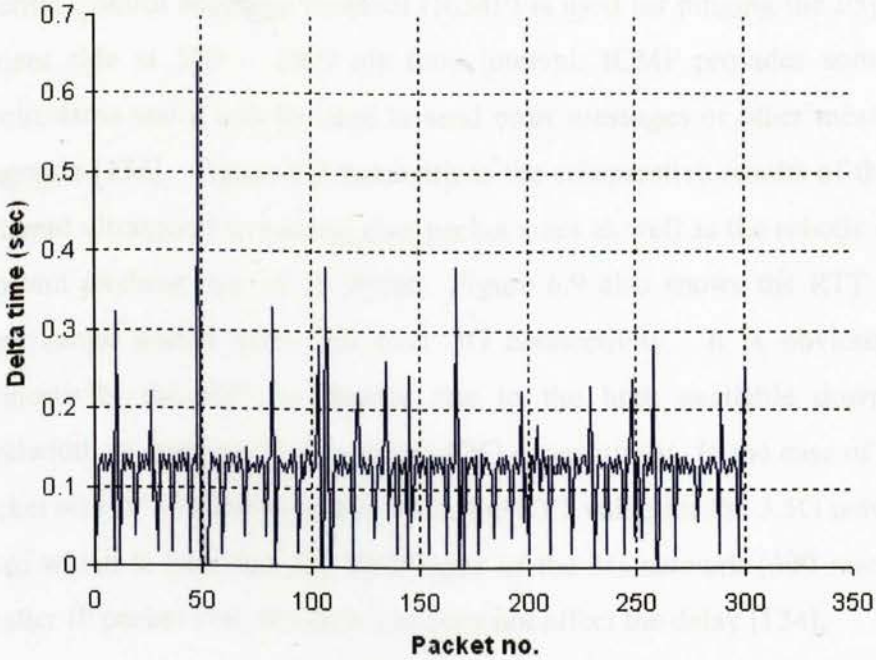

Figure 6.8 Performance of the packet delay at the Expert end.

The time delay for the expert side to request the ultrasound images is measured at 0.07sec which was based on the transmission of 16 Byte robotic control data. The average time for the packet to reach the expert end is 0.12±0.063 sec.

Therefore, the total End-to-End time delay of the system can be calculated as 0.253 sec which is within the acceptable medical requirements for robotic diagnostic quality that are quantified by 0.350 sec, as shown in table 3.3.

The delay variation (Jitter) across this system's link is considered a key factor for the reliable real-time medical ultrasound stream reception at the Expert station. As shown in figure 6.8 the average delay jitter is 0.063 (which is the standard deviation of the delta time).

In this work a fixed UDP packet size was used. However, some research suggests using variable packet sizes as mentioned in chapter 5 [118]. In order to cover this issue of variable packet size and its performance in terms of delay, different packet sizes were tested to characterize various delay performances of the 3.5G networks capability. These packet sizes were chosen to cover the possible size range of the packets generated by the video codec. One way to achieve that is by testing the RTT (Round Trip Time) delay. This is generally can be defined as the time it taken to transmit one packet from a server to a terminal plus the time it taken for the corresponding packet to be sent back from the terminal to the server [134].

Internet Control Message Protocol (ICMP) is used for pinging the Expert side from the Patient side at 500 – 1000 ms time interval. ICMP provides some error detection mechanisms and it can be used to send error messages or other messages for network diagnosis [134]. Figure 6.9 summarizes the comparative results of the RTT values for different ultrasound streaming data packet sizes as well as the robotic control data, with constant payload size of 16 Bytes. Figure 6.9 also shows the RTT measured for the same range packet sizes but over 3G connectivity. It is obvious that with 3.5G connectivity the RTT is shorter due to the high available downlink and uplink bandwidth as compared to the case of 3G connectivity. In the case of the selected UDP packet size of 300 Bytes in this work, the RTT value for the 3.5G network is about 180 msec which is less than the RTT value of the 3G network (300 msec). However for smaller IP packet size, the data rate does not affect the delay [134].

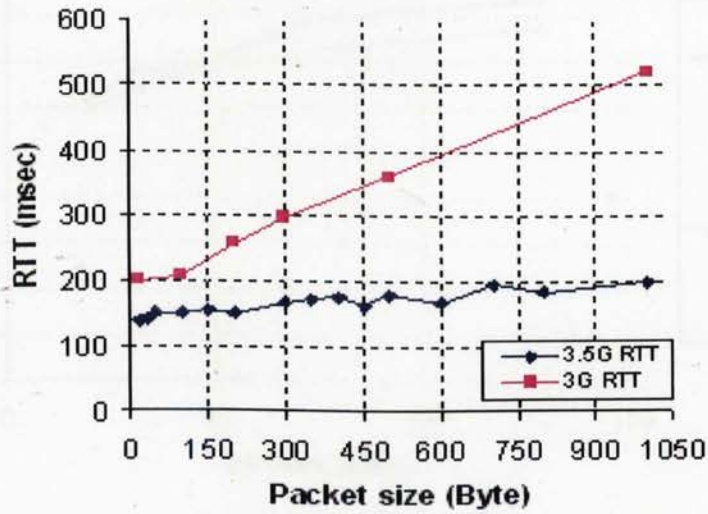

Figure 6.9 comparative RTT results of different ultrasound stream packets size and robotic packet size over 3G and 3.5G network.

(iii) Quality index measure and Arrival frame rate

As mentioned before in this chapter the Q-USR controller have been implemented on the JM 12.3 AVC test model software. As a reference for comparison, the rate control of the JM12.3 test model has been selected.

Figure 6.10 shows the comparative performance of the system firstly using the proposed rate control algorithm (Q-USR) and secondly using the rate control of JM12.3 test model in terms of PSNR for different data rate. In this test, the encoding parameters have been set exactly the same for JM12.3 in both cases in order to have a fair comparison. The GOP selected here is of IPPPP... type with 10 frames per group. For the JM12.3 test model rate control the frame rate was kept constant at 10 fps. The results show that the proposed algorithm achieves an improved PSNR with an average gain of 2.5dB. Figure 6.11 shows a comparative results between the achieved arrival frame rate with using the Q-USR control algorithm and when used the JM1.3 test model rate control algorithm. As shown in this figure, at some cases the achieved frame rate for the Q-USR controller was less than 10 fps. However, for the cases where the frame rate for both the Q-USR controller and the existing JM12.3 rate control are 10 fps, the achieved PSNR is still better in the case of Q-USR controller. In addition figures 6.10 and 6.11 show that for the proposed rate controller the achieved PSNR and Arrival frame for bit rate of over 50kbps was within the acceptable m-QoS functional bounds explained in chapter 3 (5 fps and 36 dB).

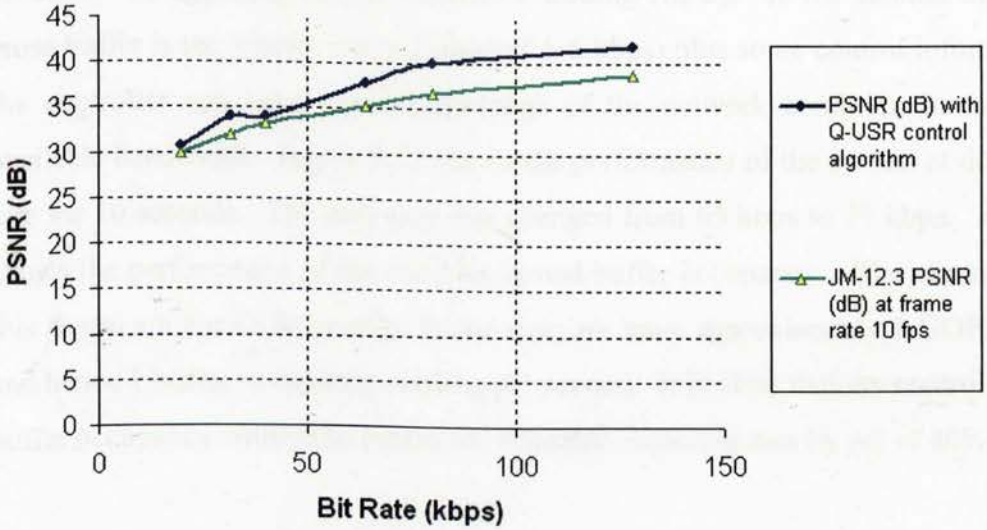

Figure 6.10 Comparative performance of the received ultrasound images PSNR at different bit rate with and without the Q-USR control algorithm.

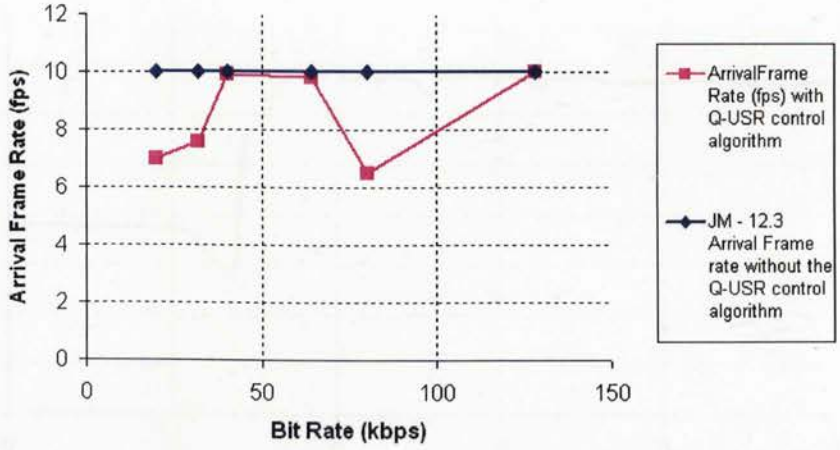

Figure 6.11 Comparative performance of the arrival frame rate of the ultrasound images at different bit rate with and without the Q-USR control algorithm.

(iv) Encoder buffer occupancy performance

The proposed algorithm adepts the sending rate according to the available bandwidth. In this work the available bandwidth was measured by measuring the average throughput for the ultrasound stream over time at the receiver using the bottleneck capacity estimation mentioned in chapter 5 (equation 5.1) and described in [129]. The measurements of this average throughput are sent from the expert station to the patient station via the TCP protocol. At the patient station the current average throughput is predicted via applying Linear Predictive Coding (LPC). If we assume that the only cross traffic is the robotic control data (of 5-6 kbps) plus some control information then the controller can have some knowledge of the network condition in terms of the available bandwidth. Figure 6.12 shows the performance of the system at different data rate for 10 seconds. The data rate was changed from 65 kbps to 79 kbps. Figure 6.13 shows the performance of the encoder virtual buffer occupancy. The measurements in this figure are per GOP average frame size; we have approximately 1 GOP per second and hence 1 buffer occupancy reading per second. It is clear that the controller kept the buffer occupancy within the maximum tolerable value (chosen by us) of 80% (0.8).

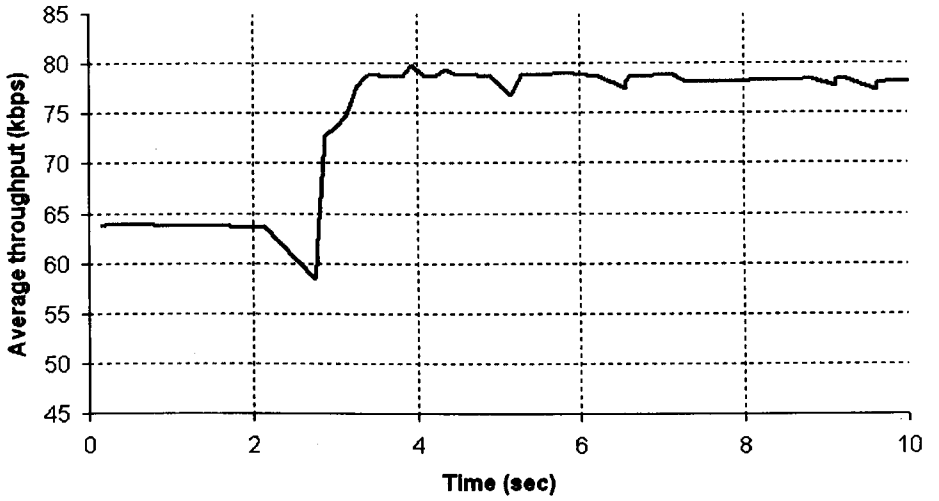

Figure 6.12 Average throughput of the generated Ultrasound stream data at different available data rate vs time

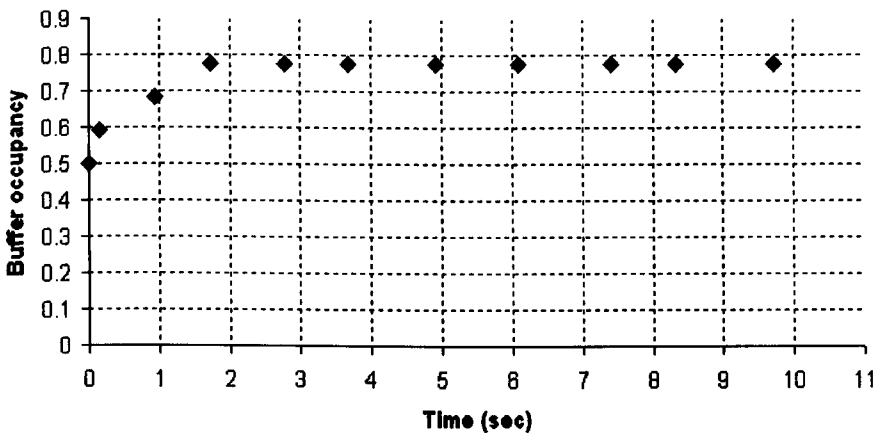

Figure 6.13 Buffer occupancy at different GOP vs time

(v) Image visual quality – objective and subjective measures

Figure 6.14 shows a sample of an ultrasound image acquired by the OTELO system, this sample is frame no. 4 of a sequence of ultrasound stream acquired by the OTELO system. Figure 6.15 shows the visual results for the ultrasound streaming images considered, the image resolution considered here is QCIF format (176x144). The original frame no. 4 is reported in figure 6.15 (a). The corresponding received video frame with the Q-USR controller applied is reported in figure 6.15 (b); presenting a high visual quality. Figure 6.15 (c) reports the corresponding received video frame without the Q-USR controller applied; evident artifacts are visible, which might impair the diagnosis.

Figure 6.14 A sample ultrasound image for abdomen, acquired by OTELO system, frame no. 4

(a)

(b)

(c)

Figure 6.15 Comparative visual results of the acquired Ultrasound streaming image frame no. 4. (a) before transmission; (b) after transmission with Q-USR controller; (c) after transmission without Q-USR controller.

In order to evaluate these images from a medical perspective, a subjective measure evaluation based on Mean Opinion Score (MOS) [94, 138] was used to assess the visual quality of the processed images in figure 6.15, in which three expert observers are asked to evaluate the quality of the processed test. Table (6.3) summarises the comparative percentage average MOS achieved by these tests (Equation 3.2). It is clear from this table that the image transmitted with Q-USR controller attains better score 60% as compared to 20% score for the image transmitted without Q-USR controller.

TABLE 6.3 PERCENTAGE AVERAGE MOS FOR THE TESTED US IMAGES WITH AND WITHOUT THE Q-USR CONTROLLER

Image title	Subjective measure- Percentage Averaged MOS
Original image before transmission (Figure 6.15 – a)	73%
Image transmission without Q-USR (Figure 6.15 – b)	60%
Image transmission with Q-USR (Figure 6.15 – c)	20%

As a conclusion of the performance analysis presented in this chapter, the following table (Table 6.4) shows a comparison between using 3G and 3.5G as the wireless communication link in this study in streaming ultrasound images. The 3G performance results shown in table 6.4 is based on an earlier publication on this thesis work [140]. The results show the better performance of the system over 3.5G in terms of higher image quality and frame rate, and lower end-to-end delay and delay jitter. This is as discussed before due to the higher bandwidth capability provided by the 3.5G connection.

TABLE 6.4 PERFORMANCE COMPARISION OF ULTRASOUND STREAMING OVER 3G AND 3.5G WIRELESS CONNECTIONS.

m-QoS metrics	3G with H.263 codec and QCIF image size	3.5G with H.264 codec and QCIF image size
Image quality/ Frame rate	35.5 dB / 5 fps (at bit rate 45kbps)	37 dB / 9.5 fps (at bit rate 63 kbps)
End-to-end delay	336 msec	253 msec
Delay jitter	70 msec	63 msec

6.4 Summary

This chapter investigated the performance of the proposed Q-USR control algorithm for robotic ultrasound streaming over 3.5G network connectivity. An overview on the 3.5G network structure was given. The video codec used here is H.264/AVC codec based using the test model JM12.3. The performance of the Q-USR control algorithm was compared with that of JM12.3 test model, the results has shown a noticeable gain in the value of PSNR when using Q-USR. In addition the performance of the system is presented and discussed in comparison with the performance over 3G network connectivity. Finally the results of a subjective image quality evaluation by the medical expert of the achieved ultrasound images were also given.

Chapter 7

Conclusions and Future Work

7.1 Introduction

This chapter presents the conclusions of the successful work reported in this thesis and the medical QoS and rate control issues in the 3G/3.5G wireless ultrasound streaming in the robotic teleultrasonography system. Suggestion for future work in this area are given for further enhancing the performance of the suggested methodology and for future implementation of the proposed methodology on future wireless systems especially in 3.75G (HSUPA) environments.

7.2 Conclusions

The contributions and achievements of this thesis work can be summarized as follows:

- A new sub-category of QoS for bandwidth demanding 3G/3.5G m-health applications (m-QoS) is introduced and defined as the '*Augmented requirements of the critical mobile health care with respect to the traditional wireless Quality of Service requirements*'. The bandwidth demanding m-health application used was the OTELO robotic system, which was briefly introduced in this thesis. The m-QoS requirements for the OTELO system over 3G/3.5G networks were justified based on experiments reported in this thesis and some important results achieved in previous work on the OTELO system. A thorough literature review proved the necessity of these new categories of QoS in medical field. These m-QoS metrics are the image quality, the ultrasound frame rate and the end to end delay. For the image quality two image quality indices were suggested and theses are the PSNR (with minimum value of 35db for QCIF and 36dB for CIF) and SSIM (with minimum value of 0.9). From this study a typical ultrasound frame rate 5 fps was accepted as minimum vale for successful medical transmission and viewing. And finally 350 msec was

medically accepted as minimum end to end delay in mobile robotic tele-ultrasonograhy system.

- To validate this new concept of m-QoS a new optimal rate control policy was proposed based on the Q-learning approach that works well in unknown environments like the wireless one. This new rate control algorithm is known here as Q-USR control algorithm.
- An end to end real time medical video streaming system was designed and successfully implemented to carry out the experimental test of the system. A real time video streaming application was built based on the client-server approach. The server represented here as the patient end of the OTELO system and the client the expert end of the OTELO system. The software used was LabVIEW. Two functional modalities of the OTELO system were implemented here: the robotic control data in terms of generating 70 bytes every 70 msec and the ultrasound streaming in terms of the real time acquisition of ultrasound images from a real ultrasound scanner.
- Medical subjective image quality measurement and assessments was carried out to test the medical acceptance of the processed image via the designed system. A subjective quality measures MOS (Mean Opinion Score) was used to assess the visual quality of the processed images. The result was that images with SSIM of 0.9 value achieved a subjective rating gain of about 80%.
- The designed system was implemented on real time 3G and 3.5G networks provided by Vodafone data cards.
- Three types of video compression techniques were used in order to analyse the performance of the new rate control algorithm. These video compression techniques were M-JPEG, H.263 and H.264/AVC. The results showed that for the QCIF image size and a data rate of 64 kbps, M-JPEG can achieve a PSNR of 32.5 dB and a frame rate of 3.75, H.263 can achieve a PSNR of 35.5 dB and a frame rate 5 fps, and H.264 can achieve a PSNR of 37dB and a frame rate of 9.5 fps. This showed that H.264 gives the best compression.
- At the sender the average throughput of the ultrasound streaming was predicated using the LPC method based on the previous average throughput readings from the receiver. This method gave a very good estimate average throughput with minimum error.

- The results showed that the designed ultrasound streaming performed better with the new Q-USR control algorithm than using the standard test model rate control algorithm (e.g. in case of H.264/AVC test model (JM12.3)). The results showed that the new algorithm achieves improved PSNR with an average gain of 2.5dB.
- The results also showed that the m-QoS was satisfied with the new rate control algorithm (Q-USR). For the 3G application and for an image size of QCIF, the result showed that a PSNR of 35dB and frame rate of 5 fps is achievable which is within the m-QoS requirements. The end to end delay was around 336 msec which is again within the m-QoS requirements for this robotic tele-ultrasonography system. In the case of 3.5G application and for an image size of QCIF, again the m-QoS in terms of PSNR and frame rate are achievable (for example for data rate of 64kbps PSNR is 37dB and frame rate is 9.5 fps). The end to end delay was 253 msec which was far inside the m-QoS of 350 msec as compared to the 3G (336 mses). Visual results of the received images showed the better diagnostic image quality of the received image under Q-USR controller.
- A comparison between the 3.5G and 3G packet transmission delay was made. One way to achieve that was via testing the RTT (Round Trip Time) delay. Different packet sizes were tested to cover the question of using variable UDP packet sizes. These packet sizes were chosen to cover the possible size range of the packets generated by the video codec. The results showed the superior performance of the 3.5G wireless connection compared to 3G wireless connection. For example for a 300 Byte packet size the 3.5G RTT was 180 msec as compared to 300 msec for 3G link capability.
- In general a comparison between using 3G and 3.5G wireless communication link in this study in streaming ultrasound images showed the better performance of the system over 3.5G in terms of higher image quality and frame rate, and lower end-to-end delay and delay jitter. This is due to the higher bandwidth capability provided by the 3.5G connection.
- Subjective quality assessment were carried out to test the acceptance of the ultrasound images quality using the Q-USR control algorithm by a number of experts. The transmitted images using Q-USR controller attained more score than that without the Q-USR controller.

7.3 Future Work

Despite the good results obtained in this thesis, there are some aspects that can be improved on to make the wireless ultrasound streaming architecture and methodology used presented by this thesis even better.

- Further investigations are needed to test the system over different 3G/3.5G wireless conditions. The network used in this thesis was a real time network and although careful work was done to test the system at different times of the day and especially at peak hours. However some wireless network simulators or emulators are needed to test the system under different wireless network conditions (e.g. bit error rate). A lot of effort was done but the solution was either the network simulators or emulators was expensive that can not be afforded. Although the MINT lab has a wireless network emulator called CLOUD but its software limitations prevented its use with the system designed in this thesis. And also time was limited to design and implement the 3G/3.5G wireless network simulator during the time of this thesis.
- Further investigation is needed to test the proposed Q-USR over the real OTELO system. In this work some of the OTELO functional modalities were emulated, for example the robotic data control transmission and delay issues.
- Error control issues were not considered in the design of the rate control algorithm. The design was based on considering the available bandwidth leaving the error control issues to the lower layer. Also the variable condition of the wireless network error control issues had to be considered in addition to the bandwidth estimation issues. This approach is well known as cross-layer design based rate control algorithms.
- For the Q-USR control algorithm itself further work is needed to have variable weighting variables in the minimax equation in chapter 4 (4.1) and to adapt these values according to the ultrasound image contents.
- Further work is needed to test the proposed system over 3.75G which is the High-Speed Uplink Packet Access (HSUPA). In order to test the effect of the increased uplink bandwidth capabilities on the performance of the new proposed rate control algorithm.

- This thesis mentions the use of the SSIM quality index measure. This was not used in the implementation part of the thesis. Further work is needed to implement the system using this quality measure in addition to the PSNR.
- Further work is needed to test the system using no-reference objective measures, where there is no need to have the original image when deciding on the processed image objective quality.
- The advantages of having variable packet size instead of fixed one need to be investigated. See section 5.2.1.
- Further work is needed to consider the design of cross layer based adaptive medical video streaming system. In this thesis an application layer based adaptive medical video streaming has been considered. Designing adaptive video streaming in general based on individual layers may give suboptimal solutions, particularly in wireless networks [19, 137]. A good review of cross layer based adaptive multimedia transmissions is provided in [141]. For example the exchange of information between the application layer source coding and the physical layer channel coding in terms of rate selection is beneficial in terms of allocating channel resources optimally and still achieving good overall distortion. This is usually known as joint source-channel coding [142]. Also the collaboration between the application layer and the link layer operations is important by allowing the link layer to perform the admission control and scheduling, not only focusing on throughput optimization but also to achieve the application layer user requirements. Figure 7.1 shows a conceptual scheme of a general cross-layer optimization.

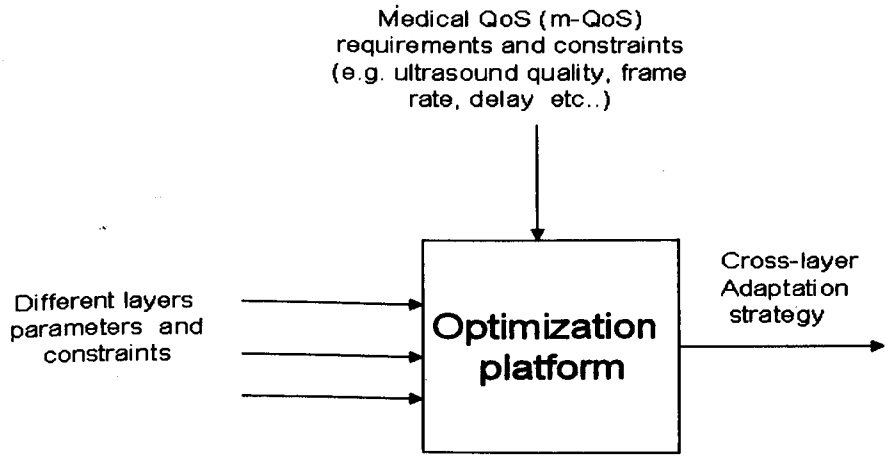

Figure 7.1 Conceptual scheme of a generic cross-layer optimization

Publications

- Istepanian, R. S. H. & Philip, N., "Non-Telephone Healthcare: The Role of 4G and Emerging, Mobile Systems for Future m-Health Systems", International Congress on Medical and Care Compunetics, L. Bos et al. (Eds.), June 2004, pp.465-471.

- Istepanian, R. S. H. & Philip, N., "Optimisation Issues of High Throughput Medical Data and Video streaming traffic in 3G wireless Environments", International Congress on Medical and Care Compunetics, L. Bos et al. (Eds.), June 2005, pp.125-131.

- Istepanian, R. S. H., Garawi, S. A. and Philip, N., "UMTS Traffic Analysis of wireless Tele-Echography Robotic system", Second Middle East Conference on Healthcare Informatics (MECHCI 2005), Dubai, 9-10 April, 2005.

- Philip, N. & Istepanian, R. S. H., "Medical Quality of Service for Wireless Ultrasound Streaming in Robotic Tele-Ultrasonography System", IEEE International Conference on Networking, Sensing and control 2007, London, pp. 245-250, April 2007.

- Philip, N., Istepanian, R. S. H., Amsou, N. and Shorvon, P., "Subjective and Qualitative Measure Issues of Agile Wireless TeleUltranogrpahy Imaging", the British Society for Gynaecology Imaging Inaugural Meeting 7-9 February 2008.

- Istepanian, R. S. H., Philip, N. and Martini, M., "Medical Quality of Service issues for Optimized Ultrasound Streaming in 3.5G Wireless System", IEEE Journal on Selected Areas of Communications – special issue on Wireless and Pervasive Communications for Healthcare (submitted in July, 2008).

- Istepanian, R. S. H., Philip, N., M. G. Martini, Amsou, N. and Shorvon, P., "Subjective and Objective Quality Assessment in Wireless TeleUltranogrpahy Imaging", the IEEE – Engineering in Medicine and Biology Society conference August 20-24 2008, Vancouver, Canada.

References

[1] World Health Organization (1997), Health-for-all policy for the 21st century, HQ (document EB101/8). Geneva.

[2] Craig, J., and Patterson, V. (2005), Introduction to the practice of telemedicine, Journal of Telemedicine and Telecare, Vol 11, No 1, pp 3-9.

[3] Yellowlees, P. (2005), Global Broadband e-Health Services, Business Briefing: Global Healthcare, 2002 Issue 3, Available: http://www.healthcare.com.au.

[4] Eysenbach, G. (2001), What is e-health?, *Journal of Medical Internet Research*. (Jun 18); 3(2):e20. Available at: http://www.jmir.org/2001/2/e20 [Accessed: 2006, March. 3].

[5] Della Mea, V. (2005), What is e-health (2): The Death of Telemedicine?, [editorial]. *Journal of Medical Internet Research,* Available at: http://www.jimir.org/2001/2/e22/ [Accessed: 2006, March. 3].

[6] Istepanian, R. and Laxminaryan, S. (2000), UNWIRED, the next generation of wireless and internatible telemedicine systems-editorial paper, *IEEEE transaction on Information Technology in Biomedicine,* Vol. 4, 189-194.

[7] Istepanian, R., Jovanov, E. and Zang, Y. (2004), Introduction to the special Section on M-Health: Beyond Seamless Mobility and Global Wireless Health-Care Connectivity, *IEEEE transaction on Information Technology in Biomedicine*, Vol. 8, No. 4.

[8] Philip, N., Istepanian, R. S. H., Wang, X. H. and Laxminarayn, S. (2004), "Non-Telephone Healthcare: The Role of 4G and Emerging Mobile Systems for Future m-Health Systems", International Congress on Medical and Care Compunetics, L. Bos et al. (Eds.), IOS Press, 2004, pp.465-471.

[9] Istepanian, R., Courreges, F., and Vieyres, P. (2004), Advances in robotic Tele-echography Services – The OTELO System, *The 26th Annual International Conference of the IEEE Engineering in Medicine and Biology Society*, San Francisco/USA.

[10] Istepanian, R. S. H., and Woodward, B. (2002), Programmable underwater acoustic telemedicine system, *Acoustica.*

[11] Istepanian, R. S. H., and Laxminaryan, S. (2000), UNWIRED, The next generation of Wireless and Internetable Telemedicine Systems- Editorial Paper, *IEEE Trans. Information Technology in Biomedicine*, Vol.4, 3, 189-194.

[12] Istepanian, R. S. H. and Pertrossian, A. (2000), Optimal Wavelet-based ECG data compression for mobile telecardiology system, *IEEE Trans. Information Technology in Biomedicine*, Vol. 4 , 3, 189-194.

[13] Istepanian, R. S. H., and Nikogossian, H. A. (2000), Telemedicine in Armenia: A Perception of Telehealth Services in the Former Soviet Republics, *J. Telemedicine and Telecare*, Vol.6, 268-272.

[14] Istepanian, R.S. H. (1999), Telemedicine in the United Kingdom, Current Status and Future Prospects, *IEEE Trans. Information Technology in Biomedicine*, Vol.3, 1, 158-159.

[15] Richards, C., Woodward, B. and Istepanian, R. S. H. (1999), Exploiting mobile telephone technology for telemedicine applications, *Medical and Biological Engineering & Computing*, Vol.37, Suppl.1, 110-111.

[16] Istepanian, R S. H., Woodward, B., Balos, P., Chen, S. and Luk, B. (1999), The comparative performance of mobile telemedical systems using the IS-54 and GSM cellular telephone standards, *Journal of Telemedicine and Telecare*, Vol.5, 2, 97-104.

[17] Tachikawa, K. (2003), Aperspective on the evolution of Mobile Communications, *IEEE Communication Magazine*, 66-73.

[18] Apostolopoulos, J., Tan, W. and Wee, S. J. (2002), Video Streaming: Concepts, Algorithms, and Systems, Mobile and Media Systems Laboratory HP Laboratories Technical Report, [Online]. Available at http://www.hpl.hp.com/ [Accessed 22 August 2006].

[19] Chakareski, J. and Frossard, P. (2007), Adaptive Systems for improved Media Streaming Experience, *IEEE Communications Magazine* Vol. 45, No. 1, pp 77-83.

[20] Istepanian, R., Pattichis, C. S., Kyriacou, E., and Voskarides, S. (2002), Wireless Telemedicine Systems: an Overview, *IEEE Antenna's Propogation Magazine*, Vol. 44, No. 2.

[21] Courreges, F., Vieyres, P., Istepanian, R., arbeille, P., and Bru, c. (2005), Clinical trials and Evaluation of a mobile robotic tele-ultrasound System, *Journal of Telemedicine and Telecare*, Vol. 11, Supp. 1, pp 46-49.

[22] Malone, F. D., Athanassiou, A., Nores, J., and dalton, M. E. (1998), Effect of ISDN bandwidth on image quality for telemedicine transmission of obstetric ultrasonography, *Telemedicine Journal and e-health*, Vol. 4, 161-165.

[23] Sublett, J. W., Dempsey, B. J., Weaver, A. C. (1995), Design and imlementation of a digital Teleultrasound System for real-Time Remote Diagnosis, Computer-Based Medical Systems, Texas, pp. 292-299.

[24] Varkarakis, I., Rais-Bahrami, S., Kavoussi L., and Stoianovici D. (2005), Robotic Surgery and Telesurgery in Urology, *Journal of Urology*, 65(5), pp. 840-846.

[25] Yokokohji, Y., Ogawa, A., Hasunuma, H., and Yoshikawa, T. (1993), Operation Modes for Cooperating with Autonomous Functions in Intelligen Teleoperation systems, *Proc. IEEE International conference on robotics and Automation,* pp. 510-515.

[26] Zivanovic, a., and Davies, B. (2000), A Robotic System for Blood Sampling, *IEEE Transactions on Information Technology in biomedicine*, vol. 4, No. 1, pp. 8-14.

[27] Video Development Initiative (ViDe) et al (2005), The videoconference cookbook, Version 4.1, [Online]. Available at http://www.vide.net/cookbook/cookbook.en/ [Accessed 06 August 2007].

[28] Burgul, R., Gilbert, F. J. and Undrill, P. E. (2000), Methods of Measurement of image quality in teleultrasound, *The British Journal of Radiology*, pp. 1306-1312.

[29] Kontaxakis, G., Walter, S. and Sakas, G. (2000), EU-TeleInViVo - An integrated portable telemedicine workstation featuring acquisition, processing and transmission over low-bandwidth lines of 3D ultrasound volume images. *Information Technology Applications in Biomedicine, ITAB 2000*, USA.

[30] Vilchis, A., Troccaz, J., Cinquin, P., Courreges, F., Poisson, G. and Tondu, B. (2001), Robotic Tele-Ultrasound System (TER) : Slave Robot Control. *1st IFAC Conference on Telematics Application in Automation and Robotics*, Weingarten, Germany, pp. 95-100.

[31] Masuda, K., Kimura, E., Tateishi, N., Ishihara, K. (2001), Remote Three dimensional motion mechanism of ultrasound probe and its application for tele-echography system, *Proceedings of International Conference of the IEEE Intelligent Robot and Systems*, pp. 1112-1116.

[32] Mitsuishi, M., Warisawa, S., Tsuda, T., Higuchi, T., Koizumi, N., Hashizume, H. and Fujiwara, K. (2001), Remote Ultrasound Diagnostic system, *IEEE ICRA, Korea*, Vol 2, pp. 1567-1573.

[33] Pierrot, F., Dombre, E., Degoulange, E., Urbain, L., Caron, P., Boudet, S., Garipy, J., and Magnien, L. J. (1999), *Hippocrate : a safe robot arm for medical applications with force feedback, Medical Image Analysis*, vol. 3, pp. 285-300.

[34] D'Attanisio, S., Tonet, O., Megali, G., Carozza, M. C. and Dario, P. (2000), *A semi-automatic hand-held mecatronic endoscope with collision avoidance capabilities, Proceedings of the Conference on Robotics and Automation*, pp. 1586-1591.

[35] De Cunha, D. and Gravez, P. (1998), The MIDSTEP system for ultrasound guided remote telesurgery, *20th Annual Intelligent of the IEEE/EMBC Engineering in Medicine and Biology Society*, Vol. 20, No 2, pp. 1266-1269.

[36] Watkins, C. J. C. H. and Dayan, P. (1992), Q-Learning Technical Note, *Machine Learning*, No. 8, pp. 279-292.

[37] Jamalipour, A. (2003), The Wireless Mobile Internet, Archetectures, Protocols and services.

[38] Pommert, A. and Hoehne, K. (2002), Evaluation of Image Quality in Medical Volume Visualization: The State of the Art, In Takeyoshi Dohi, Ron Kilinis (eds.): Medical Images Computing and Computer-Assisted Intervention, Proc., MICCAI, 2002, Part II, Lecture Notes in Computer Science 2489, Springer Verlag, Berlin, pp. 598-605.

[39] Hands, D. S., Huynh-Thu, Q., Rix, A. W., Davis, A. G. and Voelcker, R. M. (2004), Objective Perceptual Quality Measurement of 3G Video Services, *Fifth IEE International Conference on 3G Mobile Communication Technologies (3G 2004) The Premier Technical Conference for 3G and Beyond,* London, pp. 437 -441.

[40] Wang, Z., Bovik, A., Sheikh, H. and Simoncelli,E. (2004), Image quality assessment: From error measurement to structural similarity, *IEEE Trans. Image Processing*, vol. 13, No. 4, pp. 600-612.

[41] Pappas, T. N. and Safranek, R. J.(2004), Perceptual criteria for image quality evaluation, in Handbook of Image and Video Processing (A. C. Bovik, ed.), Academic Press.

[42] Liu, G. P., Yang, J., Whidborne, J. F., (2002), Multiobjective Optimisation and Control (Engineering Systems Modelling and Control Series).

[43] Jammeh, E. and Ghanbari, M. (2003), Transmission of pre-encoded video over best-effort IP network, *in 13th International Packet Video Workshop (PV2003).*

[44] Katabi, D., Bazzi, I. and Yang, X. (2001), A passive approach for detecting shared bottlenecks, *in ICCCN: IEEE International Conference on Computer Communications and Networks*, (Arizona).

[45] Obeo,R. (2001), Web-Interfaced, Forced-Reflecting Teleoperation Systems, *IEEE Transactions on Industrial Electronics*, Vol. 48, No. 6.

[46] Canero, C., Thomos, N., Triantafyllidis, G., Litos, G. and Strintzis, M. (2005), Mobile Tele-Echography: User Interface Design, *IEEE Transaction on Information Technology in Biomedicine*, Vol. 9, No. 1.

[47] Zachariadis, K. E., Boulgouris, N. V., Thomos, N., Triantafyllidis, G. A. and Strintzis, M. G. (2002), Wavelet-based communication of medical image sequences, in *Int. Workshop Enterprise Networking and Computing in Health Care Industry*, Nancy, France.

[48] Astrom, K. J. and Wittenmark, B. (1994), Adaptive Control, 2nd Edition, Prentice Hall.

[49] Wiegand, T., Sullivan, G. J., Bjontegaard, G. and Luthra, A.(2003), Overview of the H.264/AVC video coding standard, *IEEE Trans. Image Process.*, Vol. 13, No. 7, pp. 560–576.

[50] Lerouge, C., Gargield, M. and Hevner, A. (2002), Quality Attributes in Telemedicine Video Conferencing, *Proceeding of the 35th Hawaii International conference on system Sciences.*

[51] Bass, L., Clementents, P. and Katzman, R.(1998), Software Architecture in Practice, Addison-Wesley, Inc., Reading.

[52] Martini, M. G. and Mazzotti, M. (2006), Quality Driven Wireless Video Transmission for Medical Applications, IEEE *Engineering in Medicine and Biology Conference (EMBC)*, Aug-Sept, New York.

[53] Zhang, Q., Zhu, W. and Zhang, Y. (2005), End-to-End QoS for Video Delivery Over Wireless Internet, *Proceeding of the IEEE*, vol. 93, No. 1.

[54] Wroclawski, J. (1997), The Use of RSVP with IETF Integrated Services, RFC 2210..

[55] Grossman, D. (2002), New terminology and clarifications for DiffServ, RFC 3260.

[56] 3GPP TS 23. 107 (2003), Quality of Service (QoS) concept and architecture.

[57] Wu, D., Hou, Y. T. and Zhang, Y. Q. (2000), Transporting real-time video over the Internet: Challenges and Approaches, *Proceeding of IEEE*, Vol. 88, pp. 1855-1875.

[58] Garawi, S. (2006), Performance Analysis of AMobile Robotic Tele-Ultrasonography system Over 2.5G/3G Communication Networks, PhD thesis, Kingston University, London.

[59] Soomro, A. and Cavalcanti, D. (2007), Opportunities and Challenges in using WPAN and WLAN Technologies in Medical Environments, *IEEE Communications Magazine,* Vol. 45, No. 2, pp. 114-122.

[60] Jha, S. and Hassan, M. (2002), Engineering Internet QoS, Artech House.

[61] Mathis, M. et al. (1997), The Macroscopic Behavior of the TCP Congestion Avoidance Algorithm, *ACM Computer Communications Review.*

[62] Padhye, J. et al. (2000), Modeling TCP Reno Performance: A Simple Model and its Empirical Validation, *IEEE/ACM Trans. Networking*, Vol. 8, No. 2, pp. 133-145.

[63] Jacobson, V. (1988), Congestion Avoidance and Control, *ACM SIGCOMM,*NY, USA..

[64] Tan, W. and Zakhor, A. ((1999), Real-time Internet Video using Error-Resilient Scalable Compression and TCP-friendly Transport Protocol, *IEEE Trans. on Multimedia,* Vol. 1, No 2..

[65] Floyd, S. et al. (2000), Equation-based Congestion Control for Unicast Applications, *ACM SIGCOMM,* NY, USA..

[66] Schulzrinne,H., Rao, A. and Lanphier, R. (1998), Real Time Streaming Protocol (RTSP), IETF RFC 2326.

[67] Schulzrinne, H., Casner, S., Fredrick, R. and Jacobson, V. (1996), RTP: A Transport Protocol for Real-Time Applications, IETF RFC 1889.

[68] Montes, H., Gomez, G. and Fernandez, D. (2002), An end-to-end QoS Framework for Multimedia streaming services in 3G Networks, *The 13th IEEE International Symposium on Personal, Indoor and Mobile Radio Communications,* Vol. 4, pp. 1904-1908.

[69] Kontaxakis, G., Walter, S. and Sakas, G. (2005), Mobile tele-echography system:TeleInViVo – a case study, *In:M-health: emerging mobile Health Systems, R. Istepanian, S. Laxminarayan, and C. pattichis, (editors)*, Kluwer Academic/Plenum Publishers.

[70] Mogul, J. and Deering, S. (1990), Path MTU Discovery, RFC 1191 Internet Engineering Task Force.

[71] Montenegro, G., Dawkins, S., Kojo, M., Magret, V. and Vaidya, N. (2000), Long thin networks, RFC 2757.

[72] Bakre, A. and Badrinath, B. (1995), I-TCP: Indirect TCP for mobile hosts, *in Proc. 15th Int. Conf. Distributed Computing Systems (ICDCS), Vancouver, BC, Canada*, pp. 136-143.

[73] Cheung, G. and Yoshimura, T. (2002), Streaming agent: A network proxy for media streaming in 3G wireless networks, in *IEEE Packet Video Workshop*, Pittsburgh, PA.

[74] Cen, S., Cosman, P. and Voelker, G. (2003), End-to-end Differentiation of Congestion and Wireless Loss, *IEEE/ACM Transactions on Networking*, Vol. 11, No. 5, pp. 703 – 717.

[75] Biaz, S. and Vaidya, N. (1999), Discriminating congestion losses from wire-less losses using inter-arrival times at the receiver, in *Proc. IEEE Symp. Application-Specific Systems and Software Engineering and Technology*, Richardson, TX, pp. 10–17.

[76] Bhargava, A., Khan, M. F. and Ghafoor, A. (2003), QoS management in multimedia networking for telemedicine applications, *IEEE Workshop on Software Technologies for Future Embedded Systems*, pp. 39 – 42.

[77] Oberoi, V. and Chigan, C. (2005), Providing qos for sensor enabled emergency applications, *IEEE International Conference on Mobile Adhoc and Sensor Systems Conference*, pp. 157 – 159.

[78] Wac, K., Halteren, A. V. and Broens, T. (2007), Context-aware QoS Provisioning in an m-health services Platform, *International Journal of Internet Protocol Technology*, Vol. 2, No. 2, pp. 102-108

[79] Lage, A. L., Martins, J. S. B., Oliveira, J. and Cunha, W. (2004), A Quality of Service Framework for Tele-Medicine Applications, *IEEE Proceedings on WebMedia and LA-Web*, pp. 18-12.

[80] Nishantha, D., Hayashida, Y., Hayashi, T. (2004), Application Level Rate Adaptive Motion-JPEG Transmission for Medical Collaboration Systems, *IEEE Proceeding of the International conference on distributed computing Systems workshops (ICDCSW'04)*, pp. 64- 69.

[81] Busse, I., Deffner, B. and Schulzrinne, H. (1996), Dynamic QoS control of multimedia applications based on RTP, *Computer Communications*, Jan. 1996.

[82] Kim, J., Lee, J., Nam, H., Ko, S. and Yoon, J. (2005), Effective Channel Adaptive Video streaming for wireless Network, *Consumer Electronics, 2005. ICCE. 2005 Digest of Technical Papers. International*, pp. 111 - 112.

[83] Morikawa, D., Ota, S., Yamaguchi, A. and Ohashi, M. (2002), A Feedback Rate Control of Video Stream in Best-Effort High-Speed Mobile Packet Network, the 5th International Symposium on Wireless Personal Multimedia Communications, pp. 807-811.

[84] Balakrishnan, H. et al. (1997), A comparison of Mechanisims for Improving TCP Performance over Wireless Links, *IEEE/ACM Transactions on Networking (TON)*, Vol. 5 , Issue 6, pp. 256-269.

[85] Balakrishnan, H. and Katz, R. (1998), Explicit Loss Notification and wireless Web Performance, *Proc. IEEE Globecom Internet Mini-Conference*, Sydney, Australia.

[86] Tang, J. et al. (2001), RCS: A Rate control scheme for Real Time Traffic in Networks with High Bandwidth Delay Products and High Bit Error rates, *in Proc. IEEE INFOCOM 2001*, ,Vol. 1, pp. 114-122.

[87] Cen, S., Cosman, P. and Voelker, G. (2003), End-to-End Differentiation of Gongestion and wireless Losses, *IEEE/ACM Transactions on Networking (TON)*, Vol. 11, No. 5, pp.703-717.

[88] Chen, M. and Zakhor, A.(2004), Rate Control for Streaming Video over Wireless, *Twenty-third Annual Joint Conference of the IEEE Computer and Communications Societies - INFOCOM 2004*, Vol. 1, pp. 1181 – 1190.

[89] Hsu, C., Ortega, A. and Khansari, M. (1999), Rate Control for Robust Video Transmission over Burst-Error Wireless Channels, *IEEE Journal on Selected Areas in Communications*, Vol. 17, No. 5, pp. 759-773.

[90] Cheung, G., Tan, W. and Yoshimura, T. (2005), Real-Time Video Transport Optimization Using Streaming Agent Over 3G Wireless Networks, *IEEE Transactions on Multimedia,* Vol. 7, No. 4, pp. 777-785.

[91] Chande, V. and Farvardin, N. (2000), Progressive transmission of images over memoryless noisy channels, *IEEE J. Selected. Areas com.*, Vol. 18, no. 6, pp. 850-860.

[92] Chou, P. and Miao, Z. (2006), Rate-Distortion Optimized Streaming of Packetized Media, *IEEE Transactions on Multimedia*, Vol. 8, Issue 2, pp. 390 - 404 .

[93] Rijkse, K. (1996), H.263: Video Coding for Low-bit Rate Communication, *IEEE Communications Magazine*, Dec., pp. 42-45.

[94] Cosman, P., Gray, R. and Olshen, R. (1994), Evaluating Quality of Compressed Medical Images: SNR, Subjective Rating and Diagnostic Accuracy, *Proceedings of the IEEE*, Vol 82, Issue 6, pp. 919 – 932.

[95] Zhou, Y., Chen, D., Li, C., Li, X. and Feng, H. (2003), Practice of Medical Image quality evaluation, *Proceedings of the 2003 International Conference on Neural Networks and Signal Processing*, Vol. 1, pp. 204 – 207.

[96] ITU-R Recommendation BT.500-11 (2002), Methodology for the subjective Assessment of the Quality of Television Pictures.

[97] Wang, Z. and Bovik, A. C. (2002), A Universal Image Quality Index, *IEEE Signal Processing Letters,* Vol. 9, pp. 81-84.

[98] M. G. Martini, M. Mazzotti, C. Lamy-Bergot, J. Huusko and P. Amon, "Content adaptive Network Aware Joint Optimization of Wireless Video Transmission", *IEEE Communications Magazine*, Vol. 45, No. 1, pp. 84-90, January 2007.

[99] The Video Quality Experts Group. VQEG. http://www.VQEG.org.

[100] International Telecommunication Union (ITU). ITU-T Study Group 9. http://www.itu.int/ITU-T/studygroups/com09.

[101] Castellanos, C., Villa, D., Teyeb, O., Elling, J. and Wigard, J. (2006), Comparison of Available Bandwidth Techniques in Packet-Switched mobile Networks, *IEEE International Symposium on personal, Indoor and mobile Radio Communications,* pp. 1-5.

[102] Johnsson, A., Melander, B. and Bjorkman, M. (2005), Bandwidth Measurement in wireless Networks, in Mediterranean Ad Hoc Networking Workshop, Porquerolles, France.

[103] Ribeiro, V. J., Riedi, R. H., Baraniuk,, R. G., Navratil, J. and Cottrell, I. (2003), PathChirp: Efficient available bandwidth estimation for network paths, *in Passive and active Measurement Workshop.*

[104] Holma, H., Toskala, A. (2000), WCDMA for UMTS, Radio Access for third Generation Mobile Communications, U.K. John Wiley & Sons Ltd.

[105] UMTS World [Online] at http: //www.umtsworld.com/technology/overview.htm#a1 [Accessed 18 January 2007].

[106] Garawi ,S. A., Courreges, F., Istepanian, R., Zisimopoulus, H., and Gosset, P. (2004), Performance Analysis of a Compact Robotic Tele-Echography E-Health System over Terrestrial and Mobile Communication Links, *Proceeding of the 5th. IEE International Conference on 3G Mobile Communication Technologies- 3G 2004*, London, 18-20, October, 2004, pp.118-122.

[107] Cañero, C., Thomos, N.,Triantafyllidis, G., A., Litos, G. C. and Strintzis, M., G. (2005), Mobile Tele-Echography: User Interface Design, IEEE Transactions on Information Technology in Biomedicine, Vol. 9, No. 1.

[108] Garawi, S. A., Istepanian, R. S. H. and Abu-Rgheff , M. A., (2006), 3G Wireless Communication for Mobile Robotic Tele-ultrasonography Systems, *IEEE Comms. Mag.*, vol. 44, no. 4, pp.91-96.

[109] Zeng, W. and Wen, J. (2000), 3G wireless Multimedia: technologies and practical issues, Wireless Communications and Mobile, Wireless. Commun. Mob. Comput, Vol. 2, pp. 563-572.

[110] 3GPP TR 25.853. (2001), "Delay Budget within the Access Stratum,", 3GPP group (TSG); Release 4.0.0, V4.0.0.

[111] 3G TS 22.105. V3.0.0, (1999), "Technical Specification Group Services and System Aspects Service Aspects; Service and Service Capabilities".

[112] Ethereal – Protocol Network Analyzer, can be downloaded via http://www.ethereal.com/download.html, [Accessed 18 July 2007].

[113] Luna, C. E., Kondi, L. P. and Kataggelos, K. K. (2003), Maximizing User Utility in Video Streaming Applications, *IEEE Transaction on Circuts and Systems for video Technology*, Vol. 13, No. 2, pp. 141-148.

[114] Wang, Z., Sheikh, H. R. and Bovik, A. C. (2002), No-Reference Perceptual Quality Assessment of JPEG Compressed Images, *IEEE International Conference on Image Processing.*

[115] LabVIEW development system, [Online] at http://www.ni.com/labview/, [Accessed 01 August 2007].

[116] Saw, Yoo-Sok (1999), Rate-Quality Optimized Video coding, Kluwer academic Publishers.

[117] Chu, Y. C. and Ganz, A. (2004), A Mobile Teletrauma System using 3G Networks, *IEEE Transaction on Information Technology in Biomedicine,* Vol. 8, No. 4, pp. 456-462.

[118] Sadka, A. H. (2002), compressed Video Communications, John wiley & sons, Ltd.

[119] Chen, Y., Chang, C. and Ren, F. (2004), Q-Learning-Based Multirate Transmission Control Scheme for RRM in Multimedia WCDMA Systems, *IEEE Transactions on Vehicular Technology,* vol. 53, No. 1, pp. 38-48.

[120] MATLAB – the language of technical computing, [Online] at http://www.mathworks.com/products/matlab/ .

[121] Rijkse, K. (1996), H.263: video coding for low-bit-rate communication, *IEEE Communications Magazine*, Vol. 34, No. 12, pp. 42 – 45.

[122] Stockhammer, T., Hannuksela, M. M. and Wiegand, T. (2003), H.264/AVC in Wireless Environments, *IEEE Transactions on Cercuits and Systems for Video Technology,* Vol. 13, No. 7, pp. 657-672.

[123] O'Shaughnessy, D. (1987), Speech Communication Human and Machine, Addison-Wesley publishing company, Chapter-8.

[124] Yu, H., Lin, Z. and Pan, F. (2005), Applications and Improvement of H.264 in Medical Video Compression, *IEEE Transactions on Circuits and System,* Vol. 52, No. 12, December 2005, pp. 2707-2716.

[125] H.264/AVC reference model JM12.4 available [Online] at http://iphome.hhi.de/suehring/tml/, last visited on 21/10/2007.

[126] Varsa, V., Hannuksela, M. M. and Wang, Y. K. (2001), Non-Normative Error Conceakment Algorithms, *ITU-T VCEG-N62,* 2001.

[127] Wnag. Y. K., Hannuksela, M. M., Varsa, V., Hourunranta, A. and Gabbouj, M. (2002), "The error concealment feature in the H.26L test model," in *Proc. ICIP*, vol. 2, Sept. 2002, pp. 729–732.

[128] Stockhammer, T., Hannuksela, M. M. and Wiegand, T. (2003), H.264/AVC in Wireless Environments, *IEEE Transactions on Circuts and Systems for Video Technology,* Vol. 13, No. 7, July 2003, pp. 657-672.

[129] Tunali, T. and Anar, K. (2006), Adaptive available bandwidth estimation for internet video streaming, *Signal Processing: Image Communication,* Vol. 21, pp. 217-234, 2006.

[130] Korhonen, J. (2003), Introduction to 3G Mobile Communications, Second edition, Artech house, 2003.

[131] 3GPP TR 25.853. (2001), "Delay Budget within the Access Stratum," 3rd Generation Partnership Group (TSG); Release 4.0.0, V4.0.0.

[132] 3rd Generation Partnership Project (3GPP), http://www.3gpp.org/.

[133] 3rd Generation Partnership Project 2 (3GPP2), http://www.3gpp2.org/.

[134] Holma, H. & Toskala, A. (2006), HSDPA/HSUPA for UMTS – High Speed Radio Access for Mobile Communications, John Wiley & Sons Ltd, 2006.

[135] Mulvey, D. (2007), HSPA – How 3G High Speed Packet Access works, *IET Communications Engineer magazine,* February 2007.

[136] Moradi, H.; Ahmadian, M. (2003), The impact of convolution coding on the uplink performance of UMTS air interface , *6th International conference on Telecommunications in Modern Satellite, Cable and Broadcasting Service, 2003*. TELSIKS 2003, Vol. 2, 1-3 Oct. 2003, pp. 837 - 841.

[137] Ozcelebi, T., Oguz Sunay, M., Murat Tekalp, A. and Reha Civanlar, M. (2007), Cross-Layer Optimized Rate adaptation and Scheduling for Multiple-User Wireless Video streaming, *IEEE Journal on selected Areas in Communications*, vol. 25, no. 4, pp. 760-769, May 2007.

[138] Al-Fahoum, A S. and Reza, A. M. (2001), Combined Edge Crispiness and Statistical Differencing for Deblocking JPEG Compressed Images, *IEEE Transaction on Image Processing,* Vol. 10, No. 9, September 2001.

[139] Wiegand, T. Sullivan, J. (2003), Overview of the H.264/AVC Video Coding standard, *IEEE Transactions on circuits and systems for Video Technology,* Vol. 13, No. 7, July 2003.

[140] Philip, N. & Istepanian, R. S. H. (2007), Medical Quality of Service for Wireless Ultrasound Streaming in Robotic Tele-Ultrasonography System, *IEEE International Conference on Networking, Sensing and control 2007*, London, pp. 245-250, April 2007.

[141] Van der Schaar, M. and Shankar, S. (2005), Cross-Layer Wireless Multimedia Transmission: Challenges, Principles, and New Paradigms, *IEEE Wireless Communication Magazine,* vol. 12, no. 4, pp. 50-58, August 2005.

[142] Azami, S. B. Z., Duhamel, P. and Rioul, O. (1996), Joint source-channel coding: panorama of methods. *Proceeding of CNES workshop on data compression,* Toulouse, France, November 1996.

Appendix – A

Ultrasound machine type 485 Anser Vet from PieMedical

The 485 Anser Vet ultrasound system is the ultrasound machine used in this thesis work from Pie Medical: the main specifications are as follows:

- Linear, Convex imaging system
- 7" high resolution monitor
- 2 clinical image memory/recall
- Trackball controlled measurements
- Full alphanumeric keyboard
- Variable focus and frequency controls
- Two video out ports
- Probe of type Curved Array with dual frequency (3.5/5.0 MHz) and depth 40mm.

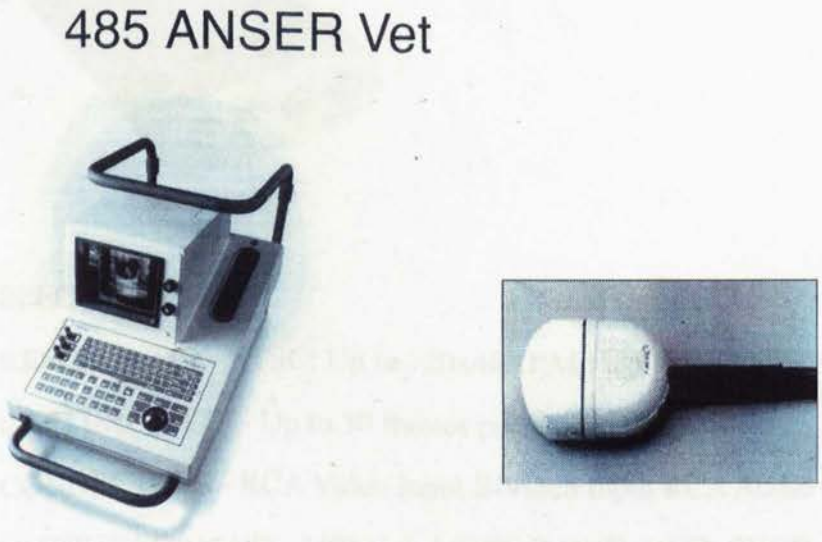

-a- -b-

Figure shows: a- the 485 ANSER Vet ultrasound scanner and b- the curved array probe used

Appendix – B

CameraMate – ProPix VideoSafe™

Zio Corp CameraMate Video Safe:

MODEL- CM-53000

VENDOR- ZIO CORP

FEATURES-

CameraMate VideoSafe With ProPix DVD - One Step Software The CameraMate VideoSafe is easiest way to convert your video tape to DVD in one easy step. You can go from Camcorder VCR, DVD player directly to DVD, VCD, or SVCD and preserve your memories as video tape is a temporary storage device - it disintegrates over time. Your video library will last forever on CD or DVD. Includes CameraMate VideoSafe, ProPix DVD Software, Quick Start Guide. Your Video Tapes will not last much longer Easy To Use ProPix DVD One Step Software Works With All Video Tapes - VHS, VHS-C, 8mm, Hi-8, DV, MiniDV Create DVD, VCD, Or SVCD From Any Video Tape.

SPECIFICATIONs

RESOLUTION - NTSC: Up to 720x480 PAL: Up to 720x576

CAPTURE RATE - Up to 30 frames per second (fps)

CONNECTORS - RCA Video Input S-Video Input RCA Audio Input (L/R)

OUTPUT FORMATS- MPEG-1, MPEG-2 DVD, VCD, SVCD

SOFTWARE - Includes ProPix DVD Software

REQUIREMENTS - Pentium III 800 MHz 256 MB RAM (512 MB Recommended)

150 MB free hard drive space for Software Installation PC must have sound card DirectX 9. 0b or Above 1024 x 768, 24 Bit Color Monitor Available USB 1. 1/2. 0 port CD Burner for VCD, S-VCD creation, DVD Burner for DVD creation. Windows 98SE/Me/2000/XP

www.Ziocorp.Com

Appendix – C

Vodafone – Mobile Connect 3G data card

State-of-the-art Type II PC Card laptop Vodafone 3G data card with speeds of up to 384 kbps

Dimensions 123 x 54 x 10mm
Weight 56g
Networks 3G UMTS, GSM900 and GSM1800
Features 2 status LEDs, CSD/HSCSD*, Dualband GSM, GPRS/3G*, Text Messaging and Type II PC Card
Download Speeds 3G: max 384kbps
GPRS: max 48kbps
Upload Speeds 3G: max 64kbps
GPRS: max 24kbps

www.vodafone.co.uk

IT reviews:

Fast Internet access for laptop users (11/05/2004)

After the years of controversy, nay-saying and all round pessimism that have dogged the development of 3G mobile phone services, it still seems a little surprising that the technology ever made it into actual, real live products. Nevertheless, the third generation mobile networks are finally up and running, albeit with limited coverage, and early adopters all over the UK are learning that the novelty of live video chat wears off a lot quicker than you'd think.

Mobile phone behemoth Vodafone has launched its first 3G product into the IT market. Rather than offering a 3G mobile handset the company has released a datacard

that allows laptop users to access the Internet via the new high-speed network. The premise is simple: plug this PCMCIA card into your laptop and you'll get broadband Internet access whenever you're in range of Vodafone's 3G network. Before we get into the details, let's answer the most important question: yes, it works, and it works pretty damned well.

We tested the card in several locations around London and, even though the signal strength varied considerably between areas, the card provided a decent connection. In areas where the reception was at full strength we achieved download speeds of around 380kbps. This is not quite as fast as a typical cable or DSL connection (512kbps) but plenty fast enough for the kind of applications mobile workers are likely to use and certainly a massive improvement over the GPRS connection mobile Internet users have been stuck with thus far.

When you move out of 3G range the card switches over to a GPRS connection, which offers speeds similar to a standard dial-up modem. We didn't expect it to work as smoothly as it did, but we have to admit that the transition between the two connections is fairly seamless nearly all of the time. Vodafone's 3G network is currently restricted to major cities but is expanding fairly rapidly, and you can get a GPRS connection just about anywhere in the country. A coverage map is available on the company's Web site.

Installation is a doddle. We set the card up on a Compaq Armada E500 running Windows 98SE (the minimum Windows version supported) and had a live connection within ten minutes. The card is managed via Vodafone's Mobile Connect dashboard, a simple application that tells you everything you need to know about your connection and even allows you to send SMS messages from your PC.

Our main gripe about the card is that in order to boost network performance, the system performs extra compression on nearly all Web page images. This includes buttons and logos as well as photographs, and there's no option to turn it off. While it's not usually that noticeable, the over-compression can sometimes make images look bad and if the quality of images in web pages is very important to you then we recommend that you try the card out in a Vodafone store before parting with cash.

The only other negative that's worth mentioning is the large antenna that comes with the card. It's about five inches long and needs to be positioned vertically for optimal performance. That said, when attached to the top of your laptop's screen it's bound to score some bonus gadget-points from other commuters when you're checking your e-

mail on the train into work.

Vodafone - Mobile Connnect 3G Datacard features - Verdict

This could be the start of a revolution in mobile Internet access, adding a fast new option to the existing wireless networking solutions available to laptop users. If and when the 3G coverage improves, datacards such as this are likely to become a staple component of the mobile worker's inventory.

Vodafone - Mobile Connnect 3G Datacard price

Buy Vodafone Mobile Connect 3G Datacard securely online at a bargain price

£100 - £200 inc. VAT depending on contract. Contracts range between £11.75 and £99.99 inc. VAT per month.

Vodafone: 08700 700 191

www.vodafone.co.uk

Appendix – D

Vodafone – Mobile Connect 3G broadband data card

The Vodafone 3G Broadband Data Card enables broadband connection to the internet. In areas where 3G is not available the card still ensures reliable and secure data connection over the widely available GPRS services.

Details:

The new 3G broadband (HSDPA) data card delivers connectivity up to 4 times faster than before, so now you can work as effective out of the office as you can when you are in the office. Check emails, transfer files or access the company network quickly, easily and securely from virtually anywhere.

The new 3G broadband data card delivers connectivity up to 4 times faster than before, so now you can work as effective out of the office as you can when you are in the office. Check emails, transfer files or access the company network quickly, easily and securely from virtually anywhere.

3G broadband achieves peak **download speeds of up to 1.4Mbps** and **upload speeds of up to 384Kbps**.

Users of this new card will also be able to take advantage of high-speed connections in Austria, France, Germany, Portugal, Spain and Hong Kong.

Specifications

• System requirements for PCs :
- Designed for WindowsR 2000 (SP2 and above) and XP Home and Professional
- Type II PC card slot with cardbus interface
- Memory: 32 MB RAM minimum, 64 MB recommended, 100MB minimum of free hard disk space

• System requirements for MACs (only for 3G Mobile Connect Card) :
- MAC OS X
- Type II PC card slot
- PowerBook G4: 15 inch or 17 inch

www.vodafone.co.uk

Appendix - E

LabVIEW^{TD} Software

LabVIEW (Laboratory **V**irtual **I**nstrumentation **E**ngineering **W**orkbench) is a platform and development environment for a visual programming language from the National Instruments http://www.ni.com. The graphical language is named "G". LabVIEW commonly used for data acquisition, instrument control, and industrial automation. The latest version of LabVIEW is version 8.5, released in August of 2007.

LabVIEW is a graphical programming language that uses icons instead of lines of text to create applications. In contrast to text-based programming languages, where instructions determine program execution, LabVIEW uses dataflow programming, where the flow of data determines execution.

In LabVIEW, you build a user interface by using a set of tools and objects. The user interface is known as the front panel. You then add code using graphical representations of functions to control the front panel objects. The block diagram contains this code. In some ways, the block diagram resembles a flowchart.

LabVIEW programs are called virtual instruments, or VIs, because their appearance and operation imitate physical instruments, such as oscilloscopes and multimeters. Every VI uses functions that manipulate input from the user interface or other sources and display that information or move it to other files or other computers.

A VI contains the following three components:

- Front panel—Serves as the user interface.
- Block diagram—Contains the graphical source code that defines the functionality of the VI.
- Icon and connector pane—Identifies the interface to the VI so that you can use the VI in another VI. A VI within another VI is called a subVI. A subVI corresponds to a subroutine in text-based programming languages.

VIs can communicate, or network, with other processes, including those that run on other applications or on remote computers.

LabVIEW supports several low-level networking protocols you can use to communicate between computers. Transmission Control Protocol (TCP) and User Datagram Protocol

(UDP) are available on all platforms LabVIEW supports Internet Protocol (IP), User Datagram Protocol (UDP), and Transmission Control Protocol (TCP) are basic tools for network communication. LabVIEW includes TCP and UDP VIs and functions you can use to create client or server VIs.

NI added machine vision to its LabVIEW product line. This is included as NI-IMAQ vision. Software options include image acquisition software to acquire images from thousands of cameras, a world-class image processing library, and a configurable interface for industrial machine vision applications.